ENERGY STORAGE MANAGEMENT AND LOAD SCHEDULING WITH RENEWABLE INTEGRATION

by

Tianyi Li

A Thesis Submitted in Partial Fulfillment
of the Requirements for the Degree of
Doctor of Philosophy
in
The Faculty of Engineering and Applied Science
Department of Electrical, Computer and Software Engineering

University of Ontario Institute of Technology

August 2015

Table of Contents

Table of Contents iii
List of Figures vii
List of Tables x
Abstract xi
Acknowledgements xiii
Chapter 1 Introduction 1
1.1 Overview 1
1.2 Energy Storage System 2
1.2.1 Renewable Generation 3
1.2.2 Battery Technology for Energy Storage 5
1.3 Energy Consumption Scheduling 8
1.3.1 System Operation Perspective 8
1.3.2 Energy Consumption Perspective 9
1.4 Motivation and Objective 10
1.5 Methodology 13
1.6 Contributions 14
1.7 Outline of the Dissertation 18
1.8 Notation 18

Chapter 2 Literature Review 20
2.1 Energy Storage Management (ESM) 20
2.2 Demand Side Management (DSM) 22
2.3 Energy Storage Management with Flexible Loads 24

2.4 Lyapunov Optimization Technique 26
2.5 Highlights of Contributions 29

Chapter 3 Real-Time Energy Storage Management with Renewable Integration: Infinite Time Approach 31

3.1 System Model 32
3.1.1 Power Sources 32
3.1.2 Battery Operation 33
3.1.3 Energy Storage Management 35
3.2 Energy Management Optimization 35
3.2.1 Real-Time Energy Storage Management Algorithm: Infinite Time Approach 36
3.2.2 Lyapunov Function and Drift 37
3.2.3 Performance of the Real-Time Control Policy 40
3.3 Centralized Storage Management System 41
3.4 Simulation Results 43
3.4.1 Stand-Alone Model 43
3.4.2 Centralized Model vs. Stand-Alone Model: Case Study 45
3.5 Appendices 52

Chapter 4 Real-Time Energy Storage Management with Renewable Integration: Finite Time Approach 57

4.1 System Model 58
4.1.1 Power Sources 58
4.1.2 Battery Operation 59
4.1.3 Energy Storage Management 61
4.2 Energy Management Optimization: Finite Horizon Approach 61
4.2.1 Problem Modification 63
4.2.2 Problem Transformation 64
4.3 Real-Time Energy Management Algorithm 66

4.3.1 Lyapunov Function and Drift 66
4.3.2 Real-Time Control Algorithm 68
4.4 Performance Analysis 73
4.4.1 Performance of Algorithm 1 74
4.4.2 Algorithm Parameter Δ_a 76
4.5 Simulation Results 77
4.5.1 Simulation Configuration 77
4.5.2 Behavior of B_t over Time 80
4.5.3 Performance Comparison under Algorithm Parameters 80
4.5.4 Performance Comparison under Battery Parameters 83
4.5.5 Guideline for Determining Δ_a 86
4.6 Energy Storage System with Sell-Back 86
4.6.1 System Model 86
4.6.2 Real-Time Energy Storage Management 89
4.6.3 Performance Analysis 95
4.6.4 Simulation Results 96
4.7 Appendices 102

Chapter 5 Real-Time Joint Energy Storage Management and Load Scheduling with Renewable Integration 117

5.1 System Model 117
5.1.1 Load Scheduling 118
5.1.2 Energy Sources and Storage 120
5.1.3 Supply and Demand Balance 122
5.2 Joint Energy Storage Management and Load Scheduling: Problem Formulation 122
5.2.1 Problem Modification 124
5.2.2 Problem Transformation 125
5.3 Joint Energy Storage Management and Load Scheduling: Real-Time

Algorithm 126
5.3.1 Virtual Queues 127
5.3.2 Real-Time Algorithm 128
5.3.3 Discussions 134
5.4 Performance Analysis 136
5.4.1 Algorithm Performance 136
5.4.2 Design Approximation 138
5.5 Simulation Results 139
5.5.1 Simulation Configuration 139
5.5.2 An Example of Load Scheduling 141
5.5.3 Effect of Scheduling Delay Constraints 141
5.5.4 Performance vs. Battery Capacity 145
5.6 Appendices 147

Chapter 6 Conclusions **157**

Chapter 7 Future Work **160**

Bibliography **163**

List of Figures

Figure 3.1 An example of energy storage and management system 33

Figure 3.2 An example of centralized energy storage and management system 41

Figure 3.3 Power grid real-time price P_t, average demands $\overline{W_t}$, average solar energy $\overline{S_t}$ 45

Figure 3.4 Long-term cost vs. C_{rc} (or C_{dc}) 46

Figure 3.5 # of recharges (discharges) vs. C_{rc} (or C_{dc}) 46

Figure 3.6 Proportion of total stored energy purchased from the grid at different price price $E_Q(P_i)$ vs. battery capacity 47

Figure 3.7 Long-term time-averaged cost vs. C_{rc} (or C_{dc}) at different V values ($B_{\max} = 1.5$ kWh) 48

Figure 3.8 Ratio ρ vs. solar integration scaler η_1 in Scenario 1 49

Figure 3.9 Ratio ρ vs. η_2 (scaled variance) in Scenario 2 49

Figure 3.10 Ratio ρ vs. correlated factor η_3 in Scenario 3 50

Figure 4.1 An example of energy storage and management system 58

Figure 4.2 System inputs $\overline{W}_t, \overline{S}_t$, and P_t over 24 hours 77

Figure 4.3 Trace of state of battery B_t vs. time slot t in a single

realization 81

Figure 4.4 Average system cost vs. Δ_a ($B_{\max} = 3$ kWh) 81

Figure 4.5 CDF of error under different values of Δ_a ($B_{\max} = 3$ kWh) .. 82

Figure 4.6 T_o-slot average system cost vs. V ($\Delta_a = 0$) 82

Figure 4.7 System cost vs. battery usage cost coefficient k ($\Delta_a = 0$) 85

Figure 4.8 System cost vs. battery capacity $B_{\max}$ 85

Figure 4.9 An example of energy storage and management system with selling-back 87

Figure 4.10 Buying (Selling) energy to (from) battery vs. $B_{\max}$ ($\eta = 0.9$) 97

Figure 4.11 Buying (Selling) energy to (from) battery vs. $B_{\max}$ ($\eta = 0.3$) 97

Figure 4.12 System cost vs. Δ_a ($B_{\max} = 3$kWh, $\eta = 0.9$) 99

Figure 4.13 CDF of mismatch under different values of Δ_a 99

Figure 4.14 System cost vs. $B_{\max}$ ($C_{\text{rc}} = 0.001$) 101

Figure 4.15 System cost vs. η ($\Delta_a = 0.1$) 101

Figure 5.1 The residential energy storage management system 118

Figure 5.2 An example of load scheduling for two arrival loads W_{t_1} and W_{t_2} 118

Figure 5.3 System inputs $\overline{W}_t, \overline{S}_t$, and P_t over 24 hours 140

Figure 5.4 A trace of load scheduling results over time 142

Figure 5.5 Average system cost vs. $d_t^{\max}$ ($d^{\max} = d_t^{\max}$) 142

Figure 5.6 Monetary cost vs. $d^{\max}$ ($\alpha = 0.005$) 144

Figure 5.7 $\overline{d_w}$ vs. $d^{\max}$ ($\alpha = 0.005$) 144

Figure 5.8 Average system cost vs. $d^{\max}$ ($d_t^{\max} = d^{\max}$) 146

Figure 5.9 Average system cost vs. $B_{\max}$ ($\alpha = 0.001$) 146

List of Tables

Table 1.1 Battery Characteristics 5

Table 3.1 Ratio ρ vs. $B_{\max}$ and C_{rc} (or C_{dc}) with $P'_H = 10P_H$ and i.i.d W_t, S_t 51

Table 3.2 Ratio ρ vs. $B_{\max}$ and C_{rc} (or C_{dc}) with $P'_H = 10P_H$ and non-stationary W_t, S_t 51

Table 3.3 Ratio ρ vs. $B_{\max}$ and C_{rc} (or C_{dc}) with non-stationary W_t and boosted non-stationary S_t 51

Abstract

In this dissertation, the energy storage management and load scheduling problems are studied. The main objective is to design real-time cost-effective control policies at a residential site with integrated renewable generation. Stochastic nature of system dynamic for renewable generation, user load, and electricity pricing has been formulated in problems. Furthermore, battery degradation costs due to battery operation have been incorporated into the system cost. Both infinite and finite time horizon approaches have been designed in this dissertation. Lyapunov optimization technique has been applied to design the real-time control algorithms that rely only on the current system dynamics. Close-form solutions have been obtained for simple implementation. The proposed algorithms are shown to have bounded performance gap to the optimal control policies.

The first problem is to minimize the long-term time-averaged system cost with i.i.d system inputs, where battery operation cost is considered. In the second problem, a finite time horizon approach is provided to minimize the system cost over a fixed time period. Non-stationary stochastic nature of system dynamics is considered in formulating the problem. Furthermore, the detailed battery operation costs is incorporated into the system cost. A special technique to tackle the technical challenges

in problem solving is developed. In the third problem, a joint energy storage management and load scheduling problem is proposed. The problem is to optimize the load scheduling and energy storage control simultaneously in order to minimize the overall system cost over a finite time horizon. In this real-time optimization design, the joint scheduling and energy storage control is separated and sequentially determined. Both scheduling and energy control decisions have close-form solutions for simple implementation. Through analysis, it is shown that the proposed real-time algorithm has a bounded performance guarantee from the optimal T-slot look-ahead solution and is asymptotically equivalent to it as the battery capacity and time period go to infinite.

Acknowledgements

I would like to express my sincere gratitude to my supervisor Prof. Min Dong for her continuous support, motivation, enthusiasm, and immense knowledge.

Chapter 1

Introduction

1.1 Overview

Over past 60 years, the term *grid* has been used to describe an electricity system that generates, transmits and distributes electricity from several central generators to a large number of consumers. A *smart grid* is an enhancement and renovation on our existing power grid. Smart grid enables two-way transmission to transmit not only electricity but also information via wired or wireless communication networks. Due to the information shared among the generators, distributors and consumers, the integration of distributed generation, renewable sources and energy storage becomes possible in a future power system, and will substantially change the current power system.

In future grid system, integrating renewable energy sources will be a vital green energy solution to reduce the energy cost and to build a sustainable society and economy. Energy storage devices will be adopted to mitigate the uncertainty introduced by the renewable generation as well as to reduce electricity cost for consumer. Developing smart appliances with flexible load will further help in stabilizing the grid and reducing the electricity cost [1]. As a result, energy delivery will be more reliable,

sustainable and economical.

The smart grid related research is broad. It involves various topics all the way from generation to consumption. Different researchers may have different visions for smart grid because of their different focuses and perspectives. From the grid operation perspective, the topics include but not limited to: Smart meter, generation phase control, micro-grid, direct load control, pricing strategies, energy distribution and distributed energy storage management. From the consumption perspective, energy storage management and demand side management can provide effective means for energy management to reduce electricity cost. In particular, energy storage can be exploited to shift energy across time, while flexible loads can be controlled to shift demand across time.

1.2 Energy Storage System

In conventional grid, centralized generation must be able to provide enough energy precisely to satisfy consumers' demands over time. This becomes problematic when generation deals with peak demand periods. Grid operators have to use generation assets called peaker plants to ensure reliability and meet the peak demand. However, peakers are expensive to operate, and they stay idle for most of the year but must be paid nevertheless [2].

In future power system, building energy storage system has the promising benefits to improve the grid reliability by reducing voltage fluctuation, and at the same time reduce energy bill for the electricity consumers. It is the promising solution for various applications. Examples of these applications include short-term power balanc-

ing services such as frequency regulation, and long-term services such as maintaining a certain level of reserve capacity [3]. Moreover, there are many types of storage with a wide range of storage characteristics for different applications: pumped hydro storage, compressed air energy storage, thermal energy storage, batteries, flywheels, capacitors, and super conducting magnetic energy storage [4].

As the incorporation of renewable energy into the grid system becomes widely adopted, designing effective energy storage management to integrate the renewable generation and harness the free energy source becomes especially important but challenging due to the inherit stochastic nature of the renewable sources. In this regard, energy storage management techniques need to be developed. The management should be able to control all the energy flows from (to) conventional generation, energy storage and renewable generation to satisfy the consumer demands and reduce the electricity costs.

Next, the main characteristics of renewable generation and battery technology will be introduced. The potential problems that the researchers may face in designing the system will be addressed in Section 1.4.

1.2.1 Renewable Generation

Currently, the largest share of electricity generation is still from fossil fuels, *e.g.,* natural gas and coal. This share is expected to increase by 29% between 2012 and 2040 to address the growing demand of energy [5]. Humanity's endless request for energy has caused the exhaustion of fossil fuels and environmental deterioration.

To address those concerns, integrating renewable generation into the grid system

has become a vital green solution to reduce the dependence of fossil fuels and to enable a transition to a sustainable society and economy [4]. Photovoltaic (PV) and wind are two renewable sources to be considered because they can be easily integrated into our power system as the distributed generation on the consumer end, capable of providing free energy and zero carbon emissions.

The renewable sources are intermittent in nature. To maximally harvest the renewable energy, mathematical methods have been developed to effectively forecast the renewable energy, including the statistical models and persistence models. Statistical models predict well in the short and medium term, *i.e.,* 1 hour up to 36 hours. Therefore, they have been widely adopted to predict accurate solar generation. The persistence model performs well for real-time wind forecast because it has accurate prediction in very short term compared to the actual data. Normally, the model's accuracy keeps within 1 hour [6]. Other possible prediction approaches may use image processing technique or meteorological information on cloudiness [7].

As renewable penetration into the power supply increases, the renewable energy with storage solution will be adopted and implemented for wide applications. This will include power balancing in a grid system, green and cost effective solution for base station power supply for wireless transmissions, low-power self-sustainable sensor network applications, as well as energy solutions for cloud data centre computing. Thus, cost effective energy management technologies to maximally harness energy from renewable sources becomes crucial for the success of green energy transition [8].

Table 1.1: Battery Characteristics

	Lead-acid	**NiCd**	**NiMH**	**Li-ion**
Technology	Matured	Matured	Matured	Developing
Hazard	Toxic	Toxic	Environmentally friendly	Safety issue
Efficiency	Low	Low	Low	High
Cost	Cheap	Cheap	Cheap	Costy
Adoptability	Poor	Moderate	Better	Best

1.2.2 Battery Technology for Energy Storage

Energy storage has been recently picked up to face the shortage and high price of fossil fuels. It is expected that most future consumer end renewable installations will be equipped with storage devices. A typical application of storage devices is electric vehicles (EVs). EVs are driven by electricity power from an array of batteries. In the near term, it is expected that EVs will be integrated to the grid system, capable of storing energy for consumers and selling it back to the grid when the grid needs it. Thankfully, many auto manufacturers have been working on the development of EVs for years and already released some models on the auto market, *e.g.,* Tesla Model S and BMW i-series.

Four types (Lead-acid, Nickel cadmium (NiCd), Nickel metal hydride (NiMH), Lithium ion (Li-ion)) of battery are listed in Table 1.1 to compare their technology maturities, hazards, storage efficiencies, investment costs and the adoptabilities to the renewable energy integration.

The detail characteristics are introduced below:

- **Lead-acid**: The lead-acid battery is the oldest and most mature technology

that has been used for electrical energy storage. **Pros**: Ideal for small-cycle renewable energy integration applications; Low investment costs and ease of maintenance; Can be discharged repeatedly by as much as 80% of their capacity. **Cons**: Limited cycle life; Poor performance at low and high ambient temperatures; Failure due to deep and continuous cycling; Environmentally unfriendly. **Adoptability to renewable energy integration**: Currently, Lead-acid is a front-runner for use in distributed generation application.

- **Nickel cadmium (NiCd)**: NiCd batteries are a robust and proven alternative to lead-acid batteries. **Pros**: Longer cycle life; Higher energy densities and low maintenance requirements. **Cons**: Contain toxic heavy metals and suffer from severe self-discharge. **Adoptability to renewable energy integration**: Compared to Lead-acid, NiCd Offer many advantages in PV applications.

- **Nickel metal hydride (NiMH)**: NiMH battery is a feasible alternative to NiCd battery. **Pros**: Environmentally friendly due to the lack of toxic substances such as cadmium, lead or mercury. Energy density is 25%−30% better than NiCd. **Cons**: Also suffer from severe self-discharge, making them inefficient for long-term energy storage. **Adoptability to renewable energy integration**: NiMH has lower costs compared to Li-ion technology; Before Li-ion batteries have lower prices, NiMH batteries could play a temporary role and are possible front-runners for renewable energy integration applications.

- **Lithium ion (Li-ion)**: The current use of Li-ion batteries is predominant in portable electronics market. **Pros**: Achieves energy storage efficiencies of

close to 100%; Highest energy density. **Cons**: High investment costs; Complicated charge management systems required; Lack of longevity; Safety issue [9]. **Adoptability to renewable energy integration**: The use of Li-ion batteries for renewable energy storage applications is very plausible in the not-so-distant future. Global investment in Li-ion research and development is estimated at over $1 billion annually. The work is aimed at reducing the capital cost and further improving reliability of this technology [10].

With the battery technology being developed, the performance and reliability of the battery have been improved drastically in recent years. However, battery operations cause battery degradation. This effect has to be considered when the storage applications are implemented. Particulary, the high depth of discharge (DoD) and the frequent charge cycling can severely cut short the lifetime of Li-ion batteries[13]. Another effect is called the battery aging effect which highly depends on internal parameters such as battery chemistry and manufacturing quality and external parameters such as temperature, charge habits and cycling regime [12].

To prolong battery life, the apparent way is to limit the number of charge cycles and restrict the DoD in each cycle. This way can ensure that the total number of cycles are always under a certain value given by the manufacture design. In practical daily cycling regime, 5 to 10 charge cycles are expected to ensure that the battery lifetime is not shortened by the operation. Alternatively, a different operation cost can be attached to the charge cycling and the DoD. If the number of cycles finished per day is more than an expected number by the design, battery lifetime is shortened

and a higher operation cost will be paid; If the deep DoD is happened, a higher cost will be paid too. In the storage system design, this research has taken into account the operation cost as described in the second way.

1.3 Energy Consumption Scheduling

Energy consumption scheduling is widely applied to stabilize the grid system and reduce operation costs at system operator side as well as reduce electricity costs at energy consumer side. This section will explain the approaches of load scheduling from system operation and energy consumption perspectives.

1.3.1 System Operation Perspective

When the system operators perform the management on the system, stabilizing the entire system is the most primary consideration. Before putting the emphasis on operator-to-consumer interaction, conventionally, system operators manage the system on the way of direct load control (DLC). The main purpose of doing that is to shave the peak-to-average ratio (PAR), which enables them to directly modify the operations of consumers' appliances during high-peak periods. As introduced in Section 1.2, peakers have to be installed at the grid operation end to meet the peak demand, which are expensive to run. Maintaining PAR at a certain level will save the operation cost for grid operators as well as reduce the possibility of outage on the consumer end.

In smart grid, more interaction between the operator and the consumer becomes possible through two-way communication techniques. To improve the system relia-

bility, instead of directly controlling consumers' demands, the system operators can design dynamic pricing strategies, *i.e.,* adjust different prices per kilowatt hour according to the real-time variation of the production capacity and the load demands. Thus, consumers will have the opportunity to see what price they will pay for energy before they buy. Although dynamic pricing is not a direct control behaved on the operator end, it provides energy consumers effective economic incentives to shift their power consumptions to low-peak periods and thus help the operators save their operation cost [11].

For example, Ontario Energy Board offers electricity price based on Time of Use (TOU). It is a fixed three-stage price with high, medium and low rates for the day. Winter and summer seasons are followed by two different rate distributions. Another promising pricing strategy is called Real-Time Pricing (RTP). where grid operators will monitor the current load consumption and adjust the price in a real time manner. Designing such a strategy to benefit both operators and consumers is difficult, since higher uncertainty may lead to less attraction from a consumer perspective. Plenty of research is aimed at designing the effective RTP strategies.

1.3.2 Energy Consumption Perspective

From a electricity consumer perspective, consumers can respond to the dynamic price set by the operators through demand scheduling. In other words, a lower electricity cost will give the consumers an incentive to re-schedule their load if the current electricity rate is high. This requires that domestic appliances can be deferred or interrupted, and must be capable of automatical starts and stops. Therefore, their

loads are flexible. For some appliances *e.g.,* lights and televisions, their starting and stopping time and operation durations are not predictable or completely unknown. Those are hard demands by consumers which must be satisfied as requested. For other appliances, such as washers, dryers and EVs, their loads are flexible and therefore are able to respond to the dynamic price. It is necessary to be pointed out that the demands for those appliances can be deferred for a few minutes or hours at little or no cost [12]. Therefore, it is possible to utilize the flexibility from those appliances, and intelligently schedule them to help consumers maximally save their electricity cost.

Moreover, some schemes have been shown that significant savings can be achieved if only a few consumers participate to the demand response, *i.e.,* rescheduling their appliances. When a higher penetration of demand response is involved among consumers, the grid stability is problematic, *i.e.,* a rebound peak of demand may occur in the originally low-rate periods due to a large number of shifted loads [2]. Therefore, to achieve notable savings for consumers and maintain a reliable grid system for operator, effective scheduling schemes need to be developed.

1.4 Motivation and Objective

As the penetration of renewable generation to the power supply increases, energy storage can be adopted to mitigate the randomness of renewable generation, reducing the power supply instability caused by renewable integration. It also provides excellent means for cost effective energy management. The renewable generation with storage solutions will become increasingly popular. At the same time, since many smart ap-

pliances have been developed, load scheduling problems have been studied to shift the energy demand in order to reduce electricity cost for consumers. Providing effective management solutions that combine both energy storage and load scheduling will be the most promising future solution for electricity consumers to reduce their energy costs.

Developing the cost effective energy storage management and load scheduling solutions are important, but faces unique challenges. Those issues mentioned below have not been fully/partially studied by other literature works.

- For the renewable generation, electricity pricing, and loads, they are all random and likely to be statistically time-varying making them difficult to predict.
- For the energy storage, there exists a double effect of electricity cost reduction and added operation costs regarding the storage degradation. Also, finite battery capacity makes the storage control decisions coupled over time and difficult to optimize.
- For the load scheduling, while minimizing the electricity cost, the delay requirements need to be met for each load and the overall service when joint design of energy storage management and load scheduling is considered. In particular, load scheduling decisions affect the energy usage and storage; vise versa, storage control and load scheduling decisions are coupled with each other over time, making joint design especially challenging.
- In addition, most energy storage management or load scheduling problems consider long-term expected cost over an infinite time horizon as the design metric.

In reality, consumers may prefer a cost saving solution in a period of time defined by their own needs. This is yet to be studied.

In this dissertation, we focus on real-time energy storage management and load scheduling at a residential site with integrated renewable generation and storage battery.

In our first problem, we study the problem of energy storage management with renewable energy integration by designing real-time control policy to minimize the long-term time-averaged system cost. We take into account system input dynamics and finite battery capacity, and incorporate the battery operation cost for energy storage into the control optimization.

In our second and third problems, we take finite time horizon approaches and consider unknown arbitrary dynamics of renewable source, load, and electricity pricing information. In addition, we provide detailed modeling of battery operation costs due to charging and discharging activities as part of the system cost.

Specifically, we consider the design of cost-effective management of energy storage with renewable integration in our second problem. We formulate the control optimization problem aiming at minimizing the system cost over a fixed time period.

In our third problem, we consider joint energy storage management and load scheduling with integrated renewable generation. We aim at optimizing the load scheduling and energy storage control simultaneously in order to minimize the overall system cost.

1.5 Methodology

In our first problem, we design a real-time storage control algorithm to meet consumer demand while minimizing the long-term system cost. We directly apply the Lyapunov optimization technique to design a real-time control algorithm that only relies on the current system dynamics. We also extend our existing model to a centralized model. Using same algorithm, we provide control solution for each user and compare two models in simulation.

In our second problem, we take a finite time horizon approach and formulate the control optimization problem over a fixed time period. The finite horizon problem prevents direct adoption of Lyapunov optimization for devising a real-time control algorithm. We develop special techniques to tackle the problem, through problem modification and transformation, which enables us to leverage Lyapunov optimization to design a real-time control algorithm. Furthermore, using same approach, we extend our existing model to a sell-back model and develop new real-time control solution.

In our last problem, we design a real-time solution for joint energy storage management and load scheduling to minimize the system cost over a finite period of time. We develop techniques to employ Lyapunov optimization technique through a sequence of problem modification and transformation for designing a real-time algorithm. The joint scheduling and energy storage control is then separated and sequentially determined in our real-time optimization algorithm.

1.6 Contributions

The contributions of this dissertation are summarized as follows:

1. Real-Time Energy Storage Management for Long-Term System Cost Minimization

We consider an energy storage management problem of minimizing the long-term time averaged system cost with renewable integration. We take into account system input dynamics, and incorporate the battery operation cost for energy storage into the control optimization. Applying Lyapunov optimization technique, we design the real-time control algorithm that only relies on the current system input. We provide a close-form control solution which renders our policy implementation with minimum complexity. Unlike existing works on energy storage which do not consider either renewable integration or battery operation cost, we incorporate both into our design for a storage control solution.

Through analysis, we show our proposed algorithm has a bounded performance to the optimal. Other literature works are lack of consideration for battery operation cost or renewable integration in their simulations. We provide the detailed studies and show that introducing renewable energy can effectively reduce the long-term cost and improve the efficiency of energy storage. In addition, we study a centralized model. Simulations show that users can further reduce their total system cost from sharing a common battery.

2. Real-Time Energy Storage Management for System Cost Minimization in a Finite Time Approach

We consider an energy storage management problem of minimizing the time averaged system cost over a finite time period. We take into account unknown arbitrary dynamics and provide detailed modeling for battery operation cost due to charging and discharging activities as part of the system cost.

The finite time horizon approach through Lyapunov optimization is not yet studied by any literature works. We are the first to investigate on this approach. However, the finite horizon problem prevents the direct adoption of Lyapunov optimization for devising a real-time control algorithm. To deal with that, we develop special techniques to tackle the problem, through problem modification and transformation, which enables us to leverage Lyapunov optimization to design a real-time storage control algorithm that relies only on the current system dynamics. Compared with other works, our design can handle unknown arbitrary dynamics, while those works can only assume the stationary system inputs.

We also extend our work by adding sell-back in the system model and provide explicit solution for each control action. We analyze our proposed algorithm and show that it has a bounded performance gap to the optimal non-causal T-slot look-ahead control solution. Furthermore, we show that our algorithm is asymptotically optimal as the battery capacity and time period go to infinity. Simulation studies show the effectiveness of our proposed algorithm as compared with two alternative real-time and non-causal algorithms.

3. Real-Time Joint Energy Storage Management and Load Scheduling for System Cost Minimization

We focus on a joint control optimization problem for energy storage management

and load scheduling with the objective of minimizing the system cost over a finite time horizon. Besides assuming unknown arbitrary system dynamics and incorporating detailed battery operational costs, we model each individual task with its own intensity, requested service duration, and maximum and average delay constraints.

The joint problem of energy storage management and load scheduling is not yet fully studied by other literature works. The existing works can only guarantee the maximum delay over all loads, or provide scheduling for each load but require known ahead information. We are the first to provide a joint solution for storage control and load scheduling that does not rely on any statistic information.

The interaction of load scheduling and energy usage, the finite battery capacity, and finite time period for optimization complicate scheduling and energy control decision making over time. To tackle this difficult stochastic problem, we develop techniques through a sequence of problem modification and transformation which enables us to employ Lyapunov optimization technique for designing a real-time algorithm that otherwise is not directly applicable. We show that the joint energy storage control and load scheduling can be separated and sequentially determined in our real-time optimization algorithm. Furthermore, both scheduling and energy control decisions have close-form solutions making the real-time algorithm simple to implement. We show that our proposed real-time algorithm has a bounded performance guarantee from the optimal T-slot look-ahead solution and is asymptotically equivalent to it as the battery capacity and time period go to infinity. Simulation results demonstrate the effectiveness of joint load scheduling and energy storage management by our proposed algorithm as compared with alternative solutions considering neither storage

nor scheduling, or storage only.

The results of this dissertation have been published/submitted in several prestigious journals and conferences as I summarize below:

1. T. Li and M. Dong, "Real-time energy storage management with renewable integration: finite-time horizon approach," accepted to *IEEE J. Select. Areas Commun.*, Sep. 2015.

2. T. Li and M. Dong, "Real-time residential-side joint energy storage management and load scheduling with renewable integration," submitted to *IEEE J. Select. Areas Commun.*, July. 2015.

3. T. Li and M. Dong, "Energy storage with renewable generation: real-time control and its application to centralized storage management," in preparation to be submitted.

4. T. Li and M. Dong, "Real-time energy storage management with sell-back: finite-time horizon approach," to be submitted to *IEEE Trans. Smart Grid*.

5. T. Li and M. Dong, "Real-time energy storage management: Finite-time horizon approach," in *Proc. IEEE Int. Conf. on Smart Grid Communications*, Venice, Italy, Nov. 2014.

6. T. Li and M. Dong, "Real-time energy storage management with renewable energy of arbitrary generation dynamics," in *Proc. Asilomar Conf. on Signals, Systems and Computers*, Pacific Grove, CA, Nov. 2013.

7. T. Li and M. Dong, "Online control for energy storage management with renewable energy integration," in *Proc. IEEE Int. Conf. Acoustics, Speech, and Signal Processing*, Vancouver, BC, May 2013.

1.7 Outline of the Dissertation

The rest of this dissertation is organized as follows: In Chapter 2, I present a review on the recent studies of energy storage management. Also, I provide a literature review on demand side management. In Chapter 3, I formulate a real-time energy storage management system with renewable integration using infinite time approach. In Chapter 4, I design the storage management through a finite horizon approach. In Chapter 5, I extend my work to consider a joint energy storage management system with load scheduling. The conclusion is provided in Chapter 6.

1.8 Notation

The main symbols used in this dissertation are summarized as below:

W_t: user's demand at time slot t

P_t: conventional grid real-time price at time slot t

$P_{\max}$: maximum electricity price

E_t: energy purchased from conventional grid at time slot t

S_t: renewable energy harvested at time slot t

$S_{w,t}$: amount of renewable energy supplied to user's demand W_t at time slot t

$S_{r,t}$: amount of renewable energy stored to battery at time slot t

Q_t: the portion of E_t stored into battery at time slot t

$R_{\max}$: maximum charging amount allowed to battery

D_t: discharging amount from battery at time slot t

$D_{\max}$: maximum discharging amount from battery

B_t: stage of battery energy level at time slot t

$B_{\min}$: minimum energy required in battery

$B_{\max}$: maximum energy allowed in battery

C_{rc}: entry cost for battery usage due to each charging

C_{dc}: entry cost for battery usage due to each discharging

$x_{e,t}$: entry cost for battery usage at time slot t as $x_{e,t} = 1_{R,t}C_{\text{rc}} + 1_{D,t}C_{\text{dc}}$

$x_{u,t}$: amount of battery energy level change in time slot t, as $x_{u,t} = |Q_t + S_{r,t} - D_t|$

$\overline{x_e}$: average entry cost for battery usage over the T_o-slot period

$\overline{x_u}$: average amount of battery energy level change over the T_o-slot period

$C_u(\cdot)$: usage cost function of the battery

$\overline{J}$: average cost of purchasing energy from the grid in T_o slots

$\mathbf{a}_t$: control action at time slot t

Δ_a: desired change amount of battery energy level in T_o slots

d_t: actual scheduling delay incurred for W_t

$d_t^{\max}$: maximum allowed delay for the load W_t before it is served

$d^{\max}$: maximum average delay for the loads within the T_o-slot period

α: positive weight for the cost of scheduling delay

$C_d(\cdot)$: cost function of scheduling delay

μ: positive weight for delay related queues in the Lyapunov function

Chapter 2

Literature Review

2.1 Energy Storage Management (ESM)

Energy storage can be located at the supply side or the demand side. With more and more renewable generation integrated, it is suggested that energy storage can be co-located with renewable generators so as to mitigate the uncertainty of renewable generation [13]. Also, the storage can be used for minimizing the users' electricity cost at the demand side. In particular, energy storage management has been considered for power balancing to counter the fluctuation of renewable generation and increase grid reliability for system operator [14–17], and to reduce electricity cost at consumption side for users [18–24].

Off-line storage control strategies for dynamic systems have been proposed [14,15, 18,19]. Using storage to mitigate the intermittent nature of renewable energy resources is studied in [14, 15]. In [14], the optimal use of distributed storage is studied where authors design their control strategies via a Linear-Quadratic based technique and show these strategies achieve asymptotically optimal for simple network topologies. The dependence of optimal performance on storage and transmission capacity is also explicitly quantified. A prediction model to study the error of the difference between

the generation and the load is proposed to ensure that the demand is satisfied as much as possible [15]. The problem is formulated as an infinite time average cost dynamic program. Threshold optimal policies are obtained.

In [18], a problem of peak shaving for the power grid using renewable generation and energy storage is studied. Renewable generation and load power consumption prediction algorithms are presented. The proposed control algorithms are separated into global tier and local tier. The global control is solved as a convex optimization problem, and the local control is solved analytically. In [19], a problem of cost saving for data centers is investigated through dynamically right-sizing the servers in data center. The optimal off-line algorithm is first proposed for dynamically turning off the servers to achieve the cost-saving. After that, the authors propose an online algorithm and show it has proven performance. In these works, renewable energy arrivals are assumed known ahead of time and the knowledge of load statistics is assumed. For real-time storage management design, [20] studies a storage management problem in order to maximize consumer energy consumption. The problem is first formulated as a Markov Decision Process (MDP), and then formulated as an online learning algorithm.

Lyapunov optimization technique [25] has been recently employed for designing real-time storage control at either grid operator side or consumer side under different system models and optimization goals [16, 17, 21–23]. Among these works, [22, 23] study the optimal demand response with energy storage management in order to minimize the system costs. Their polices show that the maximum delay is guaranteed for user demands. However, they do not consider battery operation cost due to

charging/discharging in their system models. Both renewable generation and battery operation cost are modeled in [16, 17]. The authors consider the dynamic aggregator-EVs systems and provide real-time algorithms for aggregator to fairly allocate the regulation amount among the EVs.

Energy storage is also considered in other applications besides for future grid operation. Using energy harvesting device for wireless communication has recently attracted growing interests [26–29]. The problems there focus on wireless transmission policy design, instead of energy storage management. Thus, the modeling of battery is relatively simple.

2.2 Demand Side Management (DSM)

The problems of demand side management can be designed from either the system's perspective (*e.g.,* maintaining the grid reliability, minimizing the system operational cost) or from the user's perspective (*e.g.,* minimizing the electricity cost, maximizing the energy consumption), or from the both (*i.e.,* combing the user-level objective along with the system-level objective). Many problems have been studied with different design objectives. We have summarized those works as below.

From system's perspective, load (demand) scheduling through demand side management has been studied by many for shaping the aggregate load at utility through direct load control [30–32] or pricing design [33, 34]. Among these work, [30] studies a distributed direct load control scheme for large-scale residential demand response. The problem is to reduce the mismatch between the actual aggregated demand and desired demand. An average consensus algorithm is proposed to distribute the desired

aggregated demand in a decentralized fashion. In [31], a multi-timescale scheduling scheme is proposed to optimize real-time price and manage the user demand so as to achieve system-wise reliability and efficiency. In [32], the problem of minimizing the average power grid operational cost through power demand scheduling is studied. The threshold-based control policy is proposed to ensure that every power demand is served within its deadline. For pricing design problems, [33] studies the cost minimization problem for energy provider. One algorithm for day-ahead pricing and another for estimating and refining user reaction to the prices are proposed. Dynamic programming approach is applied to solve those algorithms. In [34], an optimal real-time pricing algorithm is proposed to fairly and efficiently assign energy to each user from the aggregate utility. Convex programming techniques are applied to solve this problem.

Load scheduling has been also studied at consumer side to reduce electricity bill in response to dynamic pricing [35–40]. In [35, 36], the authors study the energy consumption scheduling problems in order to minimize the electricity cost and maximize the quality of service for appliance in household. Their problems are solved by linear-based algorithms to reduce the computation complexity. [37] considers a load scheduling problem across multiple homes in a neighborhood to deal with the issue of rebound peak. The problem is formulated and solved by dynamic programming technique. [38] considers the power consumption scheduling problem with future price uncertainty. The problem is formulated as a Markov decision process, and a threshold-based solution is obtained. [39] studies a problem of minimizing the total cost of electricity on a daily scale for home through load scheduling with total power

constraint. The proposed scheme shows a reduced peak demand for the home is achieved. A real-time opportunistic scheduling scheme based on the optimal stopping rule for smart appliances is proposed in [40]. The problem is to determine the optimal time for appliances' operation in order to reduce electricity cost.

Combining both utility side and demand side management is also considered in [41–43]. Game theory has been well applied to design the demand side management problems, such as pricing with strategic decision marking involved both the suppliers and the consumers [44]. [41, 42] have studied the distributed energy management problems through game theoretic approach. They formulate the energy consumption scheduling games between the utility operator and electricity consumers. From participating the games, their schemes show that lower costs have been achieved for the utility, and efficient load distribution has been achieved for the consumers. [43] designs a real-time pricing scheme to reduce the peak-to-average load ratio through demand response. With message exchanged between user and retailer, the optimal prices are obtained to help retailer overcome the uncertainty from users' responses, and help users determine their energy usage. The optimal solution is obtained by an iterative method.

2.3 Energy Storage Management with Flexible Loads

Since energy storage management and load scheduling are promising solutions to reduce the energy cost, some literature have focused on the designs of storage management with flexible loads. We have summarized those works as below.

Real-time energy storage management with flexible loads has been considered in [45–50]. In [45], the authors focus on local demand scheduling problem. The objective is to minimize the Micro-grid operation cost and maintain the outage probability of quality of service for electricity. [46] studies the minimization of the total energy cost of multiple residential households in a smart neighborhood. [47] studies the minimization of total operating cost for data centers where the bandwidth cost for geographically distributed data centers is considered. The utility optimal scheduling algorithm is proposed in [48] where the objective is to maximize the aggregate traffic utility with time-varying qualities of communication links. [49] studies the minimization of average energy cost by jointly determining the amount of electricity and natural gas dispatched in each time slot. [50] combines both grid operator and demand side management using distributed storage to minimize the long-term system cost.

In these works, flexible loads are modeled as the amount of total energy request. Thus, no individual task modeling or scheduling is considered. Only worst-case delay is provided. Joint energy storage and task scheduling is considered in [24], in which the electricity price is assumed to be known ahead of time. In [24, 45–50], the Lyapunov optimization technique has been applied to design the real-time control algorithms that only rely on the current system state. They show that their algorithms can significantly reduce the computational complexity and provide bounded performances to the optimal. However, those works only consider the long-term time averaged system cost as their design metric.

2.4 Lyapunov Optimization Technique

Designing real-time control strategies for energy storage management amid system unknown dynamics from renewable, demand, and pricing is particularly challenging. We have applied Lyapunov optimization technique to derive real-time solutions for storage control and load scheduling. An introduction of Lyapunov optimization is given as below.

Lyapunov optimization techniques have a long history in the field of control theory. Thanks to the pioneering works [51, 52] by Tassiulas and Ephremides, this technique was first used to design stable routing and scheduling policies for queueing networks. Those algorithms only require the knowledge of the current network state. No statistic information is needed. Later, this form of technique has been introduced for the analysis and control of stochastic networks by Michael J. Neely in [25] in which he focuses on the application to communication and network delay. Today, this technique is applicable to stochastic systems that arise in smart grid communications, where the problems can be formulated to optimize the time average of certain quantities subject with time average constraints on other quantities.

Consider a stochastic problem that operates in discrete time slots with $t \in \{0, 1, 2, \cdots\}$. Define attribute vectors $\mathbf{x}(t), \mathbf{y}(t), \mathbf{e}(t)$ as

$$\mathbf{x}(t) = (x_1(t), \ldots, x_M(t))$$

$$\mathbf{y}(t) = (y_0(t), y_1(t), \ldots, y_L(t))$$

$$\mathbf{e}(t) = (e_1(t), \ldots, \mathbf{e}_J(t))$$

where M, L, J are non-negative integers. Those attributes can be positive or negative,

and their general functions are given as

$$x_m(t) = \hat{x}_m(\alpha(t), \omega(t)) \ \forall m \in \{1, \ldots, M\}$$

$$y_l(t) = \hat{y}_l(\alpha(t), \omega(t)) \ \forall l \in \{0, 1, \ldots, L\}$$

$$e_j(t) = \hat{e}_j(\alpha(t), \omega(t)) \ \forall j \in \{1, \ldots, J\}$$

where $\omega(t)$ is a random event observed on time slot t and $\alpha(t)$ is the control action taken on time slot t. The action $\alpha(t)$ is chosen within a set $\mathcal{A}_{\omega(t)}$, *i.e.,* $\alpha(t) \in \mathcal{A}_{\omega(t)}$.

Denote $\overline{x}_m$ as the time average function of $x_m(t)$, given by

$$\overline{x}_m \triangleq \lim_{t\to\infty} \frac{1}{t} \sum_{\tau=0}^{t-1} x_m(\tau).$$

Similarly, denote $\overline{y}_l, \overline{e}_j$ as the time average functions of $y_l(t), e_j(t)$, respectively.

Define the real queues in the system with a backlog vector $\mathbf{Q}(t) = (Q_1(t), \ldots, Q_K(t))$. The dynamics is given by:

$$Q_k(t+1) = \max[Q_k(t) - b_k(t), 0] + a_k(t) \tag{2.1}$$

where $a_k(t) = \hat{a}_k(\alpha(t), \omega(t))$ and $b_k(t) = \hat{b}_k(\alpha(t), \omega(t))$.

The objective is to design an algorithm that solves the following problem

$$\textbf{Minimize}: \lim_{t\to\infty} \overline{y_0} \tag{2.2}$$

$$\text{s.t} \quad \lim_{t\to\infty} \overline{y_l} \leq 0 \quad \text{for all } l \in \{1, \ldots, L\} \tag{2.3}$$

$$\lim_{t\to\infty} \overline{e_j} = 0 \quad \text{for all } j \in \{1, \ldots, J\} \tag{2.4}$$

$$\alpha(t) \in \mathcal{A}_{\omega(t)} \quad \forall t \tag{2.5}$$

$$\text{Stability of all Network Queues.} \tag{2.6}$$

A solution is an algorithm that determines control actions $\{\alpha(t)\}$ over time to minimize the objective value of (2.2), while satisfying all constraints. For this type of stochastic problem, queueing theory plays a central role. To solve the problem, we first transform all inequality and equality constraints (2.3)-(2.5) into queue stability problems. Virtual queues are introduced to ensure the required time average constraints being satisfied, and ensure the stability of all queues. Define the dynamics of virtual queues $Z_l(t)$ and $H_j(t)$ for each $l \in \{1, \ldots, L\}$ and $j \in \{1, \ldots, L\}$ as:

$$Z_l(t+1) = \max[Z_l(t) + y_l(t), 0] \tag{2.7}$$

$$H_j(t+1) = H_j(t) + e_j(t) \tag{2.8}$$

where the virtual queue $Z_l(t)$ is to ensure constraint $\overline{y_l} \leq 0$ being satisfied, and the virtual queue $H_j(t)$ is designed to turn the time average equality constraint $\overline{e_j} = 0$ into a pure queue stability problem.

Next, the problem (2.2)-(2.6) is solved by a theory of Lyapunov drift and Lyapunov optimization. Let $\mathbf{\Theta}(t) \triangleq [\mathbf{Q}(t), \mathbf{Z}(t), \mathbf{H}(t)]$ be a vector of all actual and virtual queues, with the dynamics (2.1), (2.7) and (2.8), respectively. Define $L(\mathbf{\Theta}(t))$ as the Lyapunov function, given by

$$L(\mathbf{\Theta}(t)) \triangleq \frac{1}{2}\sum_{k=1}^{K} Q_k(t)^2 + \frac{1}{2}\sum_{l=1}^{L} Z_l(t)^2 + \frac{1}{2}\sum_{j=1}^{J} H_j(t)^2. \tag{2.9}$$

Define $\Delta(\mathbf{\Theta}(t)) = L(\mathbf{\Theta}(t+1)) - L(\mathbf{\Theta}(t))$ as the difference of Lyapunov function from one slot to the next. The objective function (2.2) is mapped to a penalty function. Instead of minimizing the existing problem, Lyapunov optimization is to greedily minimize the drift-plus-penalty function. Thus, the algorithm does not require knowledge

of the probabilities associated with the random events $\omega(t)$. This drift-plus-penalty problem is given as below

$$\Delta(\mathbf{\Theta}(t)) + V \cdot y_0(t) \tag{2.10}$$

where V is a non-negative weighted control parameter. It is easy to see that setting $V = 0$ leads our drift-plus-penalty to the drift alone problem, while $V > 0$ offers a tradeoff between backlog reduction and penalty minimization. In term of the performance bound, the time average objective value of (2.2) obtained by the drift-plus-penalty optimization is deviated by at most $O(1/V)$ from optimality.

2.5 Highlights of Contributions

In this dissertation, we design real-time energy storage management and load scheduling problems through Lyapunov optimization. Now, we highlight our contributions as follows.

We are the first to design the energy storage management in a finite horizon approach. All existing works only consider long-term time average cost as their design metric [16, 17, 21–23, 45–50]. In reality, the energy consumer may prefer the cost saving solution within a fixed period of time. We actually provide a solution suitable to such a requirement. Moreover, the existing works have to assume the renewable generation, demands (loads), and pricing information to be stationary processes. In our finite horizon approach, our problems are designed to handle the non-stationary system dynamics. This is meaningful when the problem is implemented in reality (for example, renewable energy from solar is naturally a non-stationary process). Since

Lyapunov optimization framework [25] is developed based on the infinite time horizon problem, solving finite time horizon problem is quite different. For this reason, we need to develop new techniques to overcome unique challenges, and thus employ Lyapunov optimization to design our real-time algorithms that otherwise is not directly applicable.

Specifically, for real-time energy storage management designs, the existing works either do not consider the renewable generation as one of the power sources in system [21], or battery operation cost [22,23]. We have added the renewable into the system in order to harvest the green energy, and actively modeled the detailed battery operation cost due to the charging (discharging) activities. Although both renewable generation and battery operation cost are modeled [16, 17], they only consider long-term time average cost as their design metric.

For the designs of energy storage management with flexible loads, [45–50] have modeled the flexible loads as the amount of total energy request. Thus, no individual task modeling or scheduling is considered. Only worst-case delay is provided. In our works, we have considered both individual and overall delay constraints, and provide the scheduling scheme for each task (load). A joint energy storage and task scheduling is considered in [24], while the electricity price is assumed to be known ahead of time. In our joint design, we do not require any statistic information. In the proposed real-time algorithm, we show that the joint problem has been separated, and the storage control and delay scheduling have been decoupled and sequentially determined.

Chapter 3

Real-Time Energy Storage Management with Renewable Integration: Infinite Time Approach

In this chapter, we consider the design of cost-effective management of energy storage with renewable integration by designing real-time control policy to minimize the long-term time-averaged cost. We take into account the system dynamics, and incorporate the batter operation cost for energy storage into the control optimization. Applying Lyapunov optimization technique, we design an on-line control policy that jointly optimizes the decisions for storage from two energy sources and supply to the consumer, which has bounded performance from the optimal scheme. We provide a close-form solution to our control optimization which renders our policy implementation with minimum complexity. Simulations show that introducing renewable energy can effectively reduce the long-term cost and improve the efficiency of energy storage relative to the battery operation cost. Last, we extend the basic model to a centralized model. Case studies show that users can further reduce their total cost in the centralized model.

3.1 System Model

Consider an energy storage and management system as shown in Fig. 3.1. A power consuming entity (user) can draw electricity from the power sources and/or the energy storage unit (battery) to supply its energy demand, which is denoted as W_t. Two types of power sources are considered: the conventional grid and the renewable generator. The battery is used to store energy from both power sources and to supply energy to the user[1]. We assume the system operates in discrete time slots with $t \in \{1, 2, \cdots\}$, and all operations are performed per time slot t. Details of each component are described below.

3.1.1 Power Sources

Conventional Grid: Power can be purchased at a real-time price P_t from the power grid using conventional generators. Let E_t denote the amount of energy purchased per slot. It is bounded by

$$E_t \in [0, E_{\max}] \tag{3.1}$$

where $E_{\max}$ is the maximum amount of energy can be purchased from the grid per slot. The purchased amount E_t can supply the user's demand directly and/or be stored into the battery for future use. The unit price P_t is assumed to be in a price interval $P_t \in [P_{\min}, P_{\max}]$, where $P_{\min}$ and $P_{\max}$ are the minimum and maximum electricity prices at slot t. The value of P_t is assumed known to the user and remains unchanged during time slot t. Thus, the energy purchasing cost from the grid at time slot t is

[1]Fig. 3.1 is only for illustration purpose. In practice, DC/AC converters are applied for charging/discharging to/from the battery.

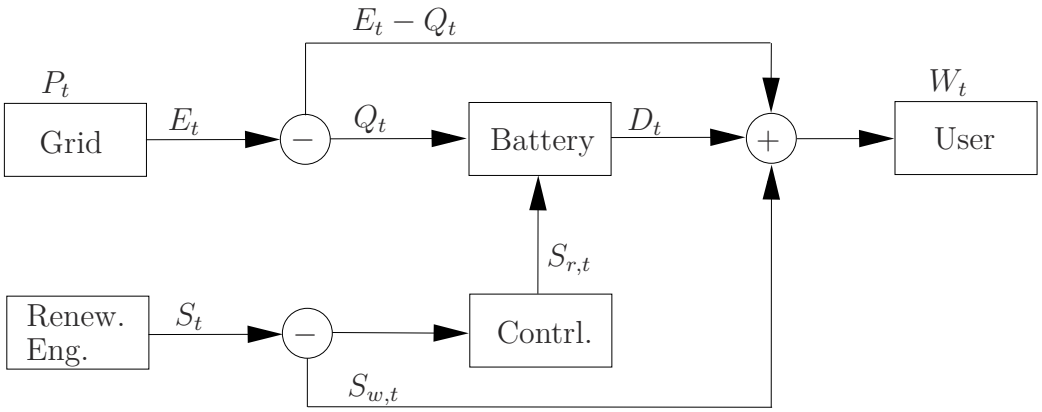

Figure 3.1: An example of energy storage and management system.

$E_t P_t$.

Renewable Generator: Assume that the priority of using S_t is to first directly supply the demand W_t. We denote this portion by $S_{w,t}$. It is given by $S_{w,t} = \min\{W_t, S_t\}$. The remaining portion of harvested energy, if any, can be stored into the battery. As we will see later, charging incurs certain cost to the battery. Thus, a controller will make a decision on whether or not to store the remaining amount into the battery. Let $S_{r,t}$ denote the amount of renewable energy stored into the battery at time slot t. We have

$$S_{r,t} \in [0, S_t - S_{w,t}]. \tag{3.2}$$

3.1.2 Battery Operation

1) Storage: We consider a simplified model for the battery charging and discharging, where there is no energy loss during charging/discharging nor leakage of stored energy over time[2]. There may be multiple sources for battery charging at the same time, *e.g.,*

[2]The energy loss during charging/discharging can be modeled as the battery efficiency level $\eta_e \in [0\%, 100\%]$. Since this parameter does not affect our fundamental problem structure and solutions, we ignore this effect and only focus on the main charging and discharging activities.

from either the grid, the renewable source, or both. Let Q_t denote the portion of E_t stored into the battery. The total amount of energy charged into battery at time slot t, *i.e.,* $Q_t + S_{r,t}$, is upper bounded by

$$Q_t + S_{r,t} \in [0, R_{\max}] \tag{3.3}$$

where $R_{\max}$ is the maximum charging amount allowed to the battery. Similarly, the discharging amount, denoted as D_t, is upper bounded by

$$D_t \in [0, D_{\max}] \tag{3.4}$$

where $D_{\max}$ denotes the maximum discharged amount allowed from the battery. We assume there is no simultaneous charging and discharging activities in the battery. This means

$$(Q_t + S_{r,t}) \cdot D_t = 0. \tag{3.5}$$

Let B_t denote the state of battery (SOB) at time slot t. For a battery with a finite capacity, the SOB B_t is upper and lower bounded by

$$B_t \in [B_{\min}, B_{\max}] \tag{3.6}$$

where $B_{\min}$ and $B_{\max}$ are the minimum energy required and maximum energy allowed in the battery, respectively; They are battery-specific characteristics and their values depend on the battery type and size. The dynamic of B_t over time due to charging and discharging activities are expressed by

$$B_{t+1} = B_t + Q_t + S_{r,t} - D_t. \tag{3.7}$$

2) Battery cost: We model battery cost as a fixed cost incurred due to each charging or discharging activity. We define two indicator functions to represent charging and discharging activities: $1_{R,t} = \{1 : \text{if } Q_t + S_{r,t} > 0;\ 0 : \text{otherwise}\}$ and $1_{D,t} = \{1 : \text{if } D_t > 0;\ 0 : \text{otherwise}\}$. Denote the cost for charging by C_{rc} and that for discharging by C_{dc}. Denote $x_{e,t}$ as the battery cost at time slot t. It is given by $x_{e,t} \triangleq 1_{R,t}C_{\text{rc}} + 1_{D,t}C_{\text{dc}}$.

3.1.3 Energy Storage Management

The energy storage management system depicted in Fig. 3.1 should satisfy the supply-demand balancing requirement at each time slot t, given by

$$W_t = E_t - Q_t + S_{w,t} + D_t. \tag{3.8}$$

3.2 Energy Management Optimization

In this section, we consider an infinite time approach is proposed, where the power purchase cost from the grid and the battery entry cost are considered. In this approach, we consider the system dynamics of user's demand, renewable source, and pricing. The control objective is to minimize the average system cost over a long-term T_o-slot time period. We first introduce a stand-alone model, where the goal is to minimize the cost for single user. Next, we study a centralized model, where users have shared battery and renewable in the system.

Denote the control actions for the energy storage management system at time slot t by $\mathbf{a}_t \triangleq [E_t, Q_t, D_t, S_{r,t}]$. The goal is to determine $\{\mathbf{a}_t\}$ to minimize the average system cost over a long-term T_o-slot period. This optimization problem is formulated

by

$$\textbf{P1:} \min_{\{\mathbf{a}_t\}} \lim_{T_o \to \infty} \frac{1}{T_o} \sum_{t=0}^{T_o-1} \mathbb{E}\{E_t P_t + x_{e,t}\}$$

$$\text{s.t. } (3.1), (3.2), (3.5), (3.8), \text{ and}$$

$$0 \leq S_{r,t} + Q_t \leq \min\{R_{\max}, B_{\max} - B_t\} \tag{3.9}$$

$$0 \leq D_t \leq \min\{D_{\max}, B_t - B_{\min}\}. \tag{3.10}$$

where $\mathbb{E}\{\cdot\}$ is taken with respect to W_t, S_t, P_t.

Remark: If the distributions of W_t, S_t, P_t are known, it is possible to solve the optimization problem **P1** through Dynamic Programming, of which we have to face the curse of dimensionality in terms of complexity. Instead, we are interested in designing an online control policy that does not rely on the statistics of W_t, S_t, P_t. To do this, we adopt Lyapunov optimization technique [25] to obtain a sub-optimal solution while satisfying all constraints in **P1**. The Lyapunov approach provides a real-time algorithm for control decision $\mathbf{a}_t$ with given system input W_t, S_t, P_t at time slot t. Furthermore, we can bound its performance gap to the optimal solution by a system design parameter.

3.2.1 Real-Time Energy Storage Management Algorithm: Infinite Time Approach

The constraints (3.9) and (3.10) depend on the SOB B_t. Due to the time-coupling dynamics of B_t over time in (3.7), the finite battery capacity imposes a hard constraint on the control actions $\{\mathbf{a}_t\}$, causing them to be correlated over time. We first relax B_t in (3.7) to a long-term time-averaged relation among Q_t, $S_{r,t}$ and D_t. It can be

shown that the following condition holds

$$\lim_{T_o\to\infty}\frac{1}{T_o}\sum_{t=0}^{T_o-1}\mathbb{E}\{Q_t+S_{r,t}-D_t\}=0. \tag{3.11}$$

We relax **P1** to the following problem.

$$\mathbf{P1_r}\ \min_{\{\mathbf{a}_t\}}\ \lim_{T_o\to\infty}\frac{1}{T_o}\sum_{t=0}^{T_o-1}\mathbb{E}\{E_tP_t+x_{e,t}\}$$
$$\text{s.t}\ \ (3.1)-(3.5),(3.8),(3.11).$$

By this relaxation, we remove the dependency of per-slot charging/discharging amount on B_t in constraints (3.9) and (3.10), and replace them by (3.3) and (3.4), respectively. Since the constraints are now relaxed, solving $\mathbf{P1_r}$ may not give a feasible solution to **P1**.

3.2.2 Lyapunov Function and Drift

Define Z_t as a virtual queue

$$Z_t \triangleq B_t - VP_{max} - D_{max} - B_{min} \tag{3.12}$$

where $V>0$ is a constant to be explained later. Note that Z_t is only a shifted version of B_t and can be negative. Due to (3.7), the dynamic of Z_t is given by

$$Z_{t+1} = Z_t + Q_t + S_{r,t} - D_t. \tag{3.13}$$

Define the Lyapunov function for Z_t as $L(Z_t)\triangleq\frac{Z_t^2}{2}$, and the conditional Lyapunov drift [25] for Z_t at time t as $\Delta Z_t \triangleq \mathbb{E}\{L(Z_{t+1})-L(Z_t)|Z_t\}$. With (3.8), we can show that ΔZ_t is bounded by

$$\Delta Z_t \le G - Z_t\mathbb{E}\{W_t - E_t - S_{w,t} - S_{r,t}|Z_t\} \tag{3.14}$$

where $G\triangleq\frac{\max\{D_{max}^2,R_{max}^2\}}{2}$.

Proof. This upper bound of ΔZ_t in (3.14) has been used to prove Proposition 3.3. Please find detail in Appendix 3.5.3. ■

The Lyapunov approach intends to minimize a drift-plus-penalty metric. The drift-plus-penalty is expressed as a weighted sum of the Lyapunov drift and the expected cost, defined as $U_t \triangleq \Delta Z_t + V\mathbb{E}\{E_t P_t + x_{e,t}\}$, where V serves as a weighted factor providing the relative weight between the cost and the drift in the metric. Using the bound above for ΔZ_t, we have the bound on the drift-plus-penalty as

$$U_t \leq G - Z_t\mathbb{E}\{W_t - E_t - S_{w,t} - S_{r,t}|Z_t\} + V\mathbb{E}\{E_t P_t + x_{e,t}\}. \tag{3.15}$$

We design our online control algorithm to minimize the upper bound of the drift-plus-penalty U_t in (3.15), with given system states $\{W_t, S_t, P_t\}$ at time t. The resulting minimization problem is given as

$$\begin{aligned} \mathbf{P2}: \min_{\mathbf{a}_t} \quad & Z_t(E_t + S_{r,t}) + V(E_t P_t + x_{e,t}) \\ \text{s.t} \quad & (3.1) - (3.5), (3.8). \end{aligned} \tag{3.16}$$

We will show later that the solution to **P2** will meet the constraints (3.9) and (3.10) of **P1**.

Now, we solve **P2** to obtain the optimal control solution $\mathbf{a}_t^* = [E_t^*, Q_t^*, D_t^*, S_{r,t}^*]$. Define the idle state of the battery as the state where there is no charging or discharging activity. We denote the control solution under this idle state by $\mathbf{a}_t^{\text{id}} = [E_t^{\text{id}}, Q_t^{\text{id}}, D_t^{\text{id}}, S_{r,t}^{\text{id}}]$. By supply-demand balancing equation (3.8), it is given by $E_t^{\text{id}} = W_t - S_{w,t}$, $Q_t^{\text{id}} = D_t^{\text{id}} = S_{r,t}^{\text{id}} = 0$. Let ξ_t denote the value of the objective in **P2** when battery is in the idle state. In this state, we have $\xi_t = (W_t - S_{w,t})(Z_t + VP_t)$. We

derive $\mathbf{a}_t^*$ in three cases below. In each case, the cost of charging (or discharging) is compared with the cost ξ_t of keeping an idle state, and the control decision is obtained by taking the one with the minimum cost. The solution is summarized below.

Proposition 3.1. *Denote* $\mathbf{a}'_t = [E'_t, Q'_t, D'_t, S'_{r,t}]$. *The optimal control solution* $\mathbf{a}_t^*$ *of* $\mathbf{P4_b}$ *is given by*

1) For $Z_t + VP_t \leq 0$*: The battery is in either charging or idle state. The solution* $\mathbf{a}'_t$ *in charging state is give by*

$$\begin{cases} D'_t = 0, \\ S'_{r,t} = \min\{S_t - S_{w,t}, R_{\max}\} \\ Q'_t = \min\{R_{\max} - S'_{r,t}, E_{\max} - W_t + S_{w,t}\} \\ E'_t = \min\{W_t + R_{\max} - S_{w,t} - S'_{r,t}, E_{\max}\}. \end{cases} \tag{3.17}$$

If $E'_t(Z_t + VP_t) + Z_t S'_{r,t} + VC_{rc}1_{R,t} < \xi_t$, *then* $\mathbf{a}_t^* = \mathbf{a}'_t$*; Otherwise,* $\mathbf{a}_t^* = \mathbf{a}_t^{id}$.

2) For $Z_t < 0 \leq Z_t + VP_t$*: The battery is either in charging, discharging, or idle state. The solution* $\mathbf{a}'_t$ *in charging or discharging state is give by*

$$\begin{cases} D'_t = \min\{W_t - S_{w,t}, D_{\max}\} \\ S'_{r,t} = \min\{S_t - S_{w,t}, R_{\max}\} \\ Q'_t = 0, \\ E'_t = [W_t - S_{w,t} - D_{\max}]^+. \end{cases} \tag{3.18}$$

If $E'_t(Z_t + VP_t) + Z_t S'_{r,t} + V(C_{rc}1_{R,t} + C_{dc}1_{D,t}) < \xi_t$, *then* $\mathbf{a}_t^* = \mathbf{a}'_t$*; Otherwise,* $\mathbf{a}_t^* = \mathbf{a}_t^{id}$.

3) For $0 \leq Z_t < Z_t + VP_t$*: The batter is in either discharging or idle state. The solution* $\mathbf{a}'_t$ *in discharging state is give by*

$$\begin{cases} D'_t = \min\{W_t - S_{w,t}, D_{\max}\} \\ S'_{r,t} = Q'_t = 0, \\ E'_t = [W_t - S_{w,t} - D_{\max}]^+. \end{cases} \tag{3.19}$$

If $E'_t(Z_t + VP_t) + VC_{dc}1_{D,t} < \xi_t$, *then* $\mathbf{a}_t^* = \mathbf{a}'_t$*; Otherwise,* $\mathbf{a}_t^* = \mathbf{a}_t^{id}$.

Proof. See Appendix 3.5.1.

The above solution can be intuitively explained as follows: case 1) corresponds to the state when energy stored in the battery is relatively low, and (3.17) reflects the incentive to recharge the battery, provided that the recharging cost C_{rc} is not high. To the opposite, case 3) indicates the scenario when the energy stored in the battery is high, and there is an incentive to discharge the battery to supply energy if C_{dc} is not high. Case 2) corresponds to the case when the battery is moderately charged, and recharging or discharging is only based on the balance between supply S_t and demand W_t.

3.2.3 Performance of the Real-Time Control Policy

We first show that the real-time control policy developed in Section 3.2.1 meets the constraints of the original problem.

Proposition 3.2. *If set* $A = B_{\min} + VP_{\max} + D_{\max}$ *and* $V \in (0, V_{\max}]$ *with* $V_{\max} = \frac{B_{\max} - D_{\max} - R_{\max} - B_{\min}}{P_{\max}}$, *the optimal control solution* $\mathbf{a}_t^*$ *for* **P2** *is a feasible policy for* **P1**, *i.e., battery finite capacity constraint* (3.6) *is satisfied.*

Proof. See Appendix 3.5.2.

Next, we show that under the i.i.d. assumption of system inputs, the performance of the real-time control policy is bounded from that of the optimal policy as follow.

Proposition 3.3. *Assume i.i.d.* $\{W_t, S_t, P_t\}$ *over time. Under the proposed control solution* $\mathbf{a}_t^*$, *the resulting long-term time averaged cost is bounded from the optimal*

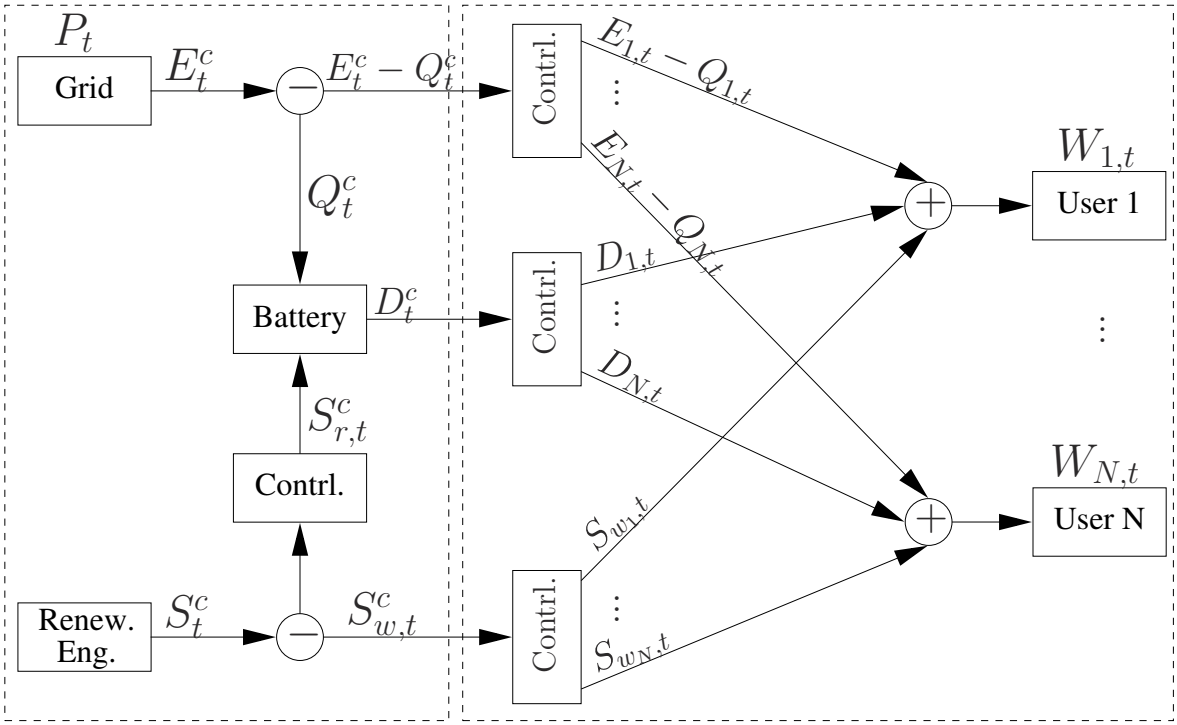

Figure 3.2: An example of energy storage and management in centralized system.

objective value ξ^o *of* **P1** *by*

$$\lim_{T_o\to\infty} \frac{1}{T_o} \sum_{t=0}^{T_o-1} \mathbb{E}\{E_t P_t + x_{e,t}\} \leq \xi^o + \frac{G}{V}. \tag{3.20}$$

Proof. See Appendix 3.5.3.

3.3 Centralized Storage Management System

In our existing model, each user has its own battery, renewable generation and grid. We call it stand-alone model. If we have N users in the grid, users are all independent from each other. Now, we consider an application of our stand-alone model, where multiple users share one battery, renewable generation and grid. As can be seen in Fig. 3.2, the left dotted frame contains the shared power sources and battery. We use superscript $(\cdot)^c$ to distinguish from the stand-alone model. Denote S_t^c as the energy harvested by renewable generation at time t. We assume each user in stand-alone

model will harvest same amount of renewable energy, *i.e.,* $S_{i,t} = S_t$, for $i = 1, 2, \ldots, N$. Thus, we set S_t^c to be N times greater than S_t. We still assume the renewable has the priority to first supply the users' demands, which is given as $S_{w,t}^c = \min\{\sum_{i=1}^N W_{i,t}, S_t^c\}$. We also set the maximum allowed amount of purchase from the grid is N times larger, *i.e.,* $E_t^c \in [0, N \times E_{\max}]$, following the price $P_t \in [P_{\min}, P_{\max}]$. Similarly, the battery charging and discharging are bounded by $Q_t^c + S_{r,t}^c \in [0, N \times R_{\max}]$ and $D_t^c \in [0, N \times D_{\max}]$, respectively.

The objective is to determine the control action $[E_t^c, Q_t^c, D_t^c, S_{r,t}^c]$ to minimize the time average system cost over N users. Compared to the stand-alone problem, it is easy to see that the problem formulation of centralized model is unchanged. As the result, we directly apply the Lyapunov optimization to design our real-time algorithm.

Once we obtain the centralized optimal control action $[E_t^{c*}, Q_t^{c*}, D_t^{c*}, S_{r,t}^{c*}]$, we distribute energy $E_t^{c*} - Q_t^{c*}$, D_t^{c*} and $S_{w,t}^c$ to N users, which are located on the right side of Fig. 3.2. We consider to distribute the energy for users proportional to their demands. This means user i is allocated $\frac{W_{i,t}}{\sum_{i=1}^N W_{i,t}}(E_t^{c*} - Q_t^{c*})$ from grid, $\frac{W_{i,t}}{\sum_{i=1}^N W_{i,t}} D_t^{c*}$ from battery discharging, and $\frac{W_{i,t}}{\sum_{i=1}^N W_{i,t}} S_{w,t}^c$ from the renewable. Thus, we ensure that the supply-demand balance constraint (3.8) for each user is still satisfied.

We have detailed case studies for this centralized model in Section. 3.4.2. From the simulation results, we show that the flexibility among users save more energy cost for the users in centralized model.

3.4 Simulation Results

To realistically set the price P_t, we use the data collected from Ontario Energy Board [53], where P_t consists of three-stage prices and is periodic every 24 hours. Fig. 3.3 shows the value of P_t within the period of 24 hours, where the three-stage prices are given as $P_H = \$0.118$, $P_M = \$0.099$, and $P_L = \$0.063$. We set the time slot duration to be 5 minutes, and approximate the renewable energy S_t and user demand W_t within each slot to be constant. We generate S_t and W_t per slot using uniform distribution within interval $[0.1/12, 2.5/12]$ kWh and $[1/12, 2/12]$ kWh, respectively. Other parameters are chosen as follows: $R_{\max} = 0.165$ kWh, $D_{\max} = 0.165$ kWh, $E_{\max} = 0.3$ kWh, $C_{\rm rc} = C_{\rm dc} = 0.001$, and $V = V_{\max}$.

3.4.1 Stand-Alone Model

First, we look at the effect of renewable energy on the objective value of **P1**. We assume $B_{\max} = 1.5$ kWh, and $B_{\min} = 0$. As shown in Fig. 3.4, the integration of renewable energy offers about 80% off in the total system cost that a user needs to pay in a grid-only system (*i.e.,* the conventional grid is the only energy source). The benefit is mainly contributed by a deduction from the purchasing cost from the grid.

For the same battery capacity, in Fig. 3.5, we study the battery recharging (discharging) activities by plotting the number of recharges (and/or discharges) vs. $C_{\rm rc}$ ($C_{\rm dc}$). We compare the performance of the system with or without renewable energy. As shown, with the renewable energy, higher battery operation cost becomes more tolerable for the system with renewable integration. For example, in a grid-only system, the control decision suggests a few charging (discharging) actions at a cost of $C_{\rm rc}$

$(C_{\text{dc}}) = 0.001, 0.003$, while this cost becomes "affordable" when the renewable energy is added, reflected by the positive number of recharges (discharges). In general, the total number of charges and discharges decreases as the cost C_{rc} (or C_{dc}) increases. Thus, the battery charging (discharging) cost directly affect the battery participation, and thus the effectiveness of the energy management system.

In Fig. 3.6, we show how the battery capacity affects the relative proportions of purchased power from grid into the battery at different prices. We plot the total amount of purchased energy at a specific price that is charged into the battery, $E_Q(P_i) \triangleq \sum_{t\in\{t:P_t=P_i\}} Q_t^*$, for $P_i = P_L, P_M, P_H$. Intuitively, as the capacity increases, the optimal decision will let the battery buy energy from the gird only if P_t is low. For our control policy, as $B_{\max}$ increases, V increases, and the performance approaches to the optimal as indicated in (3.20). This result is verified on Fig. 3.6. We see that as $B_{\max}$ increases, most energy purchased from the grid is at $P_i = P_L$.

Last, we look at the relation between V value and the objective value of **P1**. Two approaches can be used to determine the V value. To satisfy the battery capacity constraint (3.6), our algorithm has been designed to set $V \leq V_{\max}$. The resulting bound of V tightens the distance to the optimal by $\frac{G}{V_{\max}}$, which is given in (3.20). Another approach is to allow V arbitrarily large, but manually cut off or fill out the energy in the battery in order to satisfy (3.6). Based on the parameters we set, we have $V_{\max} = 9.95$ in the first approach. In the second approach, we increase $V = 20, 30, 40$. As we see in Fig. 3.7, our proposed algorithm with $V \leq V_{\max}$ leaves a distance from the optimal more than that of $V = 20$ in second approach. However, if we further increase $V = 30, 40$, we loss the optimality in second approach. From the objective

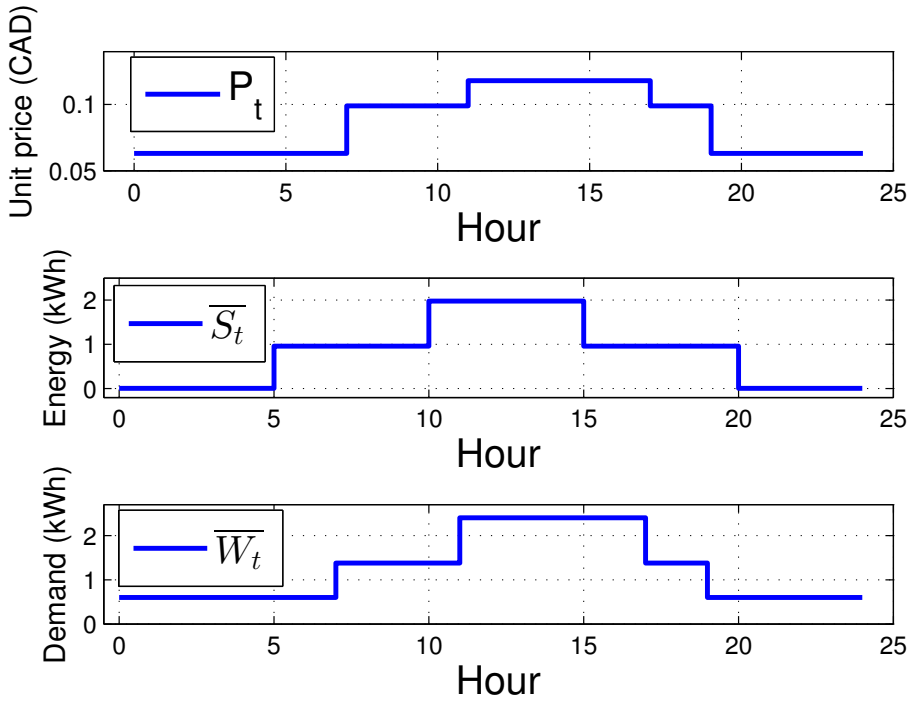

Figure 3.3: Power grid real-time price P_t, average demands $\overline{W_t}$, average solar energy $\overline{S_t}$

of **P2**, we see that a larger V value adds more weight on $E_t P_t$ in the objective, and thus, the drift is less important. As the result, the proposed algorithm will become one-slot greedy search algorithm of **P1**, *i.e.,* minimize the per slot objective of **P1**.

3.4.2 Centralized Model vs. Stand-Alone Model: Case Study

In the centralized system, the users share single battery. We believe that users can further reduce their cost by the flexibility and diversity offered in this model. We set up the total number of users $N = 64$. For the renewable energy, we assume each user will harvest same amount of energy S_t. Thus, we have $S_t^c = NS_t$. For battery, we assume the battery capacity is $NB_{\max}$. Also, this large battery will be associated

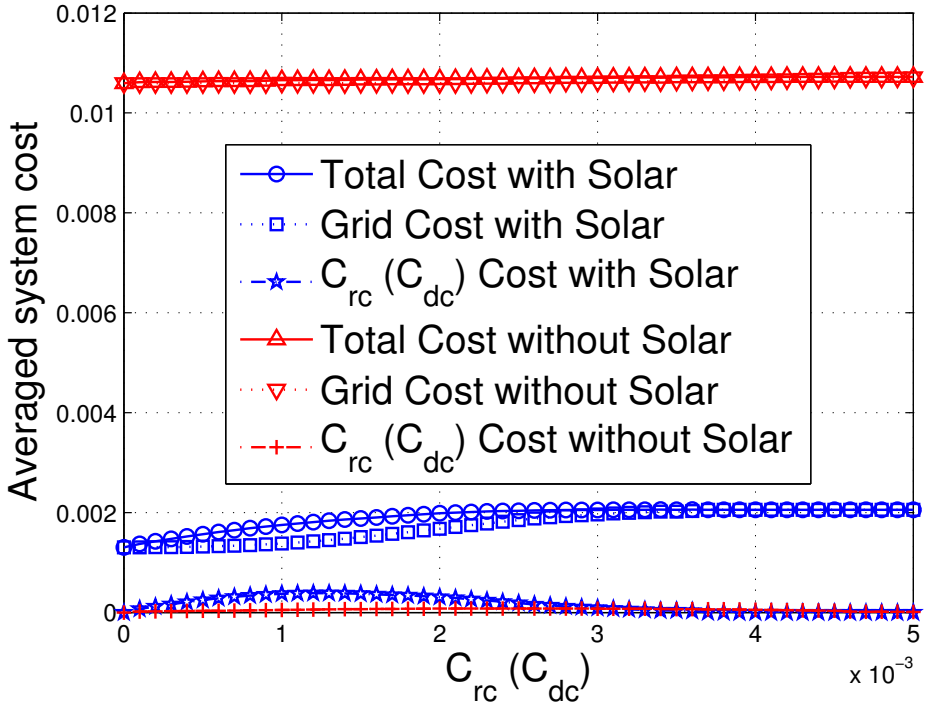

Figure 3.4: Long-term system cost vs. $C_{\rm rc}$ ($C_{\rm dc}$)

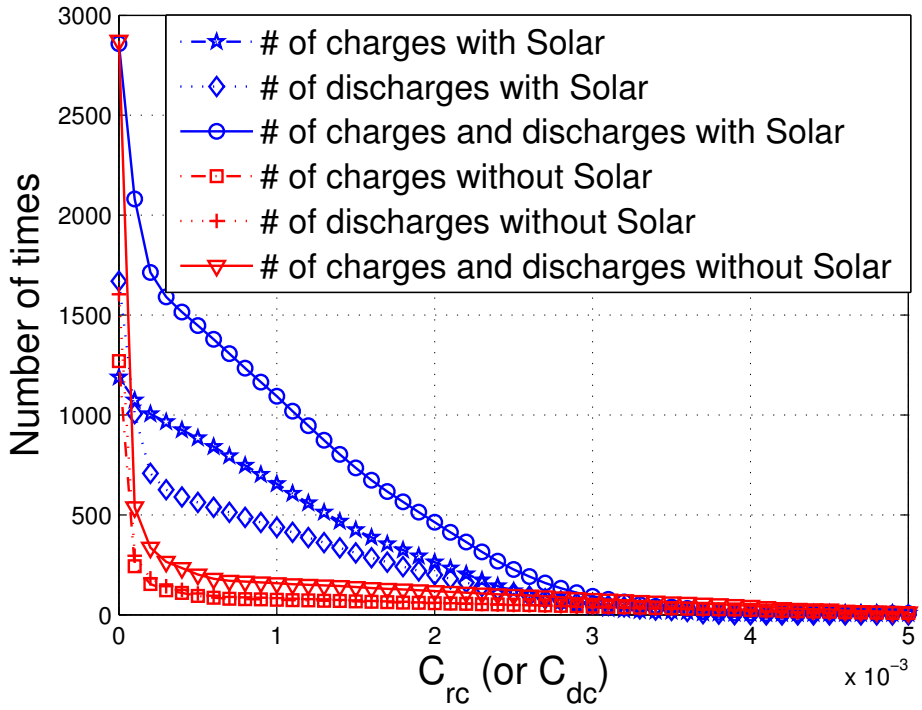

Figure 3.5: Number of charges (discharges) vs. $C_{\rm rc}$ ($C_{\rm dc}$)

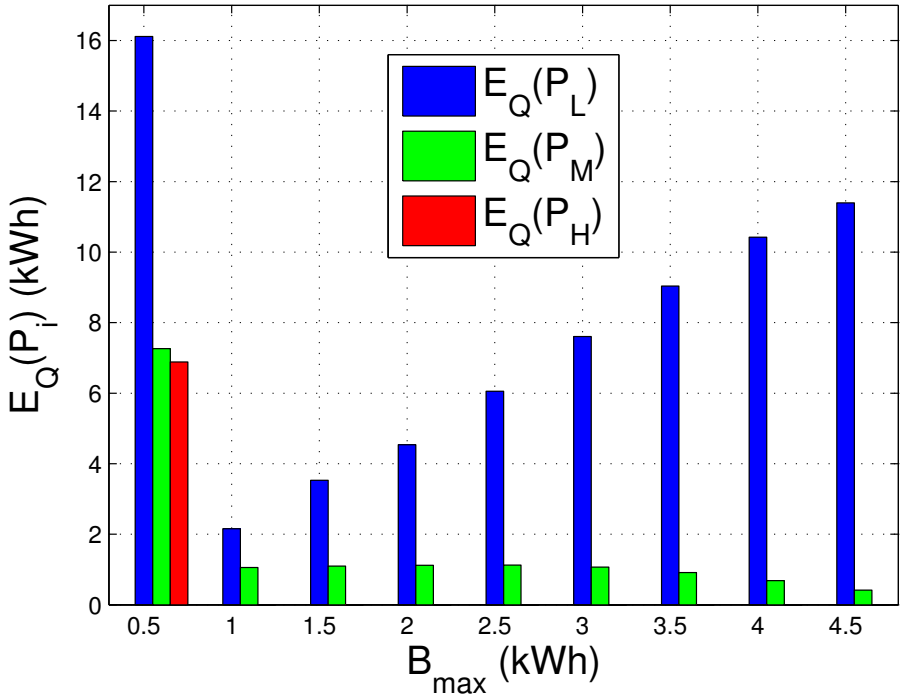

Figure 3.6: Proportion of total stored energy purchased from the grid at different price $E_Q(P_i)$ vs. battery capacity

with higher operation costs, *i.e.*, $C^c_{\rm rc} = NC_{\rm rc}$. Again, we set $C^c_{\rm rc} = C^c_{\rm dc}$.

In the following scenarios, we compare the system objective cost of **P1** obtaining from two different models, given as

$$\rho = \frac{\text{System cost in centralized model}}{\text{Total system cost over N users in stand-alone model}} \tag{3.21}$$

Scenario 1: In this scenario, we assume the renewable generation can harvest more energy. We set that S_t is uniformly generated with interval $\eta_1 \cdot [0.1/12, 2.5/12]$ kWh where $\eta_1 \in [0.8, 2]$. We set $W_{i,t}$ as uniform distribution with interval $[1/12, 3.6/12]$ kWh.

Scenario 2: In this scenario, the users' demands are more away from the mean value. We assume that $\{W_{i,t}\}_{i=1}^N$ are generated by Gaussian distribution with different values of variance $W_{i,t} \sim \mathcal{N}(\overline{W_t}, \eta_2 \cdot \overline{W_t})$ where $\eta_2 \in [0, 1]$ and $\overline{W_t} = 1.8/12$ kWh. The

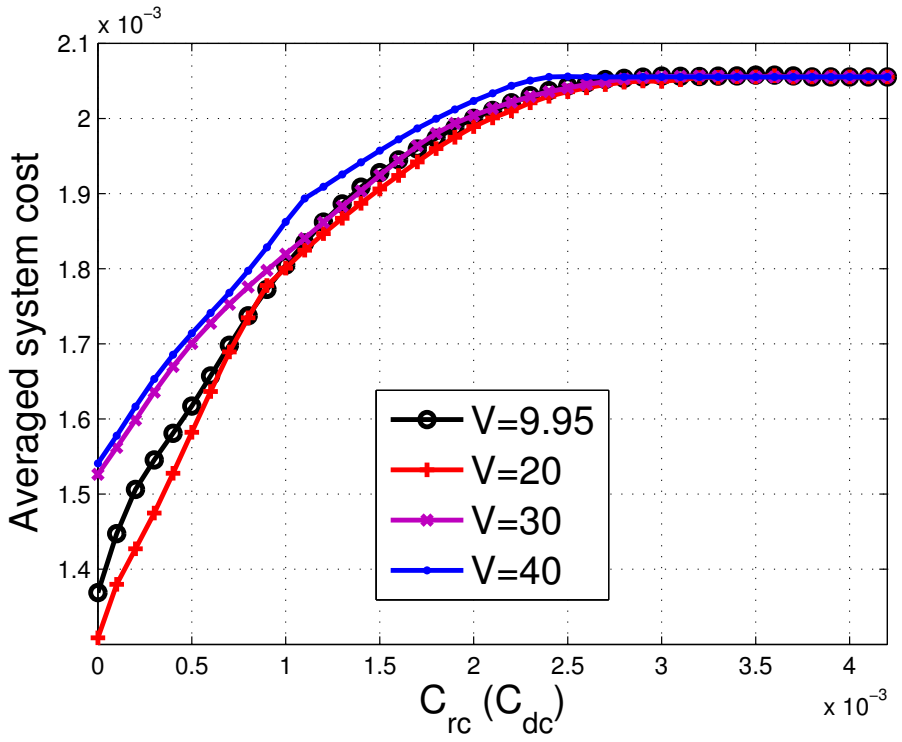

Figure 3.7: Long-term time-averaged cost vs. $C_{\rm rc}$ ($C_{\rm dc}$) at different V values ($B_{\max} = 1.5$ kWh)

renewable energy S_t is uniformly distributed with interval $[0.2/12, 5/12]$ kWh.

Scenario 3: In this scenario, the users' demands are correlated each other. Using correlation factor $\eta_3 \in [0, 1]$, we set the demands as follow

$$W_{i,t} = \eta_3 W_{f,t} + \sqrt{1-\eta_3^2} U_{i,t} + \overline{W_t} \tag{3.22}$$

where $W_{f,t} \sim \mathcal{N}(0, 0.8\overline{W_t})$ is a reference process and $U_{i,t} \sim \mathcal{N}(0, 0.8\overline{W_t})$. We set $\overline{W_t} = 1.8/12$ kWh and the renewable energy S_t is uniformly distributed with interval $[0.2/12, 5/12]$ kWh.

In scenario 1, we look at how the renewable energy achieves further cost reduction in centralized system. As can be seen in Fig. 3.8, in the range of $\eta_1 \in [0.8, 1.5]$, the users only achieve 5% cost reduction. However, with $\eta_1 > 1.5$, we see a significant

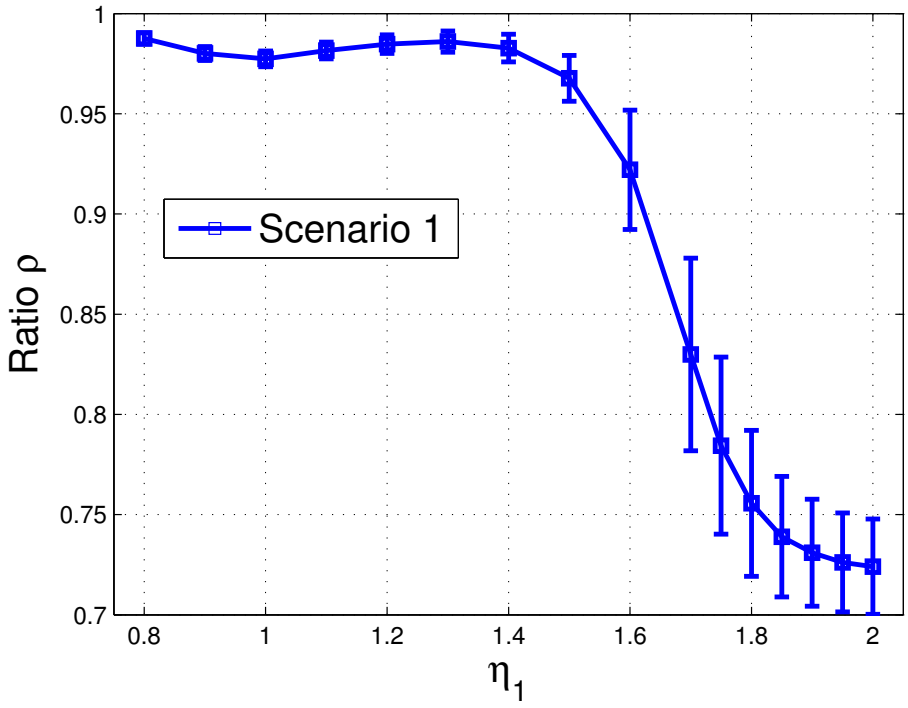

Figure 3.8: Ratio ρ vs. solar integration scaler η_1 in Scenario 1

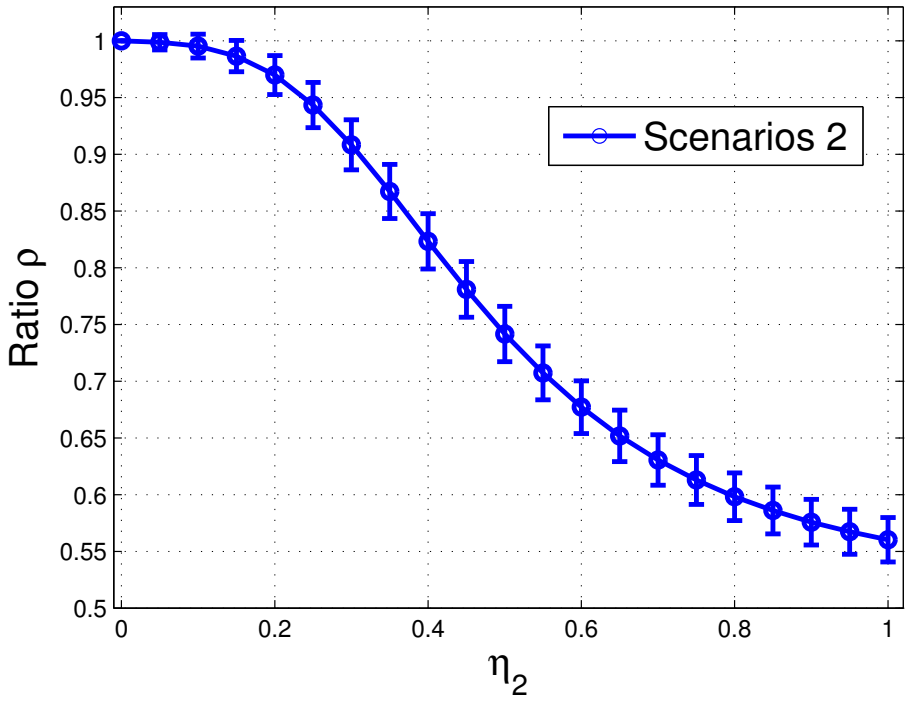

Figure 3.9: Ratio ρ vs. η_2 (scaled variance) in Scenario 2

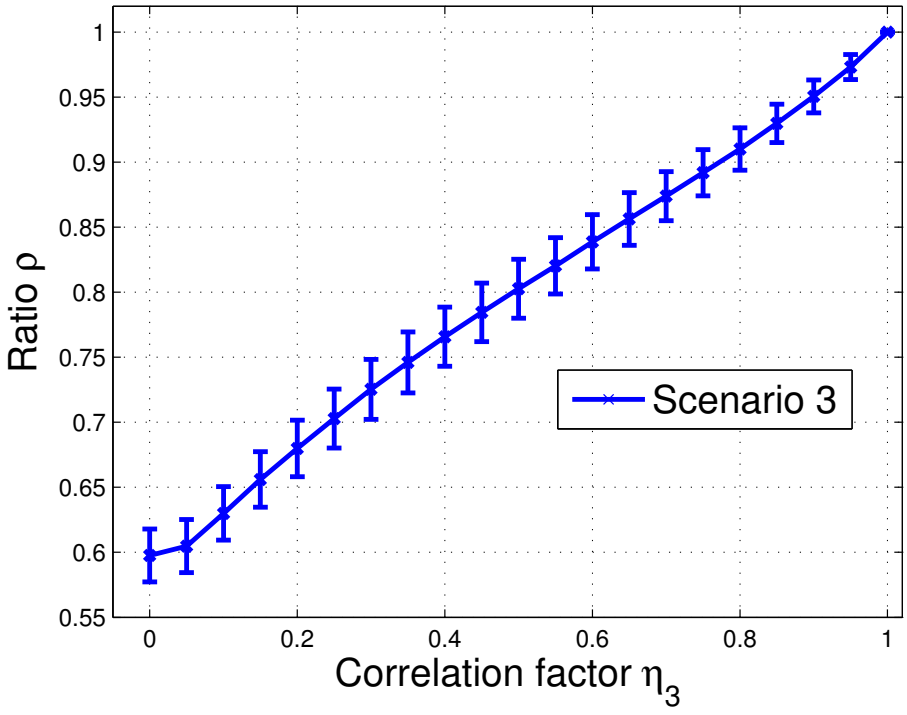

Figure 3.10: Ratio ρ vs. correlated factor η_3 in Scenario 3

reduction which is up to 30%. This is because the shared battery can store more energy from the renewable generation, which reduces the purchasing cost from the conventional grid.

In scenario 2, we diverse the users' demands by varying the standard deviation of $W_{i,t}$ with $\eta_2 \in [0, 1]$. Fig. 3.9 shows that, with the users' demands lie more than a few variances away from the mean, which realizes more diversity among the users, the system cost is reduced up to 45% over the stand-alone model. In scenario 3, we generate $\{W_{i,t}\}_{i=1}^{N}$ correlated each other. From Fig. 3.10, we know that, if the users' demands are less correlated, *i.e.*, $\eta_3 < 1$, we observe cost-saving up to 40% in the centralized system.

Next, we consider an extreme scenario by setting a new price P'_H which is 10

Table 3.1: Ratio ρ vs. $B_{\max}$ and $C_{\rm rc}$ (or $C_{\rm dc}$) with $P'_H = 10P_H$ and i.i.d W_t, S_t

$B_{\max}$ \ $C_{\rm rc}$ (or $C_{\rm dc}$)	0.001	0.005	0.01
3	0.98	0.95	0.95
4	0.95	0.91	0.92
5	0.83	0.83	0.86
6	0.77	0.78	0.82
10	0.76	0.77	0.81

Table 3.2: Ratio ρ vs. $B_{\max}$ and $C_{\rm rc}$ (or $C_{\rm dc}$) with $P'_H = 10P_H$ and non-stationary W_t, S_t

$B_{\max}$ \ $C_{\rm rc}$ (or $C_{\rm dc}$)	0.001	0.005	0.01
3	0.89	0.90	0.91
4	0.75	0.81	0.86
5	0.64	0.71	0.78
6	0.63	0.69	0.75
10	0.62	0.69	0.74

Table 3.3: Ratio ρ vs. $B_{\max}$ and $C_{\rm rc}$ (or $C_{\rm dc}$) with non-stationary W_t and boosted non-stationary S_t

$B_{\max}$ \ $C_{\rm rc}$ (or $C_{\rm dc}$)	0.001	0.005	0.01
3	0.73	0.81	0.79
4	0.73	0.81	0.79
5	0.73	0.81	0.79
6	0.73	0.81	0.79
10	0.72	0.81	0.79

times expensive than usual *i.e.,* $P'_H = 10P_H = \$1.18$. If users still purchase energy when $P_t = P_H$, they pay much more than before.

In Table 3.1, W_t and S_t are uniformly distributed within the intervals $[1/12, 3.6/12]$ kWh

and $[0.2/12, 5/12]$ kWh, respectively. When the battery capacity is limited and operation cost is high, there is no additional cost saving in the centralized system. However, we observe up to 24% in cost reduction when the capacity is large and the operation cost is cheap. As the reference, we can only obtain 12% if set P_H back to usual (not shown in table). A larger capacity can effectively reduce the cost in the centralized system. It could buy more energy when the price is low.

Next, we assume the demand $W_{i,t}$ is a non-stationary process, where the three-stage means energy $E[W_{i,t}]$ is given as $\{\overline{W}_H, \overline{W}_M, \overline{W}_L\} = \{2.4, 1.38, 0.6\}/12$ kWh with $\sigma_{W_i} = 0.5\overline{W}_i$, $i = H, M, L$, as shown in Fig. 3.3 middle. Similarly, the renewable energy S_t follows three-stage mean value $E[S_t]$ with $\{\overline{S}_H, \overline{S}_M, \overline{S}_L\} = \{1.98, 0.96, 0.005\}/12$ kWh and standard deviation $\sigma_{S_i} = 0.5\overline{S}_i$, $i = H, M, L$, as shown in Fig. 3.3 bottom. The ratio ρ with non-stationary processes is shown in Table 3.2. As can be seen, we reduce the cost by at most 38% at $B_{\max} = 10$ kWh.

Another scheme is to increase S_t as $\{\overline{S}_H, \overline{S}_M, \overline{S}_L\} = 10\{1.98, 0.96, 0.005\}/12$ kWh. With more energy coming from the renewable generation, remaining energy can be used to charge to the battery, and supply the demands when the price is high. We achieve up to 28% saving in the centralized system, which is shown in Table 3.3.

3.5 Appendices

3.5.1 Proof of Proposition 3.1

Proof. We show the solution in each case below.

1) For $Z_t + VP_t \leq 0$: Since V and P_t are both positive, we have $Z_t \leq 0$. To minimize the objective of **P2**, one possible solution is to set both E'_t and $S'_{r,t}$ as large

as possible. This means that battery is in the charging state. We have $1_{R,t} = 1$, $1_{D,t} = 0$, $D'_t = 0$, and use maximum charging rate, *i.e.,* $S'_{r,t} + Q'_t = R_{\max}$. Since Q'_t is a portion of E'_t, and $Z_t \leq Z_t + VP_t$, maximizing $S'_{r,t}$ in the above equation can further reduce the value of **P2**. By supply-demand balancing equation (3.8), we obtain Q'_t and E'_t in (3.17). Thus, the control solution $\mathbf{a}'_t$ is as in (3.17). Note that under the charging state, the entry cost C_{rc} for charging is paid. Alternatively, we consider the battery in the idle state instead, *i.e.,* $S^{\text{id}}_{r,t} + Q^{\text{id}}_t = 0$. In this case, $1_{R,t} = 0$, but E^{id}_t is smaller. The optimal $\mathbf{a}^*_t$ is then the one that achieves the minimum objective value.

2) For $Z_t < 0 \leq Z_t + VP_t$: Because $Z_t + VP_t \geq 0$, to minimize the objective of **P2**, one possible solution is to set E'_t as small as possible. This means E'_t should be only purchased to supply W_t, and not for storage, *i.e.,* $Q'_t = 0$. When $S_{w,t} = W_t$, it is possible that $S_t - S_{w,t} \geq 0$. In this case, there is no need for discharging, *i.e.,* $D'_t = 0$, and the battery could be charged from renewable source $S'_{r,t} \geq 0$. On the other hand, when $S_{w,t} < W_t$, *i.e.,* S_t is fully used to supply W_t, we have $S'_{r,t} = 0$. To meet the demand in (3.8), we could either purchase E'_t and/or let battery discharge D'_t. Based on the above, we have the control solution $\mathbf{a}'_t$ as shown in (3.18). Charging or discharging will incur entry cost C_{rc} or C_{dc}, respectively. Similar to Case 1), there exists an alternatively way which is to keep the battery idle. Thus, the optimal $\mathbf{a}^*_t$ is chosen from the three possible solutions whichever achieves the minimum objective value.

3) For $0 \leq Z_t < Z_t + VP_t$: One possible solution is to set both E'_t and $S'_{r,t}$ as small as possible to minimize the objective value of $\mathbf{P4}_b$. Thus, the battery should not be charged, *i.e.,* $Q'_t + S'_{r,t} = 0$. To satisfy the rest of demand $W_t - S_{w,t}$, energy should

be discharged from the battery. Following this, we can similarly derive the control solution $\mathbf{a}'_t$ in (3.19). Under this assumption, the entry cost $C_{\rm dc}$ for discharging is paid. Alternatively, we can keep the battery idle and only purchase energy $E_t^{\rm id}$ from the grid. This will result in more $E_t^{\rm id}$ purchased but avoid battery cost $C_{\rm dc}$. The optimal $\mathbf{a}_t^*$ is the one that achieves the minimum objective value. ■

3.5.2 Proof of Proposition 3.2

Proof. To prove Proposition 3.2, we first provide the following Lemma.

Lemma 3.1. *Under the proposed solution in Proposition 3.1, we have*

1) If $Z_t > 0$, then $Q_t^* + S_{r,t}^* = 0$.

2) If $Z_t < -VP_{\max}$, the $D_t^* = 0$.

Proof. 1) This case corresponds to Case 3) of Proposition 3.1. It is straightforward to see that $Q_t^* + S_{r,t}^* = 0$ is the optimal control action. 2) This case corresponds to Case 1) of Proposition 3.1. It is straightforward to see that $D_t^* = 0$ is the optimal control action. ■

We now prove Proposition 3.2. From Lemma 3.1 case 2, we know $D_t^* = 0$ when $Z_t < -VP_{\max}$. If $Z_t \geq -VP_{\max}$, the maximum decreasing amount of Z_t to Z_{t+1} in (3.13) in the next time slot is

$$Z_{t+1} \geq -VP_{\max} - D_{\max}, \ \forall t \tag{3.23}$$

Therefore, Z_t is lower bounded by $-VC_{\max} - D_{\max}$.

Since $Z_t = B_t - A$, we need to design A to satisfy $B_t \geq B_{\min}$ for $\forall t$. We have

$$B_t \geq -VC_{\max} - D_{\max} + A = B_{\min}. \tag{3.24}$$

Thus, we have $A = B_{\min} + VP_{\max} + D_{\max}$.

From Lemma 3.1 case 1, we have $Q_t^* + S_{r,t}^* = 0$ for $Z_t > 0$. If $Z_t \leq 0$, then the maximal increasing amount of Z_t to Z_{t+1} in (3.13) in the next time slot is

$$Z_{t+1} \leq R_{\max}, \ \forall t. \tag{3.25}$$

Therefore, Z_t is upper bounded by $R_{\max}$ for $\forall t$. We can immediately obtain that

$$Z_t = B_t - B_{\min} - VP_{\max} - D_{\max} \leq R_{\max}, \tag{3.26}$$

To ensure B_t in the above equation satisfies $B_t \leq B_{\max}$, we have

$$B_t \leq B_{\min} + VP_{\max} + D_{\max} + R_{\max} \leq B_{\max}. \tag{3.27}$$

We obtain $V \leq V_{\max}$ with $V_{\max}$ below.

$$V_{\max} = \frac{B_{\max} - D_{\max} - R_{\max} - B_{\min}}{P_{\max}}. \qquad \blacksquare$$

3.5.3 Proof of Proposition 3.3

Proof. A one-slot Lyapunov drift can be shown with its upper bound as below

$$\begin{aligned}
\Delta(Z_t) &\triangleq \mathbb{E}\{L(Z_{t+1}) - L(Z_t)|Z_t\} = \frac{1}{2}\mathbb{E}\{Z_{t+1}^2 - Z_t^2|Z_t\} \\
&= Z_t\mathbb{E}\{Q_t + S_{r,t} - D_t|Z_t\} + \frac{\mathbb{E}\{Q_t + S_{r,t} - D_t|Z_t\}^2}{2} \\
&\leq Z_t\mathbb{E}\{Q_t + S_{r,t} - D_t|Z_t\} + G.
\end{aligned} \tag{3.28}$$

Using the upper bound of drift obtained in (3.28), the drift-plus-penalty function is also upper bounded by

$$\Delta(Z_t) + V\mathbb{E}\{E_tP_t|Z_t\} \leq Z_t\mathbb{E}\{Q_t + S_{r,t} - D_t|Z_t\} + V\mathbb{E}\{(E_tP_t + x_{e,t})|Z_t\} + G. \tag{3.29}$$

Since the system inputs $\{W_t, S_t, P_t\}$ are i.i.i over time, we can show that there exists an optimal, stationary, randomized policy [25] that takes control action $\mathbf{a}^{\text{stat}}$ per slot as the function of current system state and independent of battery SOB while satisfying (3.1)-(3.5),(3.7) and providing the following solution

$$\mathbb{E}\{Q_t^{\text{stat}}\} + \mathbb{E}\{S_{r,t}^{\text{stat}}\} = \mathbb{E}\{D_t^{\text{stat}}\} \tag{3.30}$$

$$\mathbb{E}\{(E_t^{\text{stat}} P_t^{\text{stat}} + x_{e,t}^{\text{stat}}) = \xi^{\text{stat}}. \tag{3.31}$$

Substitute (3.30) and (3.31) into (3.29), we obtain

$$\begin{aligned} &Z_t \mathbb{E}\{Q_t^{\text{stat}} + S_{r,t}^{\text{stat}}(t) - D_t^{\text{stat}} | Z_t\} + V\mathbb{E}\{(E_t^{\text{stat}} P_t^{\text{stat}} + x_{e,t}^{\text{stat}}) | Z_t)\} + G \\ &= V\xi^{\text{stat}} + G \leq V\xi^o + G. \end{aligned} \tag{3.32}$$

Summing LHS of (3.29) and RHS of (3.32) over $t \in \{0, 1, 2, \cdots, T_o\}$, we have

$$\mathbb{E}\{\Delta(Z_{T_o}) - \Delta(Z_o)\} + \sum_{t=0}^{T_o-1} V\mathbb{E}\{E_t P_t + x_{emt} | Z_t\} \leq VT_o\xi^o + GT_o. \tag{3.33}$$

Take the expectation with respect to Z_t and apply the law of total expectation, then divide VT_o on both sides of (3.33) with $T_o \to \infty$, we have

$$\lim_{T_o \to \infty} \sum_{t=0}^{T_o-1} V\mathbb{E}\{E_t P_t + x_{e,t}\} \leq \frac{G}{V} + \xi^o. \qquad \blacksquare$$

Chapter 4

Real-Time Energy Storage Management with Renewable Integration: Finite Time Approach

In the previous chapter, we have used the long-term expected system cost over an infinite time horizon as the design metric, while we assume that the system dynamics are stationary processes. In this chapter, based on the existing system model, we take a finite time horizon approach and formulate the control optimization problem aiming to minimize the system cost over a fixed time period. Recognizing the unpredictable and non-stationary stochastic nature of system dynamics, we assume unknown arbitrary dynamics of renewable generation, load, and electricity pricing in formulating our problem. Furthermore, we incorporates detailed battery operation cost into the system cost. Different from the infinite time horizon problem that we have considered in the previous chapter, the coupling of control decisions over time, due to finite battery capacity, is more challenging to manage. We develop a special technique to tackle the technical challenges in solving the problem. Through problem modification and transformation, we are able to apply Lyapunov optimization to design a real-time control algorithm that only relies on the current system dynamics. The proposed con-

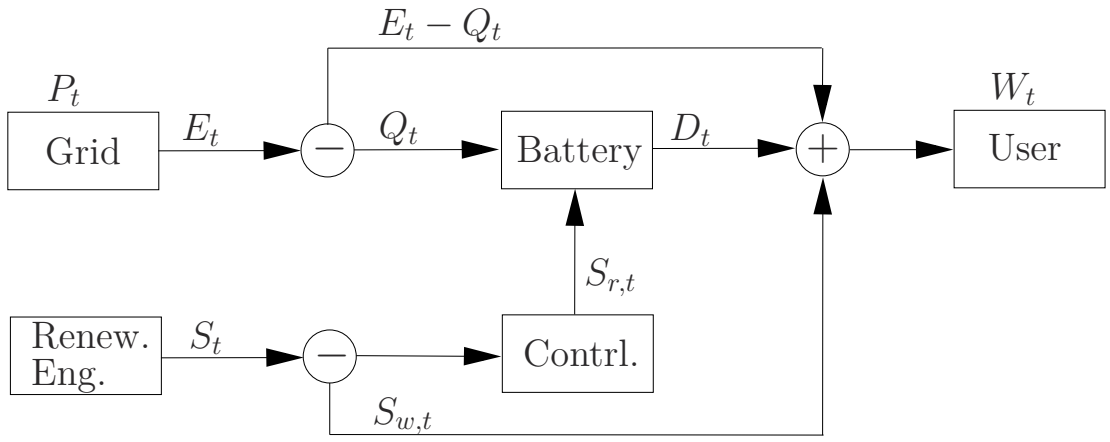

Figure 4.1: An example of energy storage and management system.

trol solution has a closed-form expression and thus is simple to implement. Through analysis, the proposed algorithm is shown to have a bounded performance gap to the optimal non-causal T-slot lookahead control policy. Simulation studies show the effectiveness of our proposed algorithm as compared with two alternative real-time and non-causal algorithms.

4.1 System Model

We consider the energy storage management system as shown in Fig. 4.1. This is the same management system as we have previously introduced in Fig. 3.1.

4.1.1 Power Sources

Conventional Grid: User can purchase amount of E_t from the grid. It is bounded by

$$E_t \in [0, E_{\max}] \tag{4.1}$$

following the real-time price P_t, which is within a range of $P_t \in [P_{\min}, P_{\max}]$.

Renewable Generator: We assume S_t is to first supply the demand W_t. The remaining portion $S_{r,t}$ of harvested energy, if any, can be charged into the battery.

Since the charging incurs certain cost to the battery, a controller will make a decision on whether or not to store the remaining amount into the battery. We have

$$S_{r,t} \in [0, S_t - S_{w,t}]. \tag{4.2}$$

4.1.2 Battery Operation

1) Storage: Battery can be charged from either the grid, the renewable source, or both. The total amount of energy charged into battery at time slot t comes from the grid and the renewable, *i.e.,* $Q_t + S_{r,t}$. The charging amount is upper bounded by

$$Q_t + S_{r,t} \in [0, R_{\max}]. \tag{4.3}$$

The discharging amount D_t is upper bounded by

$$D_t \in [0, D_{\max}]. \tag{4.4}$$

We assume there is no simultaneous charging and discharging activities in the battery. This means

$$(Q_t + S_{r,t}) \cdot D_t = 0. \tag{4.5}$$

For a battery with a finite capacity, the SOB B_t is upper and lower bounded by

$$B_t \in [B_{\min}, B_{\max}]. \tag{4.6}$$

The dynamics of B_t over time due to charging and discharging activities are expressed by

$$B_{t+1} = B_t + Q_t + S_{r,t} - D_t. \tag{4.7}$$

2) Battery degradation cost: It is well known that frequent charging/discharging activities cause a battery to degrade [54]. We model two types of battery degradation cost: *entry cost* and *usage cost*. The entry cost is a fixed cost incurred due to each charging or discharging activity. We define two indicator functions to represent charging and discharging activities: $1_{R,t} = \{1 : \text{if } Q_t + S_{r,t} > 0;\ 0 : \text{otherwise}\}$ and $1_{D,t} = \{1 : \text{if } D_t > 0;\ 0 : \text{otherwise}\}$. Denote the entry cost for charging by C_{rc} and that for discharging by C_{dc}. Denote $x_{e,t}$ as the entry cost for battery usage at time slot t. It is given by $x_{e,t} \triangleq 1_{R,t}C_{\text{rc}} + 1_{D,t}C_{\text{dc}}$.

The battery usage cost is the cost associated with the charging/discharging amount. Let $x_{u,t} \triangleq |Q_t + S_{r,t} - D_t|$ denote the net amount of battery energy level change at time slot t due to charging or discharging. From (4.3) and (4.4), it follows that $x_{u,t}$ is bounded by

$$x_{u,t} \in [0, \max\{R_{\max}, D_{\max}\}]\,. \tag{4.8}$$

We model the usage cost as a function of average net amount of battery energy level change over a period of time, defined as $C(\overline{x})$, where $\overline{x}$ is the average net amount of change.[1] It is known that faster charging/discharging within a fixed period has a more detrimental effect on the life time of the battery. Thus, we assume $C(\cdot)$ is a continuous, convex, non-decreasing function with maximum derivative $C'(\cdot) < \infty$. Such convex cost function has been adopted in literature [34, 46, 55].

[1]In general, the battery usage cost is associated with a charge cycle (charging the battery and then discharging it to the same level is considered a charge cycle). The charge cycle typically lasts for a period of time. To approximate this, we model the associated usage cost function in terms of average amount of energy change in the battery over a time period.

4.1.3 Energy Storage Management

The energy storage management system depicted in Fig. 4.1 should satisfy the supply-demand balancing requirement at each time slot t, given by

$$W_t = E_t - Q_t + S_{w,t} + D_t. \tag{4.9}$$

The goal of the management system is to control the supply and storage to minimize the overall system cost within a given period of operation time (defined in Section 4.2).

Note that power demand, renewable source, and pricing $\{W_t, S_t, P_t\}$ are the random system inputs at time slot t. Their statistical behaviors are often difficult to obtain or predict. For example, for renewable sources such as solar, the dynamics of the generation amount over time is complicated: S_t is correlated over time and furthermore is typically non-stationary. Thus, assuming certain (known) statistics on S_t would not be realistic in practice. The same applies to W_t and P_t. Instead, in this work, we do not make any assumption on the dynamics of these system inputs $\{W_t, S_t, P_t\}$. We intend to design a real-time control algorithm that is able to handle such arbitrary and unknown system inputs.

4.2 Energy Management Optimization: Finite Horizon Approach

Our control objective is to minimize the average system cost within a pre-defined period of time T_o. The system cost includes both power purchasing cost and battery degradation costs. Define the average cost of purchasing energy from the grid over a T_o-slot period by $\overline{J} \triangleq \frac{1}{T_o}\sum_{t=0}^{T_o-1} E_t P_t$. For the battery degradation cost, define the

average entry cost over the T_o-slot period by

$$\overline{x_e} \triangleq \frac{1}{T_o} \sum_{t=0}^{T_o-1} x_{e,t}. \tag{4.10}$$

As described in Section 4.1.2, the battery average usage cost over the T_o-slot period is based on the average net changing amount over the T_o-slot period. Define the average net amount of change over the T_o-slot period by

$$\overline{x_u} \triangleq \frac{1}{T_o} \sum_{t=0}^{T_o-1} x_{u,t}. \tag{4.11}$$

From (4.8), it is straightforward to see that $\overline{x_u}$ is bounded by[2]

$$\overline{x_u} \in [0, \max\{R_{\max}, D_{\max}\}], \tag{4.12}$$

and the battery average usage cost is $C(\overline{x_u})$. Overall, the average battery degradation cost over the T_o-slot period is given by $\overline{x_e} + C(\overline{x_u})$.

Denote the control actions for the energy storage management system at time slot t by $\mathbf{a}_t \triangleq [E_t, Q_t, D_t, S_{r,t}]$. Our goal is to determine $\{\mathbf{a}_t\}$ to minimize the average system cost within the T_o-slot period. This optimization problem is formulated by

$$\begin{aligned} \textbf{P1:} \min_{\{\mathbf{a}_t\}} \ & \overline{J} + \overline{x_e} + C(\overline{x_u}) \\ \text{s.t.} \ & (4.1), (4.2), (4.5), (4.9), (4.12), \text{and} \\ & 0 \le S_{r,t} + Q_t \le \min\{R_{\max}, B_{\max} - B_t\} \qquad (4.13) \\ & 0 \le D_t \le \min\{D_{\max}, B_t - B_{\min}\}. \qquad (4.14) \end{aligned}$$

Remark: The challenges in solving the above optimization problem are two-fold: First, the constraints (4.13) and (4.14) depend on the SOB B_t. Due to the time-coupling dynamics of B_t over time in (4.7), the finite battery capacity imposes a

[2]Note that tighter bounds can be obtained depending on different initial capacity value or total capacity of the battery and the length of T_o.

hard constraint on the control actions $\{\mathbf{a}_t\}$, causing them to be correlated over time. Second, the optimization problem under a finite horizon is much more challenging than those considered under the infinite horizon in the existing works [21, 24, 56]. Specifically, for the infinite horizon where $T_o \to \infty$, it can be shown that the average battery charging amount and discharging amount over long term are equal, *i.e.*, $\lim_{T_o\to\infty} \frac{1}{T_o} \sum_{t=0}^{T_o-1} D_t = \lim_{T_o\to\infty} \frac{1}{T_o} \sum_{t=0}^{T_o-1} (S_{r,t} + Q_t)$. This is a key relation that is relied upon in developing the techniques for designing the real-time control. For the problem with a finite period, however, the above relation no longer holds. New techniques need to be developed for a real-time control solution.

In the following, we first apply a sequence of modification and transformation of **P1**, and then we propose a real-time control algorithm to solve the resulting energy storage management problem and ensure the solution is feasible to the original problem **P1**. Although the resulting real-time solution is suboptimal to **P1**, we show in Section 4.4 that our proposed algorithm has a provable performance bound on its suboptimality.

4.2.1 Problem Modification

As mentioned earlier, **P1** is a challenging problem because the charging/ discharging amount depends on the current SOB B_t as in constraints (4.13) and (4.14). This makes the control actions couple over time. To remove such coupling, we modify the constraints on the charging and discharging amounts. Based on the dynamic of SOB B_t in (4.7), we have the following relation over the T_o-slot period.

$$B_{T_o} - B_0 = \sum_{t=0}^{T_o-1} (Q_t + S_{r,t} - D_t). \tag{4.15}$$

We now set a constraint on the change of SOB over the T_o-slot period to be equal to a desired value Δ_a, *i.e.,*

$$\sum_{t=0}^{T_o-1}(Q_t + S_{r,t} - D_t) = \Delta_a. \tag{4.16}$$

It is easy to see that $|\Delta_a| \leq \Delta_{\max} \triangleq \min\{B_{\max} - B_{\min},\ T_o \max\{R_{\max}, D_{\max}\}\}$. Note that, Δ_a is only a desired value we set; it may not be achieved by an control algorithm at the end of T_o-slot period. In Section 4.4, we will quantify the amount of mismatch with respect to Δ_a under our proposed control algorithm.

With the constraint (4.16), we now modify **P1** to the follow optimization problem

$$\begin{aligned} \textbf{P2:} \min_{\{\mathbf{a}_t\}} \quad & \overline{J} + \overline{x_e} + C(\overline{x_u}) \\ \text{s.t} \quad & (4.1) - (4.5), (4.9), (4.12), (4.16). \end{aligned}$$

Note that from **P1** to **P2**, we impose the new constraint (4.16) on the change of SOB over the T_o-slot period, and remove the battery capacity constraint (4.6). By doing so, we remove the dependency of per-slot charging/discharging amount on B_t in constraints (4.13) and (4.14), and replace them by (4.3) and (4.4), respectively.

4.2.2 Problem Transformation

In the objective of **P2**, the battery average usage cost $C(\overline{x_u})$ is a function of a time-averaged quantity, which complicates the problem. Adopting the technique introduced in [57], we now transform the problem to one that contains the time-average of the function. Specifically, we introduce an auxiliary variable γ_t with the following

constraints

$$\gamma_t \in [0, \max\{R_{\max}, D_{\max}\}], \ \forall t \tag{4.17}$$

$$\overline{\gamma} = \overline{x_u} \tag{4.18}$$

where $\overline{\gamma} \triangleq \frac{1}{T_o}\sum_{\tau=0}^{T_o-1}\gamma_t$. The above constraints indicate that the auxiliary variable γ_t and $x_{u,t}$ lie in the same range and have the same time average behavior over the T_o-slot period. Define $\overline{C(\gamma)} \triangleq \frac{1}{T_o}\sum_{t=0}^{T_o-1}C(\gamma_t)$ as the time average of $C(\gamma_t)$ over T_o slots. By using γ_t instead of $x_{u,t}$, we transform the optimization problem **P2** into the following optimization problem

$$\begin{aligned} \textbf{P3:} \min_{\{\gamma_t, \mathbf{a}_t\}} \ & \overline{J} + \overline{x_e} + \overline{C(\gamma)} \\ \text{s.t} \ & (4.1) - (4.5), (4.9), (4.16) - (4.18) \end{aligned}$$

where the objective now is to minimize the T_o-slot time average of system cost. The following lemma shows the equivalence of **P2** and **P3**.

Lemma 4.1. P2 *and* **P3** *are equivalent, i.e., at optimality, their objective values are identical, and an optimal control solution* $\{\mathbf{a}_t^*\}$ *for* **P2** *is optimal for* **P3**, *and vise versa.*

Proof. See Appendix 4.7.1.

P3 is still a difficult problem to solve. Nonetheless, by the modification and transformation from **P1** to **P3**, we are able to utilize Lyapunov optimization techniques to design real-time control algorithm for **P3**. In the following, we propose a real-time control policy to solve **P3** by adopting the Lyapunov optimization technique [25]. Note that the solution to **P3** may not be feasible to **P1** due to the modification in

(4.16). However, we will show later that by properly designing our control parameters A_o and V, we can ensure the produced solution is also feasible to **P1**.

4.3 Real-Time Energy Management Algorithm

4.3.1 Lyapunov Function and Drift

Using the Lyapunov optimization framework, based on the time-averaged constraints (4.16) and (4.18), we introduce the following two virtual queues Z_t and H_t, respectively

$$Z_{t+1} = Z_t + Q_t + S_{r,t} - D_t - \frac{\Delta_a}{T_o}, \tag{4.19}$$

$$H_{t+1} = H_t + \gamma_t - x_{u,t}. \tag{4.20}$$

Under the Lyapunov optimization, it can be shown [25] that satisfying constraints (4.16) and (4.18) is equivalent to maintaining the stability of queues Z_t and H_t, respectively.

Recall that constraint (4.16) is under the assumption that $B_{T_o} - B_0 = \Delta_a$ for the T_o-slot period. From the updating dynamics in (4.7) and (4.19), we see that Z_t and B_t have the following relation

$$Z_t = B_t - A_t \tag{4.21}$$

where $A_t \triangleq A_o + \frac{\Delta_a}{T_o}t$ is a time-dependent shift consisting of two parts: the first term is a constant $A_o > 0$ which expands the range of Z_t to be the entire real line, *i.e.,* $Z_t \in \mathbb{R}$ for $B_t \in \mathbb{R}^+$; The second term is a linear time function $\frac{\Delta_a}{T_o}t$ which is to ensure that the constraint (4.15) is satisfied given the dynamics of Z_t in (4.19). The value of A_o will be determined later to ensure that the solution we develop is feasible for **P1**, *i.e.,* the constraint (4.6) is satisfied.

Let $\mathbf{\Theta}_t \triangleq [Z_t, H_t]$ be the vector of the virtual queues defined above. We define a quadratic Lyapunov function $L(\mathbf{\Theta}_t)$ for $\mathbf{\Theta}_t$ as $L(\mathbf{\Theta}_t) \triangleq \frac{1}{2}(Z_t^2 + H_t^2)$. Divide T_o slots into M sub-frames of T-slot duration, *i.e.,* $T_o = MT$, for positive integers M and T. We define a one-slot sample path Lyapunov drift[3] as

$$\Delta(\mathbf{\Theta}_t) \triangleq L\left(\mathbf{\Theta}_{t+1}\right) - L(\mathbf{\Theta}_t) \tag{4.22}$$

which only depends on the current system inputs $\{W_t, S_t, P_t\}$. Instead of directly minimizing the system cost considered in **P3**, we now consider a drift-plus-cost metric defined by

$$\Delta(\mathbf{\Theta}_t) + V[E_t P_t + x_{e,t} + C(\gamma_t)] \tag{4.23}$$

which is a weighted sum of the drift $\Delta(\mathbf{\Theta}_t)$ and the system cost at current time slot t.[4] The constant $V > 0$ sets the relative weight between the drift and the system cost.

We first provide the following lemma presenting an upper bound on the drift $\Delta(\mathbf{\Theta}_t)$, which will be used in our subsequent design of the real-time control algorithm.

Lemma 4.2. *The one-slot Lyapunov drift* $\Delta(\mathbf{\Theta}_t)$ *is upper bounded by*

$$\Delta(\mathbf{\Theta}_t) \leq G + Z_t\left(Q_t + S_{r,t} - D_t - \frac{\Delta_a}{T_o}\right) + H_t\left[\gamma_t - (E_t + S_{r,t} + l_t)\right] \tag{4.24}$$

where

$$l_t \triangleq \begin{cases} W_t - S_{w,t} & \text{if } H_t < 0, \\ S_{w,t} - W_t & \text{otherwise.} \end{cases}$$

and $G = \frac{1}{2}\max\left\{(R_{\max} - \frac{\Delta_a}{T_o})^2, (D_{\max} + \frac{\Delta_a}{T_o})^2\right\} + \frac{1}{2}\max\left\{R_{\max}^2, D_{\max}^2\right\}$.

[3]We can also define a T-slot sample path Lyapunov drift $L\left(\mathbf{\Theta}_{t+T}\right) - L(\mathbf{\Theta}_t)$. However, for $T \geq 2$, $L(\mathbf{\Theta}_{t+T})$ and thus the drift are functions of future system inputs. To design a real-time control algorithm with causal inputs, we only consider one-slot Lyapunov drift with the current system input $\{W_t, S_t, P_t\}$

[4]By Lyapunov optimization theory [25], essentially the Lyapunov drift in the drift-plus-cost metric is used to maintain the time-averaged constraints (4.16) and (4.18) being satisfied.

Proof. See Appendix 4.7.2.

Using the upper bound on $\Delta(\mathbf{\Theta}_t)$ in (4.24), we immediately have the upper bound on the drift-plus-cost metric in (4.23).

4.3.2 Real-Time Control Algorithm

In the following, we design the real-time algorithm to minimize the upper bound of drift-plus-penalty metric at every time slot t. By removing the constant terms independent of control action $\mathbf{a}_t$, this problem is equivalent to the following optimization problem

$$\begin{aligned}\mathbf{P4}: \min_{\gamma_t, \mathbf{a}_t} \quad & V[E_t P_t + x_{e,t} + C(\gamma_t)] + H_t\gamma_t + (E_t + S_{r,t})(Z_t - H_t) \\ \text{s.t.} \quad & (4.1) - (4.5), (4.9), \text{ and } (4.17).\end{aligned}$$

Denote the optimal solution of $\mathbf{P4}$ by $(\gamma_t^*, \mathbf{a}_t^*)$. Regrouping the terms in the objective of $\mathbf{P4}$ with respect to the control actions γ_t and $\mathbf{a}_t$, we can split $\mathbf{P4}$ into two sub-problems below to solve separately

$$\mathbf{P4_a}: \min_{\gamma_t} \quad H_t\gamma_t + VC(\gamma_t) \quad \text{s.t. } (4.17).$$

$$\begin{aligned}\mathbf{P4_b}: \min_{\mathbf{a}_t} \quad & E_t(Z_t - H_t + VP_t) + S_{r,t}(Z_t - H_t) + V(1_{R,t}C_{\text{rc}} + 1_{D,t}C_{\text{dc}}) \\ \text{s.t.} \quad & (4.1) - (4.5), \text{ and } (4.9).\end{aligned}$$

After determining $(\gamma_t^*, \mathbf{a}_t^*)$, we update Z_t and H_t through their respective updating equations.

We now find γ_t^* and $\mathbf{a}_t^*$ by solving $\mathbf{P4}_a$ and $\mathbf{P4}_b$, respectively. Furthermore, we provide the conditions under which the control solution $\mathbf{a}_t^*$ is feasible to $\mathbf{P1}$.

1) The optimal γ_t^*: We first consider $\mathbf{P4}_a$. Since $C(\cdot)$ is convex, the objective of $\mathbf{P4}_a$ is convex. Let $C'(\cdot)$ denotes the first derivative of $C(\cdot)$ and $C'^{-1}(\cdot)$ denote the inverse function of $C'(\cdot)$. Solving $\mathbf{P4}_a$, we obtain the optimal solution γ_t^* below.

Lemma 4.3. *The optimal solution γ_t^* of $\mathbf{P4_a}$ is given by*

$$\gamma_t^* = \begin{cases} 0 & \text{if } H_t \geq 0 \\ \Gamma & \text{if } H_t < -VC'(\Gamma) \\ C'^{-1}\left(-\frac{H_t}{V}\right) & \text{otherwise.} \end{cases} \tag{4.25}$$

where $\Gamma \triangleq \max\{R_{\max}, D_{\max}\}$.

Proof. See Appendix 4.7.3.

As we will see next, Lemma 4.3 is also useful to ensure $\mathbf{a}_t^*$ to be feasible to **P1**. The feasibility of $\mathbf{a}_t^*$ to **P1** relies on the design of A_o and V, which requires H_t to be bounded. The optimal solution γ^* in (4.25) essentially ensures a bounded H_t.

2) The optimal $\mathbf{a}_t^*$ feasible to **P1**: Now, we solve $\mathbf{P4_b}$ to obtain the optimal control solution $\mathbf{a}_t^* = [E_t^*, Q_t^*, D_t^*, S_{r,t}^*]$. Define the idle state of the battery as the state where there is no charging or discharging activity. We denote the control solution under this idle state by $\mathbf{a}_t^{\text{id}} = [E_t^{\text{id}}, Q_t^{\text{id}}, D_t^{\text{id}}, S_{r,t}^{\text{id}}]$. By supply-demand balancing equation (4.9), it is given by $E_t^{\text{id}} = W_t - S_{w,t}$, $Q_t^{\text{id}} = D_t^{\text{id}} = S_{r,t}^{\text{id}} = 0$. Let ξ_t denote the value of the objective in $\mathbf{P4_b}$ when battery is in the idle state. In this state, we have $\xi_t = (W_t - S_{w,t})(Z_t - H_t + VP_t)$. We derive $\mathbf{a}_t^*$ in three cases below. In each case, the cost of charging (or discharging) is compared with the cost ξ_t of keeping an idle state, and the control decision is obtained by taking the one with the minimum cost. The solution is summarized below.

Proposition 4.1. *Denote* $\mathbf{a}'_t = [E'_t, Q'_t, D'_t, S'_{r,t}]$. *The optimal control solution* $\mathbf{a}^*_t$ *of* $\mathbf{P4_b}$ *is given by*

1) For $Z_t - H_t + VP_t \leq 0$*: The battery is in either charging or idle state. The solution* $\mathbf{a}'_t$ *in charging state is give by*

$$\begin{cases} D'_t = 0, \\ S'_{r,t} = \min\{S_t - S_{w,t}, R_{\max}\} \\ Q'_t = \min\{R_{\max} - S'_{r,t}, E_{\max} - W_t + S_{w,t}\} \\ E'_t = \min\{W_t + R_{\max} - S_{w,t} - S'_{r,t}, E_{\max}\}. \end{cases} \tag{4.26}$$

If $E'_t(Z_t - H_t + VP_t) + (Z_t - H_t)S'_{r,t} + VC_{rc}1_{R,t} < \xi_t$, *then* $\mathbf{a}^*_t = \mathbf{a}'_t$*; Otherwise,* $\mathbf{a}^*_t = \mathbf{a}^{id}_t$.

2) For $Z_t - H_t < 0 \leq Z_t - H_t + VP_t$*: The battery is either in charging, discharging, or idle state. The solution* $\mathbf{a}'_t$ *in charging or discharging state is give by*

$$\begin{cases} D'_t = \min\{W_t - S_{w,t}, D_{\max}\} \\ S'_{r,t} = \min\{S_t - S_{w,t}, R_{\max}\} \\ Q'_t = 0, \\ E'_t = [W_t - S_{w,t} - D_{\max}]^+. \end{cases} \tag{4.27}$$

If $E'_t(Z_t - H_t + VP_t) + (Z_t - H_t)S'_{r,t} + V(C_{rc}1_{R,t} + C_{dc}1_{D,t}) < \xi_t$, *then* $\mathbf{a}^*_t = \mathbf{a}'_t$*; Otherwise,* $\mathbf{a}^*_t = \mathbf{a}^{id}_t$.

3) For $0 \leq Z_t - H_t < Z_t - H_t + VP_t$*: The batter is in either discharging or idle state. The solution* $\mathbf{a}'_t$ *in discharging state is give by*

$$\begin{cases} D'_t = \min\{W_t - S_{w,t}, D_{\max}\} \\ S'_{r,t} = Q'_t = 0, \\ E'_t = [W_t - S_{w,t} - D_{\max}]^+. \end{cases} \tag{4.28}$$

If $E'_t(Z_t - H_t + VP_t) + VC_{dc}1_{D,t} < \xi_t$, *then* $\mathbf{a}^*_t = \mathbf{a}'_t$*; Otherwise,* $\mathbf{a}^*_t = \mathbf{a}^{id}_t$.

Proof. See Appendix 4.7.4.

Remark: Proposition 4.1 shows that the optimal control decision $\mathbf{a}_t^*$ is determined in three cases, depending on the value of $Z_t - H_t$ and $Z_t - H_t + VP_t$. Since Z_t is related to B_t, and H_t is related to battery usage cost $x_{u,t}$, the three cases essentially represent the control decision when the battery energy level is at low, moderate, or high, as in case 1), 2), or 3), respectively. When both the battery energy level and electricity price are low, the battery tends to charge to store energy (or idle if the battery cost is high). When battery energy level is high, the battery tends to discharge to supply energy (or idle if the battery cost is high). Between the two levels, the battery may choose either charge or discharge, depending on the electricity price and battery cost (or idle if the battery cost is high).

The optimal solution $\mathbf{a}_t^*$ of $\mathbf{P4_b}$ provides a real-time solution for **P3**. However, it may not be feasible to **P1**, because the battery capacity constraint (4.6) on B_t may be violated. By properly designing A_o and V, we can guarantee that $\mathbf{a}_t^*$ satisfies constraint (4.6), and ensure the feasibility of the solution. The result is stated below.

Proposition 4.2. *For the optimal solution* $\mathbf{a}_t^*$ *of* **P4**, *set* A_t *in* (4.21) *with*

$$A_o = \begin{cases} B_{\min} + VP_{\max} + VC'(\Gamma) + \Gamma + D_{\max} + \frac{\Delta_a}{T_o}, & \text{if } \Delta_a \geq 0 \\ B_{\min} + VP_{\max} + VC'(\Gamma) + \Gamma + D_{\max} + \frac{\Delta_a}{T_o} - \Delta_a, & \text{if } \Delta_a < 0 \end{cases} \tag{4.29}$$

and $V \in (0, V_{\max}]$ *with*

$$V_{\max} = \frac{B_{\max} - B_{\min} - R_{\max} - D_{\max} - 2\Gamma - |\Delta_a|}{P_{\max} + C'(\Gamma)} \tag{4.30}$$

the resulting B_t *satisfies the battery capacity constraint* (4.6), *and* $\{\mathbf{a}_t^*\}$ *is feasible to* **P1**.

Proof. Here we provide a brief outline of our proof. The details are provided in

Appendix 4.7.5. Using the solutions γ_t^* and $\mathbf{a}_t^*$ of $\mathbf{P4_a}$ and $\mathbf{P4_b}$, respectively, we can show that both Z_t and H_t are upper and lower bounded. Then, by applying these bounds to (4.21) and using the battery capacity constraint (4.6), we obtain A_o as the minimum value that can be achieved with a given value of Δ_a. With A_o obtained, we derive the upper bound of V, *i.e.,* $V_{\max}$, to ensure that (4.6) is satisfied. ■

Remark 1: Since $V > 0$, for $V_{\max}$ in (4.30) to be positive, the battery storage capacity should be larger than several times the maximum of charging and discharging amounts, provided $|\Delta_a|$ is set small. This is generally satisfied for the battery used for storage and the time slot duration not being too long.

Remark 2: Since Δ_a is set as a desired value, the solutions $\{\mathbf{a}_t^*\}$ from **P4** may not satisfy constraint (4.16) at the end of the T_o-slot period, and thus may not be feasible to **P2**. Nonetheless, by Proposition 4.2, setting A_o and V as in (4.29) and (4.30) guarantees the control solutions $\{\mathbf{a}_t^*\}$ being feasible to **P1**.

We summarize the proposed real-time control algorithm in Algorithm 1 and provide the following remarks.

Remark 3: We here summarize our overall approach. To seek a solution to **P1**, we have performed a sequence of modification and transformations from **P1** to **P4**. These problems have tight connections as follows: we modify **P1** to **P2** by removing the battery capacity constraint on per-slot charging and discharging amounts in (4.13) and (4.14), and instead imposing a new constraint (4.16) on the overall change of battery energy level over T_o slots. Problems **P2** and **P3** are equivalent by Lemma 4.1. Although **P3** is still difficult to solve, we are able to leverage Lyapunov optimization technique, and propose a real-time algorithm for **P3**, which is solving per-slot opti-

Algorithm 1 Real-time battery management control algorithm

Initialize: $Z_0 = H_0 = 0$.
Determine T_o.
Set $\Delta_a \in [-\Delta_{\max}, \Delta_{\max}]$.
Set A_o and $V \in (0, V_{\max}]$ as in (4.29) and (4.30), respectively.
At time slot t:

1: Observe the system input $\{W_t, S_t, P_t\}$ and queues Z_t and H_t.
2: Solve $\mathbf{P4_a}$ and obtain γ_t^* in (4.25); Solve $\mathbf{P4_b}$ and obtain $\mathbf{a}_t^*$ by following cases (4.26)-(4.28).
3: Use $\mathbf{a}_t^*$ and γ_t^* to update Z_{t+1} and H_{t+1} in (4.19) and (4.20), respectively.
4: Output control decision $\mathbf{a}_t^*$.

mization problem **P4**. From **P1** to **P4**, the only constraint we removed from **P1** is the battery capacity constraint. Thus, we design system parameters A_o and $V_{\max}$ to ensure our proposed real-time solution satisfies the battery capacity constraint and thus is feasible to **P1**. As a result, Algorithm 1 provides a real-time suboptimal solution to **P1**. Although suboptimal, we will see in Section 4.4 that Algorithm 1 has a provable performance bound on its suboptimality.

Remark 4: Note that, our proposed real-time control solution is provided in closed-form and thus is very simple to implement. Furthermore, our proposed algorithm does not rely on any statistical assumption on the pricing, demand, and renewable processes $\{W_t, S_t, P_t\}$. Thus, it can be applied to general scenarios, especially when such process is non-stationary or difficult to predict in a highly dynamic environment and over a short time period.

4.4 Performance Analysis

We have proposed a real-time control solution (Algorithm 1) for the original energy storage problem **P1**. As mentioned earlier, it is a feasible but suboptimal solution for

P1. In this section, we analyze the performance of Algorithm 1.

4.4.1 Performance of Algorithm 1

We first analyze the performance of Algorithm 1 with respect to the objective of **P1**. Let $u^*(V)$ denote the T_o-slot average system cost objective of **P1** achieved by Algorithm 1, where we explicitly show the dependency of the cost on the weight V in the drift-plus-cost metric. Partition T_o slots into T frames with $T_o = MT$, for some integers $M, T \in \mathbb{N}^+$. Let u_m^{opt} denote the minimum T-slot average cost achieved by a T-slot look-ahead optimal control solution over the mth frame. In other words, assuming a full knowledge of $\{W_t, S_t, P_t\}$ for the entire frame beforehand, we solve **P1** with T-slot average cost objective for this frame and obtain its minimum objective value u_m^{opt}. Thus, the T-slot look-ahead optimal solution is a non-causal solution. The following theorem provides a bound of the cost performance under our proposed real-time algorithm to u_m^{opt} under the T-slot lookahead optimal solution.

Theorem 1. *Consider $\{W_t, S_t, P_t\}$ being any arbitrary processes over time. Assume any $M, T \in \mathbb{N}^+$ with $T_o = MT$. Under Algorithm 1, the resulting T_o-slot average system cost is bounded by*

$$u^*(V) - \frac{1}{M}\sum_{m=0}^{M-1} u_m^{opt} \leq \frac{GT}{V} + \frac{L(\mathbf{\Theta}_0) - L(\mathbf{\Theta}_{T_o})}{VT_o} + \frac{C'(\Gamma)(H_0 - H_{T_o})}{T_o}. \tag{4.31}$$

In particular, as $T_o \to \infty$, we have

$$\lim_{T_o\to\infty} u^*(V) - \lim_{T_o\to\infty} \frac{1}{M}\sum_{m=0}^{M-1} u_m^{opt} \leq \frac{GT}{V}. \tag{4.32}$$

Proof. We provide a brief proof here. Please find detailed proof in Appendix 4.7.6. Using the upper bound on $\Delta(\mathbf{\Theta}_t)$ in Lemma 4.1, we have the upper bound of the

drift-plus-penalty metric. Summing the bound over $m \in \{0, \dots M-1\}$ and dividing by VT_o, we obtain the upper bound for $u^*(V)$. Using Jensen's inequality in the convex function $C(\overline{\gamma})$ yields the above bound. ■

Note that, as shown in Appendix 4.7.5, both $L(\mathbf{\Theta}_t)$ and H_t are bounded. Thus, the upper bound in (4.31) is finite. We also have the following remarks.

Remark 1: First, Theorem 1 presents an upper bound on the performance gap of Algorithm 1 to the T-slot lookahead optimal solutions, for all possible $MT = T_o$. The gap is in the order of $\mathcal{O}(1/V)$. Thus, for the best performance, we should always set $V = V_{\max}$. Second, since $V_{\max}$ in (4.30) increases with $B_{\max}$, the solution by Algorithm 1 is asymptotically optimal, as it is asymptotically equivalent to the optimal T-slot lookahead solution as the battery capacity increases and T_o increases.

Remark 2: The average system cost under the T-slot lookahead optimal solution decreases with increasing T. This is because more system inputs are known beforehand and better optimization can be made. Thus, although the upper bound in (4.31) bounds the gap between Algorithm 1 and T-slot lookahead, the actual gap between $u^*(V)$ and that of T-slot lookahead is smaller with smaller T. It is also possible that $u^*(V)$ is lower than the average system cost of T-slot lookahead optimal solution for small value of T, as we will see in the simulation results.

Remark 3: The bound in (4.32) provides the performance gap of long-term time-averaged sample-path system cost of Algorithm 1 and T-slot lookahead. As $T_o \to \infty$, Algorithm 1 essentially provides the control solution under the infinite time horizon.

4.4.2 Algorithm Parameter Δ_a

As mentioned earlier, when modifying **P1** to **P2**, we impose a new constraint (4.16), where we set Δ_a to be a desired value for the change of battery energy level in T_o slots. This value may not be achieved by our proposed algorithm at the end of T_o slots. We now quantify the amount of mismatch with respect to Δ_a by Algorithm 1. Denote the mismatch by $\epsilon \triangleq \sum_{\tau=0}^{T_o-1}(Q_\tau + S_{r,\tau} - D_\tau) - \Delta_a$. We have the following result.

Proposition 4.3. *For any system input $\{W_t, S_t, P_t\}$, under Algorithm 1, for any initial queue value $Z_0 \in \mathbb{R}$, the mismatch ϵ for constraint* (4.16) *is given by*

$$\epsilon = Z_{T_o} - Z_0, \tag{4.33}$$

and is bounded by

$$|\epsilon| \leq 2\Gamma + R_{\max} + VP_{\max} + VC'(\Gamma) + D_{\max}. \tag{4.34}$$

Proof. See Appendix 4.7.7.

Proposition 4.3 provides the exact expression of the mismatch ϵ, as well as an upper bound for it. This upper bound may be loose in the actual implementation. As we will see in the simulation results, the actual error ϵ is much smaller than this upper bound.

Since Δ_a needs to be set in Algorithm 1, the solution and its performance depend on Δ_a. Note from (4.30) that $V_{\max}$ increases as $|\Delta_a|$ decreases. As discussed in Remark 1 following Theorem 1, the larger $V_{\max}$, the closer performance to the optimal T-slot look-ahead solution. Thus, in terms of performance bound, a smaller $|\Delta_a|$ is

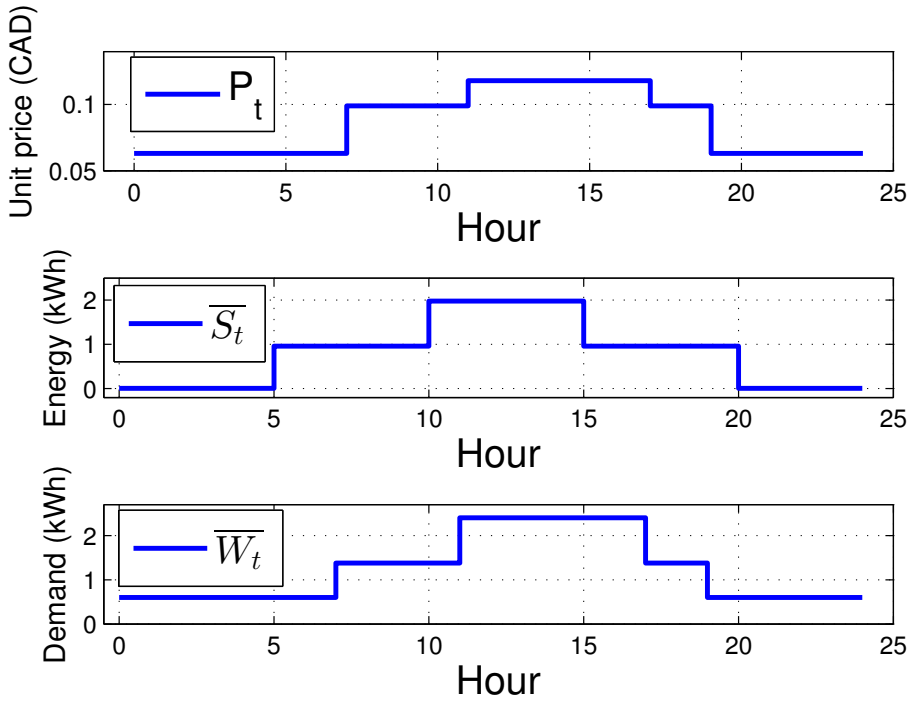

Figure 4.2: System inputs $\overline{W}_t, \overline{S}_t$, and P_t over 24 hours.

preferred. In Section 4.5, we provide detailed simulation analysis of the effect of Δ_a on the performance, and provide a guideline for determining Δ_a in Section 4.5.5.

4.5 Simulation Results

4.5.1 Simulation Configuration

We study the performance of our proposed battery management control algorithm through simulation. We set the slot duration to be 5 minutes, and assume P_t, S_t and W_t within each slot being constant. We use the data collected from Ontario Energy Board [53] to set the price P_t. As shown Fig. 4.2 top, it follows a three-stage price pattern as $\{P_h, P_m, P_l\} = \{\$0.118, \$0.099, \$0.063\}$ and is periodic every 24 hours. We consider $\{S_t\}$ being generated by solar energy. It is a non-stationary process, with the mean amount $\overline{S}_t = \mathbb{E}[S_t]$ changing periodically over 24 hours, and

having three-stage values as $\{\overline{S}_h, \overline{S}_m, \overline{S}_l\} = \{1.98, 0.96, 0.005\}/12$ kWh and standard deviation as $\sigma_{S_i} = 0.4\overline{S}_i$, for $i = h, m, l$, as shown in Fig. 4.2 middle. We assume the load $\{W_t\}$ is a non-stationary process, having three-stage mean values $\overline{W}_t = \mathbb{E}[W_t]$ as $\{\overline{W}_h, \overline{W}_m, \overline{W}_l\} = \{2.4, 1.38, 0.6\}/12$ kWh with standard deviation as $\sigma_{W_i} = 0.2\overline{W}_i$, for $i = h, m, l$, as shown in Fig. 4.2 bottom. We set other parameters as follows: $R_{\max} = 0.165$ kWh, $D_{\max} = 0.165$ kWh, $E_{\max} = 0.3$ kWh, $C_{\rm rc} = C_{\rm dc} = 0.001$, $B_{\min} = 0$, and the initial battery energy level $B_0 = B_{\max}/2$. Unless specified, we set $B_{\max} = 3$ kWh as the default value.[5]

We consider a 24-hour duration and thus set $T_o = 288$ slots. Based on constraint (4.16), a positive (negative) Δ_a allows battery to charge (discharge) more than discharge (charge) over T_o-period. Note that in the practical implementation, fixing Δ_a ($\neq 0$) over multiple periods will eventually drive the energy in the battery to its maximum or minimum, and render its setting meaningless.[6] Thus, in simulation, we set the value of $|\Delta_a|$ and alternate the sign of Δ_a over each T_o-slot period to control this tendency. Specifically, we set $\Delta_a = +c$ for the odd T_o-slot periods and $\Delta_a = -c$ for the even T_o-slot periods, for some constant $c > 0$. The respective values of A_o and $V_{\max}$ are set as in (4.29) and (4.30). Unless specified, we set $V = V_{\max}$ as the default value.

Quadratic Battery Usage Cost: We consider an exemplary case where the battery usage cost is a quadratic function, given by $C(\overline{x_u}) = k\overline{x_u}^2$, where the constant $k > 0$

[5]The current storage battery products in the market are with capacity ranging from 1.2 kWh to 7 kWh [58–60].

[6]The battery eventually reaches its maximum storage capacity (or empty) and may not be able to charge (or discharge) even if $\Delta_a > 0$ (or < 0) is set over all T_o-slot periods.

is the battery cost coefficient depending on the battery characteristics, and $\overline{x_u}$ is given in (4.11). By Lemma 4.3, the optimal γ_t^* of $\mathbf{P4}_a$ with this particular $C(\overline{x_u})$ can be straightforwardly obtained as below

$$\gamma_t^* = \begin{cases} 0 & \text{if } H_t > 0 \\ \Gamma & \text{if } H_t < -2kV\Gamma \\ -\frac{H_t}{2kV} & \text{otherwise} \end{cases}. \tag{4.35}$$

We use this cost function throughout our simulation study. Unless specified, we set $k = 0.2$ as the default value.

Other Algorithms for Comparison: We consider two other algorithms, one being a non-causal solution and the other being a real-time algorithm: i) *3-slot look-ahead*: We consider the non-causal T-slot look-ahead optimal solution with $T = 3$. Specifically, assuming $\{P_t, W_t, S_t\}$ are known non-causally 3-slot ahead, for each 3-slot frame, we solve **P1** with the objective being a 3-slot average cost objective and obtain u_m^{opt} for mth frame.[7] ii) *One-slot greedy*: a greedy algorithm that minimizes the per-slot system cost, based on the current input $\{P_t, W_t, S_t\}$. That is, we solve **P1** with the objective being 1-slot cost objective. Using it in the T_o-slot period, it essentially is the T-slot look-ahead solution with $T = 1$. Note that, due to the battery operation cost, to minimize per-slot system cost, the greedy solution is to directly purchase energy from the grid to meet the demand without utilizing battery storage (after use up the energy initially stored in the battery). Thus, the greedy algorithm is a solution that does not utilize storage.

[7]Here we only consider 3-slot look-ahead optimal solution. It is obtained through exhaustive search. Finding T-slot look-ahead optimal solution for larger T becomes increasingly more difficult.

4.5.2 Behavior of B_t over Time

We first show the state of battery energy level B_t over time slot t under Algorithm 1. Fig. 4.3 top is generated assuming both $\{S_t\}$ and $\{W_t\}$ are i.i.d. processes with uniform distribution with interval $[1, 15]/60$ kWh and $[1, 4]/12$ kWh, respectively. Fig. 4.3 bottom is generated with non-stationary $\{S_t\}$ and $\{W_t\}$ with the default setting as described in Section 4.5.1 and Fig. 4.2. We see that, in both cases, the change of B_t roughly follows the change of three-stage price P_t in Fig. 4.2 top. For the non-stationary case, due to the change of mean renewable energy $\overline{S}_t$ and mean demand $\overline{W}_t$, we observe the changes of B_t at some time durations are less random (e.g. more renewable S_t to supply W_t directly), and at other time duration can be more drastic (e.g. when the mean $\overline{S}_t$ and $\overline{W}_t$ change).

4.5.3 Performance Comparison under Algorithm Parameters

1) Effect of desired Δ_a: We first evaluate how the average system cost objective of **P1** under our proposed Algorithm 1 (*i.e.,* $u^*(V)$) varies with Δ_a in Fig. 4.4. We run our control algorithm over a total duration of T_{tot} slots, with $T_{\text{tot}} = \{4, 6\}T_o$. As we see, the cost increases with Δ_a. In particular, a positive Δ_a results in a higher cost. This is because that, to satisfy the desired $\Delta_a(> 0)$ at the end of the T_o-slot period, more energy needs to be stored in the battery. A larger Δ_a results in more cost due to energy purchasing from the grid. When $\Delta_a < 0$, more discharging than charging is required, resulting in less cost because no energy purchase from the grid is needed. A larger value of $|\Delta_a|$ for $\Delta_a < 0$ leads to less requirement of energy purchase, even though the battery usage cost $C(\overline{x_u})$ is higher. Thus, the overall system cost is lower.

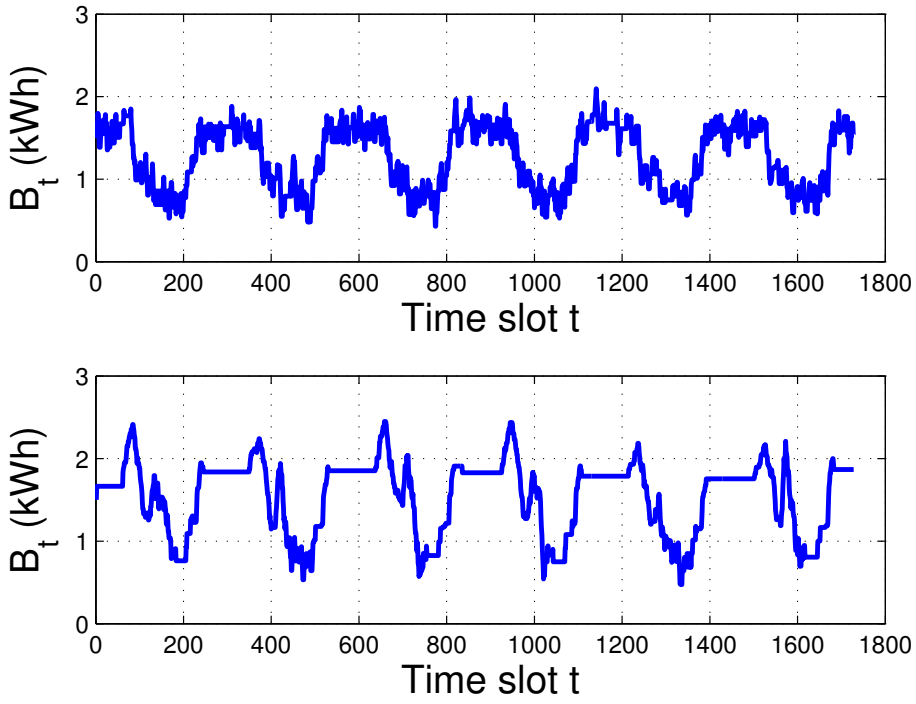

Figure 4.3: Trace of state of battery B_t vs. time slot t in a single realization: Top: i.i.d $\{W_t\}$ and $\{S_t\}$; Bottom: non-stationary $\{W_t\}$ and $\{S_t\}$ using Fig. 4.2).

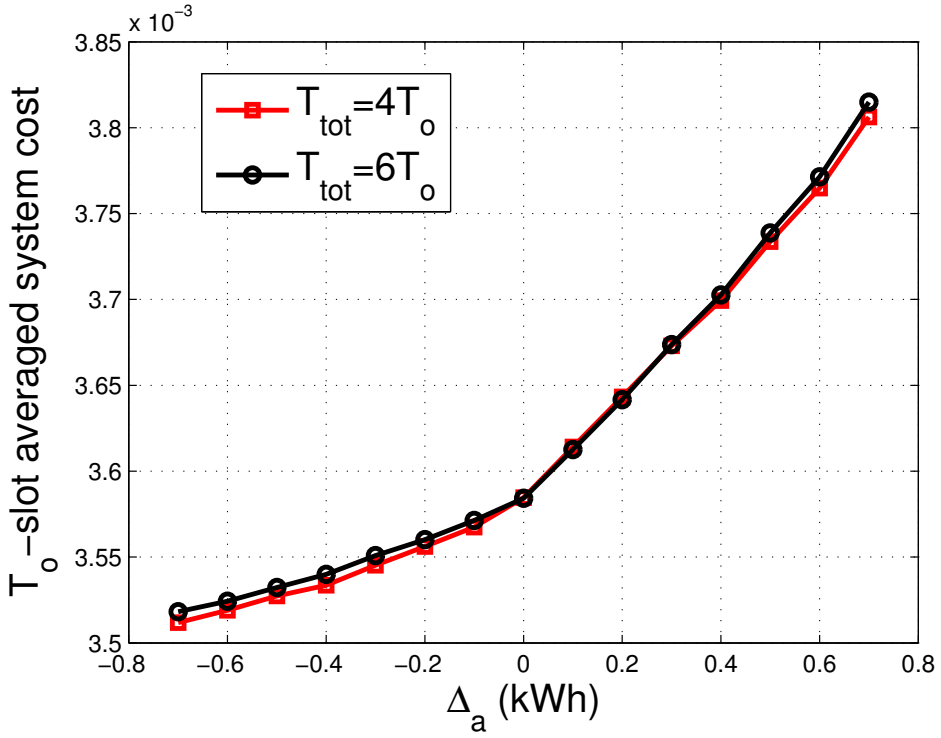

Figure 4.4: Average system cost vs. Δ_a ($B_{\max} = 3$ kWh).

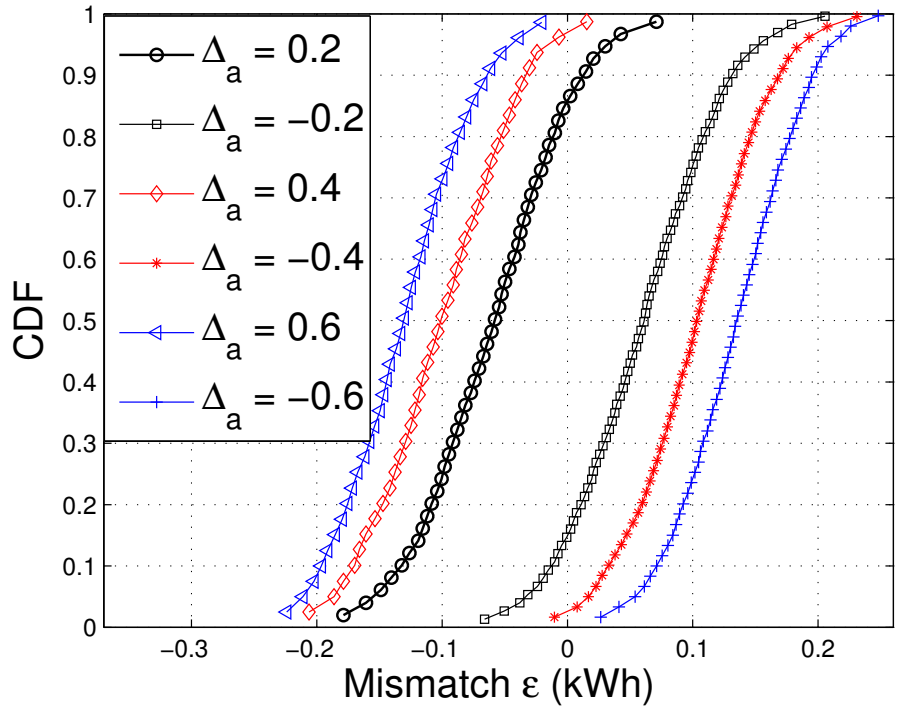

Figure 4.5: CDF of error under different values of Δ_a ($B_{\max} = 3$ kWh).

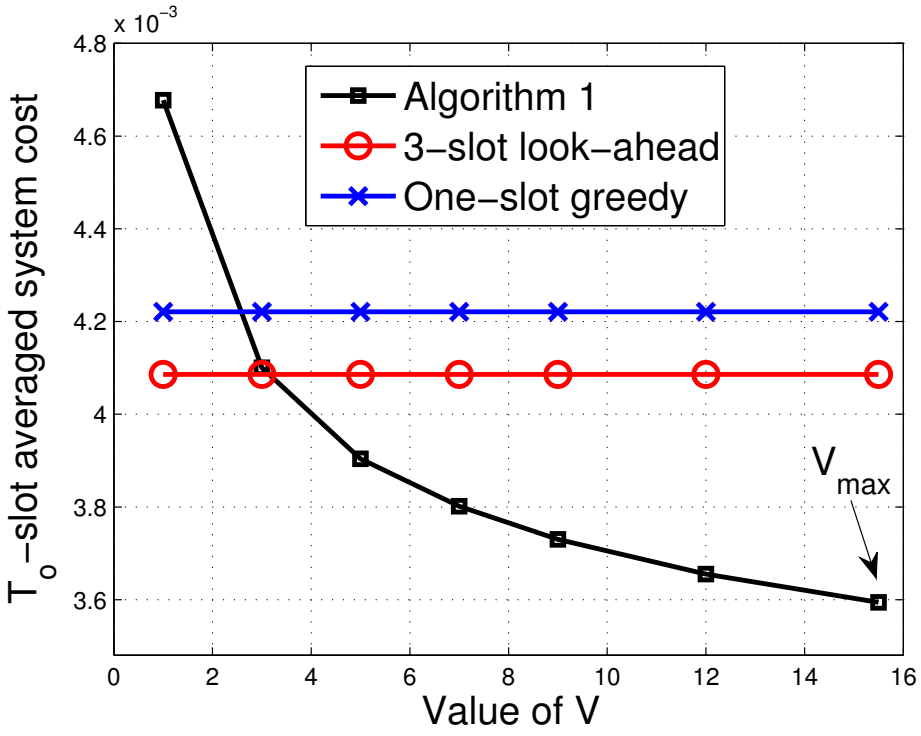

Figure 4.6: T_o-slot average system cost vs. V ($\Delta_a = 0$).

2) Mismatch ϵ: We study the resulting mismatch ϵ for the constraint (4.16) under Algorithm 1 as described in Proposition 4.3. In Fig. 4.5, we plot the CDF of the mismatch ϵ over 500 realizations of $\{W_t, S_t\}$, for $\Delta_a = \pm 0.2, \pm 0.4, \pm 0.6$. The duration of $T_{\text{tot}} = 6T_o$. We see that for a small $|\Delta_a| = 0.2$, the absolute mismatch $|\epsilon|$ is also relatively small, and the range of the CDF curves is closer to 0. When $|\Delta_a|$ increases to 0.6, the value of $|\epsilon|$ becomes larger accordingly. This is because requiring battery discharging or charging to meet larger $|\Delta_a|$ may not be achieved at the end of T_o, causing larger absolute mismatches. We also observe that ϵ and Δ_a are in opposite sign. This shows that $|\sum_{\tau=nT_o}^{(n+1)T_o-1}(Q_\tau + S_{r,\tau} - D_\tau)| < |\Delta_a|$, *i.e.,* the net change of energy amount in the battery is less than the desired amount we set.

3) Effect of parameter V: In Fig. 4.6, we evaluate the average system cost under Algorithm 1 for $V \in (0, V_{\max}]$. We set $\Delta_a = 0$ and $T_{\text{tot}} = 6T_o$. As we see, under our proposed algorithm, the system cost reduces as V increases. This observation is consistent with the result in Theorem 1 that the upper bound of the performance to the optimal T-slot lookahead solution reduces as V increases. In contrast, both 3-slot look-ahead and one-slot greedy algorithms do not depend on V, and thus the average system cost is flat.

4.5.4 Performance Comparison under Battery Parameters

1) Effect of battery usage cost: Fig. 4.7 shows the average system cost vs. battery usage cost coefficient k under Algorithm 1 and the two alternative algorithms. We set $\Delta_a = 0$. Note that since k affects the battery usage cost, the system cost under Algorithm 1 increases with k. So does that of the 3-slot look ahead solution. However,

one-slot greedy algorithm does not depend on k, because the optimal control decision to minimize the per slot system cost objective of **P1** is to purchase the exact amount of $W_t - S_{w,t}$ without storing energy (after all energy is the battery is used up). Thus, the battery storage is bypassed under this algorithm. We see from Fig. 4.7 that our proposed real-time solution under Algorithm 1 outperforms the other two algorithms over a wide range of values of k. Note that as already discussed in Remark 2 after Theorem 1, it is possible that our proposed real-time solution performs better than T-slot look-ahead optimal solution for small T.

2) Effect of battery storage capacity $B_{\max}$: In Fig. 4.8, we study the effect of battery capacity $B_{\max}$ on the system cost under Algorithm 1, for $\Delta_a = 0, \pm 0.2, \pm 0.4$. We set $C_{\rm rc} = C_{\rm dc} = 0.001$. As we see, the system cost reduces as $B_{\max}$ increases. This is because a larger battery capacity allows charging/discharging to be more flexible based on the current need and electricity price, resulting in a lower system cost. Also, consistent with previous simulation results, we see that setting $\Delta_a \leq 0$ results in a smaller system cost. Under Algorithm 1, when $\Delta_a > 0$, the battery is forced to store more energy, resulting in a higher system cost. When $\Delta_a \leq 0$, the battery discharges more energy to meet the desired Δ_a, resulting in a lower system cost. The performance difference between $\Delta_a = 0$ and $\Delta_a = -0.2$ is negligible for a low to medium battery capacity, but is more noticeable for a larger battery capacity.

As a comparison, the optimal 3-slot look-ahead algorithm also benefits from a larger battery capacity $B_{\max}$ and the system cost reduces. However, the cost is unchanged under the one-slot greedy algorithms as it bypasses the battery. We observe that our proposed real-time control solution under Algorithm 1 outperforms these two

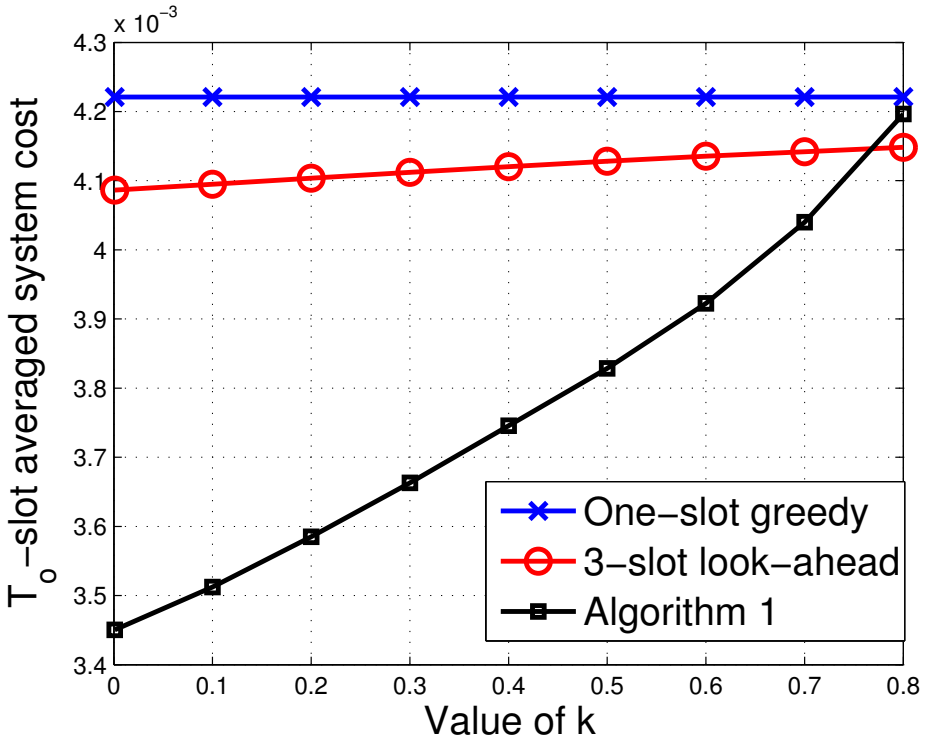

Figure 4.7: System cost vs. battery usage cost coefficient k ($\Delta_a = 0$).

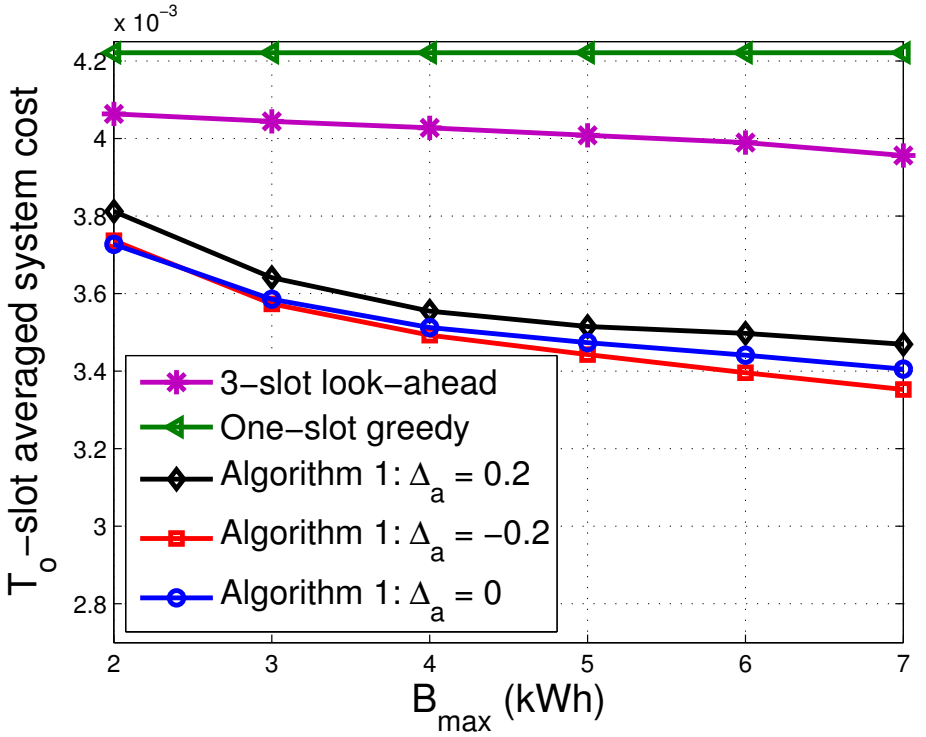

Figure 4.8: System cost vs. battery capacity $B_{\max}$.

algorithms over a wide range of $B_{\max}$ and Δ_a.

4.5.5 Guideline for Determining Δ_a

For setting the value of Δ_a, a user has his own choices depending on what he prefers in this period. If the user wants to store more energy, a positive Δ_a can be set; If the user prefers to use more energy from the battery to supply the user demand, then a negative Δ_a can be set. In Section 4.5.3.1)-2), we have studied the effect of Δ_a in terms of its setting value and mismatch ϵ on the performance in Figs. 4.4 and 4.5. Furthermore, we have shown the effect of Δ_a to the system cost in Fig. 4.8. These studies provide us a guideline on determining the value of Δ_a. To summarize, the overall system cost increases with Δ_a, and the change is smaller when $\Delta_a \leq 0$ than when $\Delta_a > 0$. In addition, a smaller value of $|\Delta_a|$ results in a smaller mismatch as shown in Fig. 4.5. Thus, in general, setting $\Delta_a \leq 0$ with $|\Delta_a|$ being a relatively small value in Algorithm 1 is desirable for the system cost.

4.6 Energy Storage System with Sell-Back

In this section, we extend our current model to sell-back model. As shown in Fig. 4.9, the energy discharged from the battery and harvested from the renewable generation can be sold back to the grid.

4.6.1 System Model

Energy Consumption: This part has been introduced in Section 4.1. We only provide a brief description as below. For renewable generation, we assume S_t is first supplied to the user's demand. We have $S_{w,t} = \min\{W_t, S_t\}$. Also, user can purchase energy

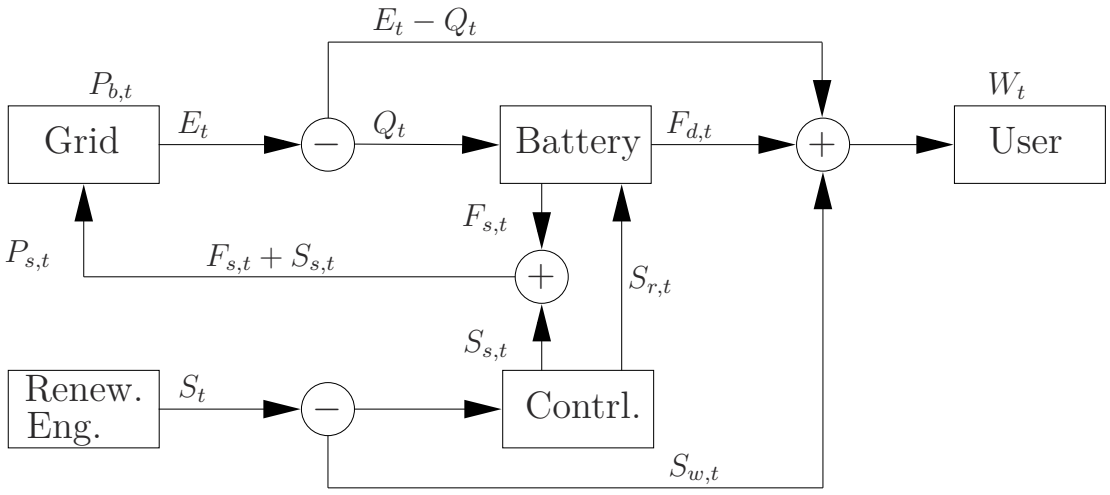

Figure 4.9: An example of energy storage and management system with selling-back from the conventional grid at a real-time buying price $P_{b,t}$. It is assumed to be in a price interval $P_{b,t} \in [P_b^{\min}, P_b^{\max}]$, where $P_b^{\min}$ and $P_b^{\max}$ are the minimum and maximum buying prices, respectively. The value of $P_{b,t}$ is assumed known to the user and remains unchanged during the slot. The amount of energy E_t buying from the grid is bounded by

$$E_t \in [0, E_{\max}] \tag{4.36}$$

Let $F_{d,t}$ denote the amount of energy discharged from the battery used to supply the user demand. By the demand-and-supply relation, the demand W_t must be satisfied at each time slot t. We have

$$W_t = E_t - Q_t + S_{w,t} + F_{d,t}. \tag{4.37}$$

Energy Production: Let $S_{s,t}$ denote the amount of energy sold back to the grid from the renewable generation and $F_{s,t}$ denote the amount of energy discharged from the battery used to sell back to the grid. The total amount for selling is bounded by

$$F_{s,t} + S_{s,t} \in [0, U_{\max}] \tag{4.38}$$

where $U_{\max}$ is the maximum amount of energy allowed to sell back to the grid. Similar to E_t, $F_{s,t} + S_{s,t}$ is followed with a real-time selling price $P_{s,t} \in [P_s^{\min}, P_s^{\max}]$, where $P_s^{\min}$ and $P_s^{\max}$ are the minimum and maximum selling prices. $P_{s,t}$ is assumed known to the user and remains unchanged during the slot. We assume $P_{b,t} > P_{s,t}$ for $\forall t$.

Remark: Our algorithm can handle $P_{b,t} \leq P_{s,t}$. However, with energy storage being considered, it is not appropriate to set $P_{b,t} \leq P_{s,t}$, *i.e.,* user will always sell stored energy with high price and buy the same amount with lower price at same time. From the utility perspective, this should not be allowed.

Essentially, the user can only be in one of stages, *i.e.,* either electricity-hungry or electricity-satiated. The corresponding behavior allows user either to buy or sell, but not both at same time. Since $S_{s,t}$ is separate from any supply-related activity, the renewable energy should be able to sell $S_{s,t}$ at any time without any constraint. Thus, user must satisfy the following constraint

$$E_t \cdot F_{s,t} = 0. \tag{4.39}$$

For $F_{s,t} > 0$, we must have $E_t = 0$. It implies that battery would sell energy back to the grid only if the user doesn't need to buy any energy from the grid to supply its demand at the moment; For $E_t > 0$, we must have $F_{s,t} = 0$. It implies that user requests to buy extra energy from the grid. Thus, the user needs energy and cannot sell any energy at the moment. Later, we will show (4.39) is not a sufficient condition, but it is the necessary condition. Running our algorithm can ensure (4.39) being satisfied.

Battery Operation: After $S_{w,t}$ is used to directly supply the user's demand, a

controller will help user decide how to utilize the remaining energy harvested by the renewable generator. Let $S_{r,t}$ be the amount of energy charged into the battery. Consider together with $S_{s,t}$, we have

$$S_{r,t} + S_{s,t} \in [0, S_t - S_{w,t}], \tag{4.40}$$

and with Q_t, we have

$$S_{r,t} + Q_t \in [0, R_{\max}]. \tag{4.41}$$

The total discharged amount from the battery that is used to supply the user demand and sell back to the grid is bounded by

$$F_{d,t} + F_{s,t} \in [0, D_{\max}]. \tag{4.42}$$

We assume there is no simultaneous charging and discharging activities happened at the same time. Thus, we have

$$(S_{r,t} + Q_t) \cdot (F_{d,t} + F_{s,t}) = 0. \tag{4.43}$$

The dynamic of SOB B_t due to charging and discharging activities is given as

$$B_{t+1} = B_t + S_{r,t} + Q_t - F_{d,t} - F_{s,t}. \tag{4.44}$$

4.6.2 Real-Time Energy Storage Management

Our control objective is to minimize the average system cost within a pre-defined period of time T_o. The system cost includes the power buying cost, selling profit and the battery degradation cost. Let $\overline{J} \triangleq \frac{1}{T_o} \sum_{t=0}^{T_o-1} E_t P_{b,t} - (F_{s,t} + S_{s,t}) P_{s,t}$ be the average net cost for energy buying and selling over a T_o-slot period. The average

battery degradation cost over the T_o-slot period is same to the previous model, given by $\overline{x_e} + C(\overline{x_u})$.

At time slot t, the system input is $\{W_t, S_t, P_{b,t}, P_{s,t}\}$. The control action is $\mathbf{a}_t \triangleq \{E_t, Q_t, F_{d,t}, F_{s,t}, S_{r,t}, S_{s,t}\}$. Our optimization problem is formulated as follows

$$\textbf{P1:} \min_{\{\mathbf{a}_t\}} \ \overline{J} + \overline{x_e} + C(\overline{x_u})$$

$$\text{s.t.} \ \ (4.36), (4.37), (4.38), (4.40), (4.43),$$

$$\overline{x_u} \in [0, \max\{R_{\max}, D_{\max}\}] \tag{4.45}$$

$$0 \leq S_{r,t} + Q_t \leq \min\{R_{\max}, B_{\max} - B_t\} \tag{4.46}$$

$$0 \leq F_{d,t} + F_{s,t} \leq \min\{D_{\max}, B_t - B_{\min}\}. \tag{4.47}$$

Since the problem formulation for this sell-back system is similar to our previous work, *i.e.,* without sell-back, we apply the same approach for problem modification and transformation. Specifically, for problem modification, we set a new constraint on the change of SOB over the T_o-slot period to be equal to a desired value Δ_a, *i.e.,*

$$\sum_{\tau=0}^{T_o-1} (Q_\tau + S_{r,\tau} - F_{d,\tau} - F_{s,\tau}) = \Delta_a. \tag{4.48}$$

For problem transformation, we introduce the auxiliary variable γ_t with constraints (4.17) and (4.18). Thus, we are able to utilize Lyapunov optimization techniques to design the real-time control algorithm. Please find detail for problem formulation in Section 4.2, and Lyapunov function and drift in Section 4.3. The resulting real-time

optimization problem is provided as follow

$$\begin{aligned}
\mathbf{P4_a}: \min_{\gamma_t} \quad & H_t\gamma_t + VC(\gamma_t) \\
\text{s.t.} \quad & \gamma_t \in [0, \max\{R_{\max}, D_{\max}\}],\ \forall t \qquad (4.49)\\
\mathbf{P4_b}: \min_{\mathbf{a}_t} \quad & E_t(Z_t - H_t + VP_{b,t}) + S_{r,t}(Z_t - H_t) \\
& - F_{s,t}(Z_t - |H_t| + VP_{s,t}) - S_{s,t}VP_{s,t} + V(1_{R,t}C_{\text{rc}} + 1_{D,t}C_{\text{dc}}) \\
\text{s.t.} \quad & (4.36)\text{-}(4.38), (4.40)\text{-}(4.43).
\end{aligned}$$

We now find γ_t^* and $\mathbf{a}_t^*$ by solving $\mathbf{P4}_a$ and $\mathbf{P4}_b$, respectively. Furthermore, we provide the conditions under which the control solution $\mathbf{a}_t^*$ is feasible to $\mathbf{P1}$.

1) The optimal γ_t^*: See Lemma 4.3.

2) The optimal $\mathbf{a}_t^*$ feasible to $\mathbf{P1}$: Now, we solve $\mathbf{P4_b}$ to obtain the optimal control solution $\mathbf{a}_t^* = [E_t^*, Q_t^*, F_{d,t}^*, F_{s,t}^*, S_{r,t}^*, S_{s,t}^*]$. Define the idle state of the battery as the state where there is no charging or discharging activity. Under this state, the control solution, denoted by $\mathbf{a}_t^{\text{id}} = [E_t^{\text{id}}, Q_t^{\text{id}}, F_{d,t}^{\text{id}}, F_{s,t}^{\text{id}}, S_{r,t}^{\text{id}}, S_{s,t}^{\text{id}}]$, is given by $E_t^{\text{id}} = W_t - S_{w,t}$, $Q_t^{\text{id}} = F_{d,t}^{\text{id}} = F_{s,t}^{\text{id}} = S_{r,t}^{\text{id}} = 0$, and $S_{s,t}^{\text{id}} = \min\{S_t - S_{w,t}, U_{\max}\}$. Let ξ_t denote the value of the objective in $\mathbf{P4_b}$ when battery is in the idle state. In this state, we have $\xi_t = (W_t - S_{w,t})(Z_t - H_t + VP_{b,t}) - \min\{S_t - S_{w,t}, U_{\max}\}VP_{s,t}$. We derive $\mathbf{a}_t^*$ in cases below. In each case, the cost of charging (or discharging) is compared with the cost ξ_t of keeping an idle state, and the control decision is obtained by choosing the one with the minimum objective cost. The solution is summarized below.

Proposition 4.4. *Denote $\mathbf{a}_t' = [E_t', Q_t', F_{d,t}', F_{s,t}', S_{r,t}', S_{s,t}']$. If the renewable energy is*

used to charge the battery, i.e., $S'_{r,t} > 0$*, for* $S'_{r,t}(Z_t - H_t) + VC_{rc} < -S'_{s,t}VP_{s,t}$*, let*

$$\begin{cases} S'_{r,t} = \min\{S_t - S_{w,t}, R_{\max}\} \\ S'_{s,t} = \min\{S_t - S_{w,t} - S'_{r,t}, U_{\max}\}, \end{cases} \tag{4.50}$$

for $S'_{r,t}(Z_t - H_t) + VC_{rc} \geq -S'_{s,t}VP_{s,t}$*, let*

$$\begin{cases} S'_{s,t} = \min\{S_t - S_{w,t}, U_{\max}\} \\ S'_{r,t} = \min\{S_t - S_{w,t} - S'_{s,t}, R_{\max}\}. \end{cases} \tag{4.51}$$

The optimal control solution $\mathbf{a}_t^*$ *of* $\mathbf{P4_b}$ *is given by*

1) For $Z_t - H_t + VP_{b,t} \leq 0$*: The battery can either charge or stay idle. Let*

$$\begin{cases} F'_{d,t} = F'_{s,t} = 0 \\ S'_{r,t} \text{ and } S'_{s,t} \text{ follow (4.50) or (4.51)} \\ Q'(t) = \min\{R_{\max} - S'_{r,t}, E_{\max} - W_t + S_{w,t}\} \\ E'_t = \min\{W_t + R_{\max} - S_{w,t} - S'_{r,t}, E_{\max}\}. \end{cases} \tag{4.52}$$

If $E'_t(Z_t - H_t + VP_{b,t}) - S'_{s,t}VP_{s,t} + (Z_t - H_t)S'_{r,t} + V1_{R,t}C_{rc} < \xi_t$*, then* $\mathbf{a}_t^* = \mathbf{a}'_t$*; Otherwise,* $\mathbf{a}_t^* = \mathbf{a}_t^{id}$*.*

2) For $\min\{Z_t - H_t, Z_t - |H_t| + VP_{s,t}\} > 0$*: The battery can either discharge or stay idle.* If $H_t \geq 0$ or $\{H_t < 0,\ Z_t + H_t \geq 0\}$*: Battery sells back prior to the renewable. Let*

$$\begin{cases} F'_{d,t} = \min\{W_t - S_{w,t}, D_{\max}\} \\ F'_{s,t} = \min\{D_{\max} - F'_{d,t}, U_{\max}\} \\ S'_{s,t} = \min\{S_t - S_{w,t}, U_{\max} - F'_{s,t}\} \\ S'_{r,t} = Q'(t) = 0 \\ E'_t = [W_t - S_{w,t} - D_{\max}]^+, \end{cases} \tag{4.53}$$

else the renewable sells first, i.e., $\{H_t < 0,\ Z_t + H_t < 0\}$*. Let*

$$\begin{cases} F'_{d,t} = \min\{W_t - S_{w,t}, D_{\max}\} \\ S'_{s,t} = \min\{S_t - S_{w,t}, U_{\max}\} \\ F'_{s,t} = \min\{D_{\max} - F'_{d,t}, U_{\max} - S'_{s,t}\} \\ S'_{r,t} = Q'(t) = 0 \\ E'_t = [W_t - S_{w,t} - D_{\max}]^+. \end{cases} \tag{4.54}$$

If $E'_t(Z_t - H_t + VP_{b,t}) - S'_{s,t}VP_{s,t} - F'_{s,t}(Z_t - |H_t| + VP_{s,t}) + V1_{D,t}C_{dc} < \xi_t$, *then* $\mathbf{a}^*_t = \mathbf{a}'_t$; *Otherwise,* $\mathbf{a}^*_t = \mathbf{a}^{id}_t$.

3) *For* $\max\{Z_t - H_t, Z_t - |H_t| + VP_{s,t}\} < 0 \leq Z_t - H_t + VP_{b,t}$: *The battery can either charge (only from* $S_{r,t}$*) or discharge (only from* $F_{d,t}$*). Let*

$$\begin{cases} F'_{d,t} = \min\{W_t - S_{w,t}, D_{\max}\} \\ F'_{s,t} = Q'(t) = 0 \\ S'_{r,t} \text{ and } S'_{s,t} \text{ follow (4.50) or (4.51)} \\ E'_t = [W_t - S_{w,t} - D_{\max}]^+, \end{cases} \tag{4.55}$$

If $E'_t(Z_t - H_t + VP_{b,t}) + S'_{r,t}(Z_t - H_t) - S'_{s,t}VP_{s,t} + V(C_{rc}1_{R,t} + C_{dc}1_{D,t}) < \xi_t$, *then* $\mathbf{a}^*_t = \mathbf{a}'_t$; *Otherwise,* $\mathbf{a}^*_t = \mathbf{a}^{id}_t$.

4) *For* $Z_t - H_t < 0 < Z_t - |H_t| + VP_{s,t}$: *Battery can either charge (only from* $S_{r,t}$*) or discharge. Due to no simultaneous charging and discharging constraint* (4.43)*, if* $F_{s,t} \geq 0$ *and* $S_{r,t} = 0$, *let*

$$\begin{cases} F'_{d,t} = \min\{W_t - S_{w,t}, D_{\max}\} \\ S'_{s,t} = \min\{S_t - S_{w,t}, U_{\max}\} \\ F'_{s,t} = \min\{D_{\max} - F'_{d,t}, U_{\max} - S'_{s,t}\} \\ S'_{r,t} = Q'(t) = 0 \\ E'_t = [W_t - S_{w,t} - D_{\max}]^+; \end{cases} \tag{4.56}$$

If $S_{r,t} \geq 0$ *and* $F_{s,t} = 0$, *let*

$$\begin{cases} F'_{d,t} = \min\{W_t - S_{w,t}, D_{\max}\} \\ S'_{r,t} \text{ and } S'_{s,t} \text{ follow (4.50) or (4.51)} \\ F'_{s,t} = Q'(t) = 0 \\ E'_t = [W_t - S_{w,t} - D_{\max}]^+, \end{cases} \tag{4.57}$$

Choose the control action $\mathbf{a}'_t$ *achieving the minimum value for the objective. If* $E'_t(Z_t - H_t + VP_{b,t}) + S'_{r,t}(Z_t - H_t) - F'_{s,t}(Z_t - |H_t| + VP_{s,t}) - S'_{s,t}VP_{s,t} + V(C_{rc}1_{R,t} + C_{dc}1_{D,t}) < \xi_t$, *then* $\mathbf{a}^*_t = \mathbf{a}'_t$; *Otherwise,* $\mathbf{a}^*_t = \mathbf{a}^{id}_t$.

5) For $H_t < 0$ and $Z_t + H_t + VP_{s,t} < 0 < Z_t - H_t$: Let

$$\begin{cases} F'_{d,t} = \min\{W_t - S_{w,t},\ D_{\max}\} \\ F'_{s,t} = S'_{r,t} = Q'(t) = 0 \\ S'_{s,t} = \min\{S_t - S_{w,t}, U_{\max}\} \\ E'_t = [W_t - S_{w,t} - D_{\max}]^+. \end{cases} \tag{4.58}$$

If $E'_t(Z_t - H_t + VP_{b,t}) + VC_{dc}1_{D,t} - S'_{s,t}VP_{s,t} < \xi_t$, then $\mathbf{a}^*_t = \mathbf{a}'_t$; Otherwise, $\mathbf{a}^*_t = \mathbf{a}^{id}_t$.

Proof. See Appendix 4.7.8.

Remark: Proposition 4.4 shows that the optimal control decision $\mathbf{a}^*_t$ is determined in those five cases, depending on the values of $Z_t - H_t + VP_{b,t}$, $Z_t - H_t$, $Z_t - |H_t| + VP_{s,t}$ and $VP_{s,t}$. Since Z_t is related to B_t as shown in (4.21), and H_t is related to battery usage cost $x_{u,t}$, the cases essentially represent the control decision when the battery energy is at certain levels. When the battery energy level is low as case 1), the battery tends to charge to store energy (or idle if the battery cost is high). When the battery energy level is high as case 2), the battery tends to discharge to supply energy (or idle if the battery cost is high). Between the two levels as cases 3)-5), the battery may choose either charge or discharge, depending on the prices and battery cost (or idle if the battery cost is high). There is one exception for $S^*_{s,t}$. It is not determined by the battery level due to $VP_{s,t} > 0$. This means the selling direct from the renewable only depends on the selling-price. It is advantageous when the control solution chooses not to charge $S_{r,t}$, the remaining energy from the renewable will be utilized for selling.

The optimal solution $\mathbf{a}^*_t$ of $\mathbf{P4_b}$ provides a real-time solution for **P3**. However, it may not be feasible to **P1**, because the battery capacity constraint (3.6) on B_t may be violated. By properly designing A_o and V, we can guarantee that $\mathbf{a}^*_t$ satisfies

constraint (3.6), and ensure the feasibility of the solution. The result is stated below.

Proposition 4.5. *Under our proposed real-time control algorithm, for* A_t *in* (4.21) *with*

$$A_o = \begin{cases} B_{\min} + VP_b^{\max} + VC'(\Gamma) + \Gamma + D_{\max} + \frac{\Delta_a}{T_o}, & \text{if } \Delta_a \geq 0 \\ B_{\min} + VP_b^{\max} + VC'(\Gamma) + \Gamma + D_{\max} + \frac{\Delta_a}{T_o} - \Delta_a, & \text{if } \Delta_a < 0 \end{cases} \tag{4.59}$$

and $V \in (0, V_{\max}]$ *with*

$$V_{\max} = \begin{cases} \frac{B_{\max} - B_{\min} - R_{\max} - D_{\max} - 2\Gamma - |\Delta_a|}{P_b^{\max} + C'(\Gamma)}, & \text{if } P_s^{\min} > C'(\Gamma) \\ \frac{B_{\max} - B_{\min} - R_{\max} - D_{\max} - 2\Gamma - |\Delta_a|}{P_b^{\max} + 2C'(\Gamma) - P_s^{\min}}, & \text{if } P_s^{\min} \leq C'(\Gamma) \end{cases} \tag{4.60}$$

the resulting B_t *satisfies the battery capacity constraint* (4.6)*, and* $\{\mathbf{a}_t^*\}$ *is feasible to* **P1**.

Proof. We use similar approach for Proposition 4.2 to prove Proposition 4.5. See Appendix 4.7.5 for detail.

4.6.3 Performance Analysis

Since the algorithm for this sell-back model is unchanged, we omit the analysis for the performance bound. Please find Theorem 1 in Section 4.4.1 for detail.

Similar to Proposition 4.3 in Section 4.4.2, we quantify the mismatch ϵ as follows.

Proposition 4.6. *For any system input* $\{W_t, S_t, P_{b,t}, P_{s,t}\}$*, under Algorithm 1, for any initial queue value* $Z_0 \in \mathbb{R}$*, the mismatch* ϵ *for constraint* (4.48) *is given by*

$$\epsilon = Z_{T_o} - Z_0, \tag{4.61}$$

and is bounded by

$$\begin{aligned} |\epsilon| \leq \max\{&2\Gamma + VC'(\Gamma) + VP_b^{\max} + R_{\max} + D_{\max}, \\ &2\Gamma + 2VC'(\Gamma) + VP_b^{\max} + R_{\max} + D_{\max} - VP_s^{\min}\} \end{aligned} \tag{4.62}$$

Proof. We use similar approach for Proposition 4.3 to prove Proposition 4.6. See the proof in Appendix 4.7.7 for detail.

Last, as we expect in (4.39), buying energy for $E_t > 0$ and selling-back from battery for $F_{s,t} > 0$ should not happen at same time. By the optimal control solution (4.52)-(4.58), we have the following result.

Proposition 4.7. *For any system inputs* $\{W_t, S_t, P_{b,t}, P_{s,t}\}$*, under Algorithm 1, the optimal control solution* a_t^* *can guarantee* (4.39) *being satisfied.*

Proof. See Appendix 4.7.9.

4.6.4 Simulation Results

Please find our simulation configuration in Section 4.5.1.

Effects of Selling-Back Price $P_{s,t}$: We fist study the battery buying and selling behaviors varied with the selling-back price $P_{s,t}$. We assume the selling price is proportional to the buying price. Since we set 3-stage selling price with low, medium and high rates as P_b^l, P_b^m, P_b^h, the selling price is also followed by the 3-stage, but it has the rate $P_s^i = \eta P_b^i$ with $0 < \eta < 1$ and $i = l, m, h$. Define the average charging amount Q_t and sell-back amount $F_{s,t}$ at each stage as follows

$$E_Q(P_b^i) \triangleq \frac{1}{T_i} \sum_{t=\{t:P_{b,t}=P_b^i\}} Q_t^*, \ i = h, m, l \tag{4.63}$$

$$E_{F_s}(P_s^i) \triangleq \frac{1}{T_i'} \sum_{t=\{t:P_{s,t}=\eta P_b^i\}} F_{s,t}^*, \ i = h, m, l \tag{4.64}$$

where $T_i \triangleq \sum_{t=\{t:P_{b,t}=P_b^i\}} 1$ and $T_i' \triangleq \sum_{t=\{t:P_{s,t}=\eta P_b^i\}} 1$. We assume η is known and kept unchanged over T_o time slots. We set parameters to $\Delta_a = 0.1$ and $\eta = 0.9, 0.3$.

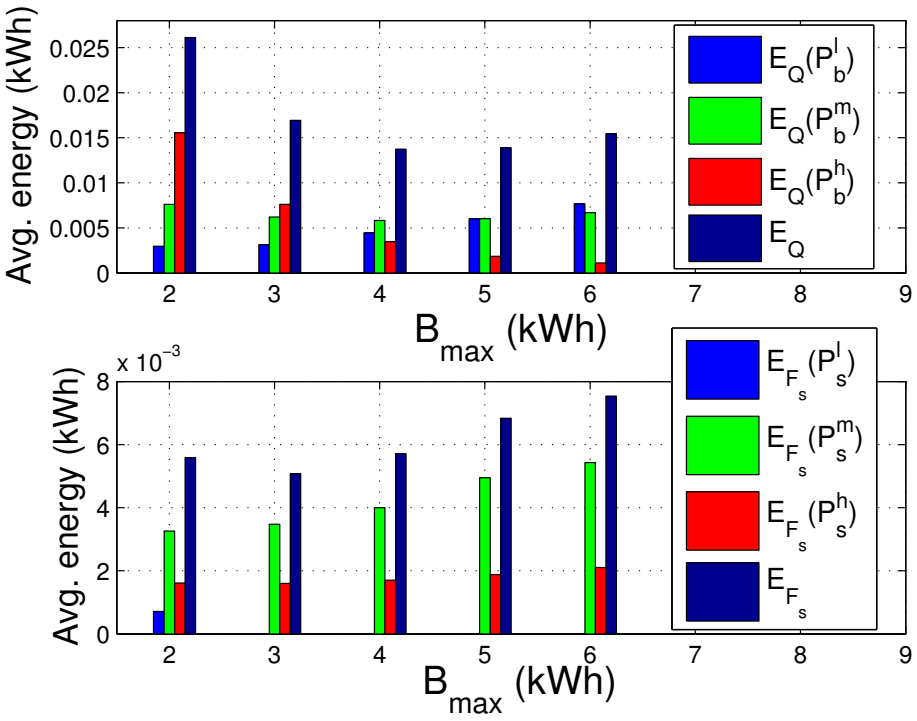

Figure 4.10: Buying (Selling) energy to (from) battery vs. $B_{\max}$ ($\eta = 0.9$).

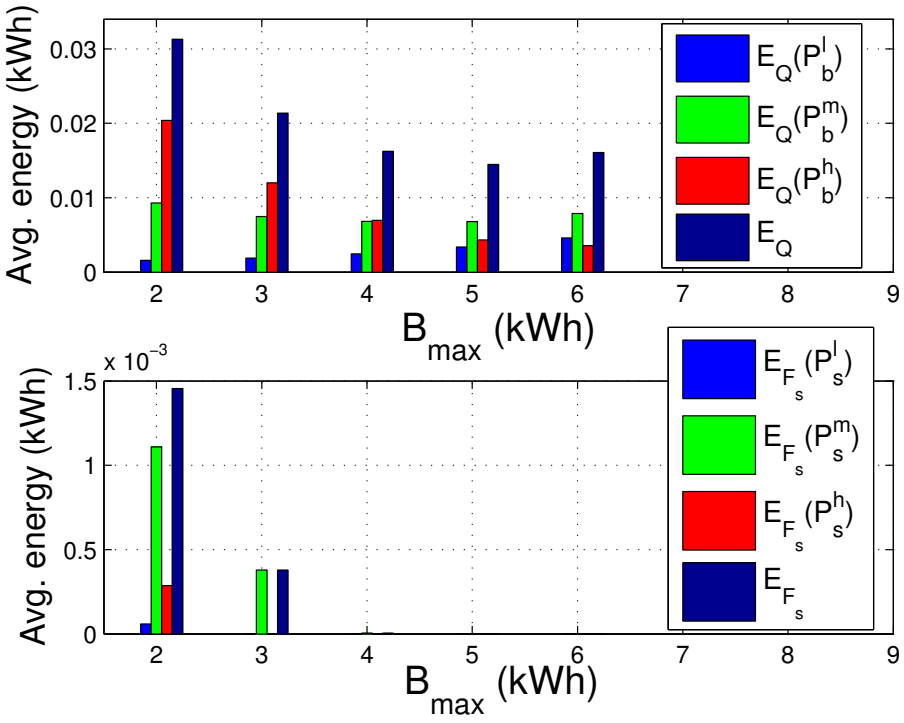

Figure 4.11: Buying (Selling) energy to (from) battery vs. $B_{\max}$ ($\eta = 0.3$).

If set $\eta = 0.9$, as shown in Fig. 4.10 bottom, more energy is sold back to the grid. This is because selling back energy in high price can profit user; If set $\eta = 0.3$, as shown in Fig. 4.11 bottom, battery chooses to keep the energy, not selling back. This is because the selling price is cheap, energy will be kept in the battery for future usage. Moreover, when the battery capacity $B_{\max}$ increases, we see more energy is sold back to the grid on medium and high rates, *i.e.,* $i = m, h$. This is because a large size of capacity offers more flexibility for charging and discharging activities. Thus, user only sells energy when the price is high enough. On the contrary, as shown in Fig. 4.10 top and Fig. 4.11 top, the amount of energy purchased from the grid with high rate of $P_{b,t}$ is decreased as the battery capacity increases.

Effects of Desired Δ_a and Mismatch ϵ: We evaluate how the average system cost objective of **P1** under our proposed Algorithm 1 (*i.e.,* $u^*(V)$) varies with Δ_a in Fig. 4.12. We run our control algorithm over a total duration of T_{tot} slots, with $T_{\text{tot}} = \{4, 6\}T_o$. We see that the cost increases with Δ_a. A positive Δ_a results in a higher cost. This is because more energy needs to be stored into the battery to satisfy the desired Δ_a (> 0). More purchasing energy from grid causes the higher cost. When $\Delta_a < 0$, more discharging is required than the charging, resulting in less cost since less energy is purchased from the grid. Although, the battery usage cost $C(\overline{x_u})$ is higher, the overall system cost is still lower.

We study the resulting mismatch ϵ for the constraint (4.16) under Algorithm 1. In Fig. 4.13, we plot the CDF of the mismatch ϵ over 500 realizations, for $\Delta_a = \pm 0.2, \pm 0.4, \pm 0.6$. The duration of $T_{\text{tot}} = 6T_o$. For a small $|\Delta_a| = 0.2$, we see that the absolute mismatch ϵ is also relatively small, and the range of the CDF curves is closer

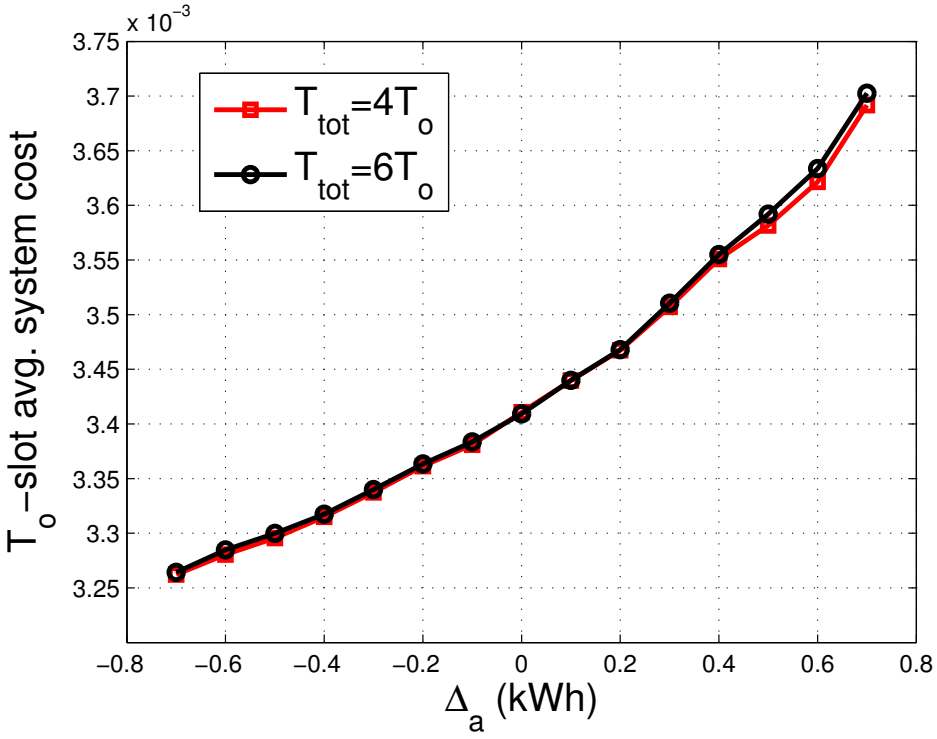

Figure 4.12: System cost vs. Δ_a ($B_{\max} = 3$kWh, $\eta = 0.9$).

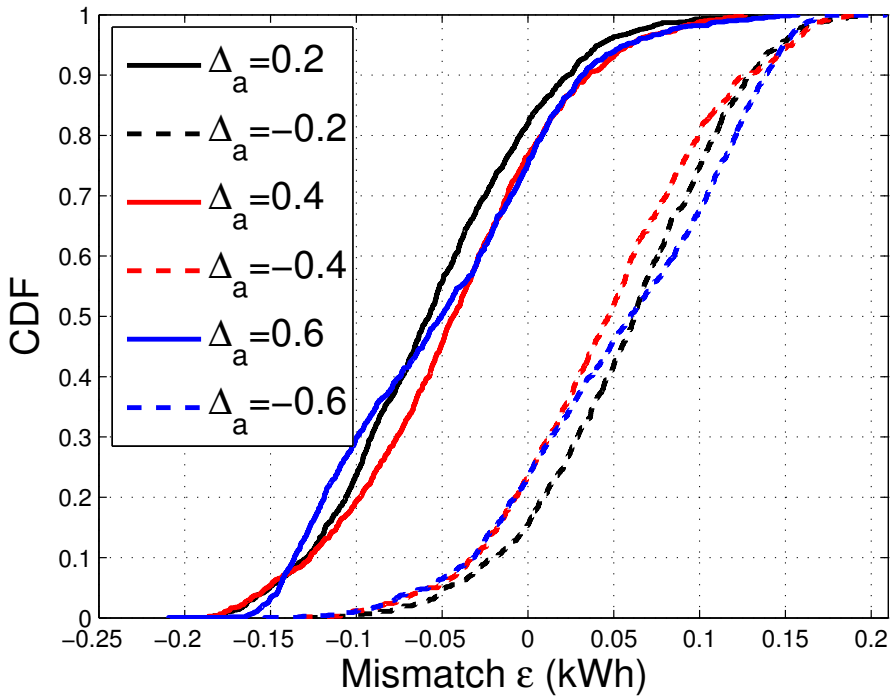

Figure 4.13: CDF of mismatch under different values of Δ_a ($B_{\max} = 3$ kWh, $\eta = 0.9$).

to 0. For large $|\Delta_a| = 0.4, 0.6$, the range of the CDF curves are similar to $|\Delta_a| = 0.2$. This is because the selling-back amount $F_{s,t}$ keeps the mismatch amount relatively small to meet the desired large $|\Delta_a|$.

Effect of Battery Capacity $B_{\max}$ on System Cost: In Fig. 4.14, we study the effect of battery capacity $B_{\max}$ on the system cost under algorithm 1 over algorithm parameters for $|\Delta_a| = 0, 0.2, 0.4$ and $\eta = 0.9, 0.3$. We set $T_{\text{tot}} = 6T_o$ and $C_{\text{rc}} = C_{\text{dc}} = 0.001$. First, we observe that, consistent with previous simulation results, setting $\Delta_a = 0$ always results in the lowest system cost. This is because, for any $|\Delta_a| > 0$, higher cost is incurred since the battery is either forced to charge or discharge to meet the desired value of Δ_a, leading to unnecessary purchasing cost with respect to $E_t P_{b,t}$ or discharging cost with respect to $x_{u,t}$. Second, we find that the system cost reduces as $B_{\max}$ increases. This is because a larger battery capacity allows charging (discharging) to be more flexible. Thus, the system cost is reduced. Also, we look at the effect of η. With higher selling price, the system cost is reduced. Setting high selling price can effectively promote user to sell more energy back to the grid, helping user reduce the system cost.

Performance Comparison under Difference Algorithms: We compare our proposed algorithm to a 3-slot look-ahead algorithm. In Fig. 4.15, different capacities of $B_{\max}$ is considered. With large η, *i.e.,* $P_{s,t}$ is higher, the cost difference between these two algorithms are less. The 3-slot look-ahead algorithm may benefit more from selling back energy with higher repayment, while our proposed algorithm sells less and intends to store more energy for future usage. With larger capacity of $B_{\max}$, from (4.31), we know that our algorithm performs closer to the optimal with larger value of V, which

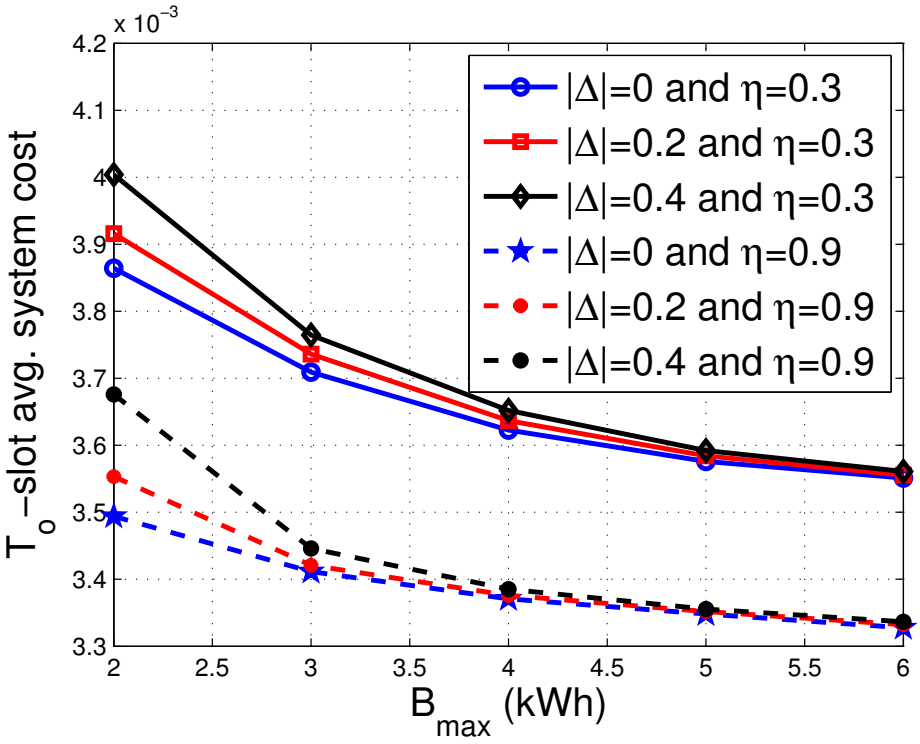

Figure 4.14: System cost vs. $B_{\max}$ ($C_{\rm rc} = 0.001$).

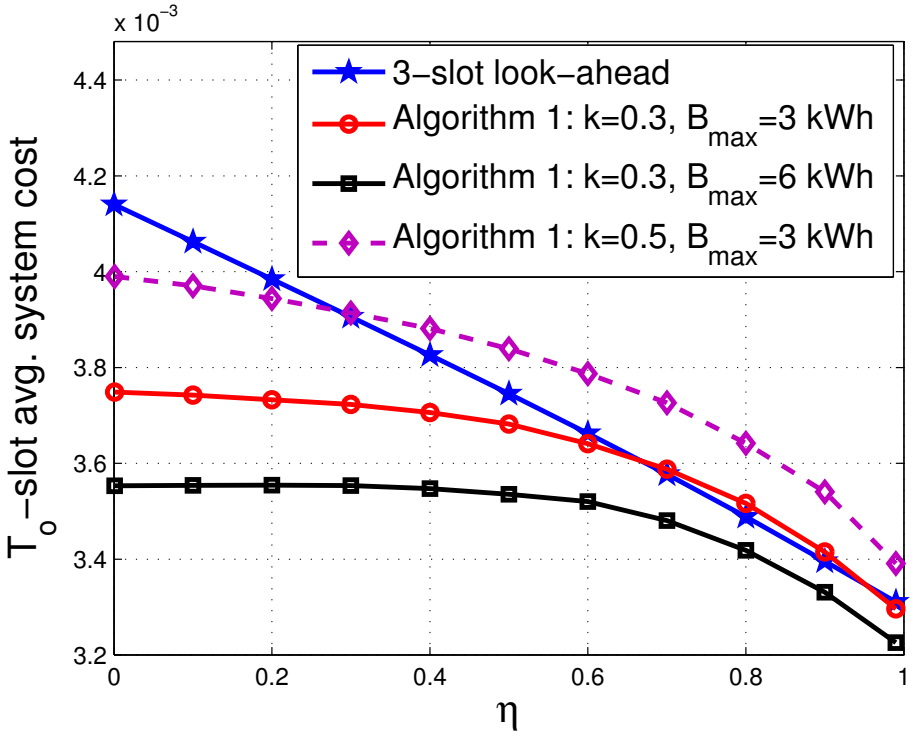

Figure 4.15: System cost vs. η ($\Delta_a = 0.1$).

is proportional to $B_{\max}$ as shown in (4.30). A large battery provides more flexibility, resulting the reduced cost. Also we consider different values in battery coefficient k. As can be seen, our proposed algorithm is close to the optimal over a wide range of k.

4.7 Appendices

4.7.1 Proof of Lemma 4.1

Proof. The proof follows the general argument in [57]. Note that the optimal solution of **P2** satisfies all constraints of **P3**, and therefore it is a feasible solution of **P3**. Let u_2^o and u_3^o denote the minimum objective values of **P2** and **P3**, respectively. Thus, we have $u_3^o \leq u_2^o$. By Jensen's inequality and convexity of $C(\cdot)$, we have $\overline{C(\gamma)} \geq C(\overline{\gamma}) = C(\overline{x_u})$. This means $u_3^o \geq u_2^o$. Hence, we have $u_2^o = u_3^o$ and **P3** and **P2** are equivalent. ■

4.7.2 Proof of Lemma 4.2

Proof. From the definition of $\Delta(\mathbf{\Theta}_t)$ in (4.22), we have

$$\begin{aligned}\Delta(\mathbf{\Theta}_t) = L(\mathbf{\Theta}_{t+1}) - L(\mathbf{\Theta}_t) &= \frac{1}{2}\left(Z_{t+1}^2 - Z_t^2 + H_{t+1}^2 - H_t^2\right) \\ &= Z_t\left(Q_t + S_{r,t} - D_t - \frac{\Delta_a}{T_o}\right) + H_t(\gamma_t - x_{u,t}) \\ &\quad + \frac{\left(Q_t + S_{r,t} - D_t - \frac{\Delta_a}{T_o}\right)^2}{2} + \frac{(\gamma_t - x_{u,t})^2}{2}. \end{aligned} \tag{4.65}$$

Let g_t denote the sum of the last two terms in (4.65). Note that from (4.16), we have $\frac{\Delta_a}{T_o} \leq \max\{R_{\max}, D_{\max}\}$. For a given value of Δ_a, by (4.3), (4.4), (4.8) and (4.17), g_t

is upper bounded by

$$g_t \leq \frac{\max\left\{\left(R_{\max} - \frac{\Delta_a}{T_o}\right)^2, \left(D_{\max} + \frac{\Delta_a}{T_o}\right)^2\right\}}{2} + \frac{\max\{R_{\max}^2, D_{\max}^2\}}{2} \triangleq G. \tag{4.66}$$

We now find the upper bound of $-H_t x_{u,t}$ in the second term of (4.65). By the supply-demand balancing requirement in (4.9), we have $x_{u,t} = |Q_t + S_{r,t} - D_t| = |E_t + S_{r,t} + S_{w,t} - W_t|$. Note that $S_{w,t}$, W_t and H_t are known for the current time slot t. Also, $S_{w,t} - W_t \leq 0$, because $S_{w,t} = \min\{W_t, S_t\}$. The upper bound of $-H_t x_{u,t}$ is obtained as follows:

1) For $H_t \geq 0$: Let $l_t \triangleq S_{w,t} - W_t$. It is easy to see that the following inequality holds

$$-H_t|E_t + S_{r,t} + S_{w,t} - W_t| < 0 \leq -H_t[E_t + S_{r,t} + l_t].$$

2) For $H_t < 0$: Let $l_t \triangleq W_t - S_{w,t}$. We have

$$-H_t|E_t + S_{r,t} + S_{w,t} - W_t| \leq -H_t(|E_t + S_{r,t}| + |S_{w,t} - W_t|) = -H_t[E_t + S_{r,t} + l_t].$$

Combining the above results and (4.66), we have the upper bound of $\Delta(\mathbf{\Theta}_t)$ in (4.24). ■

4.7.3 Proof of Lemma 4.3

Proof. Given $\gamma_t \in [0, \Gamma]$ in (4.17) and $C(\gamma_t)$ as a continuous, convex, non-decreasing function in γ_t with maximum derivative $C'(\Gamma) < \infty$, the optimal γ_t^* is determined by examining the derivative of the objective function $H_t + VC'(\gamma_t)$. Note that $C'(\gamma_t) \geq 0$ and is increasing with γ_t. We have

1) For $H_t \geq 0$: $H_t + VC'(\gamma_t) > 0$, thus the objective of $\mathbf{P4}_a$ is a monotonically increasing function, and its minimum is obtained with $\gamma_t^* = 0$.

2) For $H_t < -VC'(\Gamma)$: Since $VC'(\Gamma) \geq VC'(\gamma_t)$, we have $H_t + VC'(\gamma_t) < 0$ The objective of $\mathbf{P4}_a$ is a monotonically decreasing function, and its minimum is reached with $\gamma_t^* = \Gamma$.

3) For $-VC'(\Gamma) \leq H_t \leq 0$: In this case, γ_t^* is the root of $H_t + VC'(\gamma_t) = 0$, we have $\gamma_t^* = C'^{-1}\left(-\frac{H_t}{V}\right)$.

Thus, we have γ_t^* as in (4.25). ■

4.7.4 Proof of Proposition 4.1

Proof. We show the solution in each case below.

1) For $Z_t - H_t + VP_t \leq 0$: Since V and P_t are both positive, we have $Z_t - H_t \leq 0$. To minimize the objective of $\mathbf{P4}_b$, one possible solution is to set both E_t' and $S_{r,t}'$ as large as possible. This means that battery is in the charging state. We have $1_{R,t} = 1$, $1_{D,t} = 0$, $D_t' = 0$, and use maximum charging rate, *i.e.,* $S_{r,t}' + Q_t' = R_{\max}$. Since Q_t' is a portion of E_t', and $Z_t - H_t \leq Z_t - H_t + VP_t$, maximizing $S_{r,t}'$ in the above equation can further reduce the value of $\mathbf{P4}_b$. By supply-demand balancing equation (4.9), we obtain Q_t' and E_t' in (4.26). Thus, the control solution $\mathbf{a}_t'$ is as in (4.26). Note that under the charging state, the entry cost C_{rc} for charging is paid. Alternatively, we consider the battery in the idle state instead, *i.e.,* $S_{r,t}^{\text{id}} + Q_t^{\text{id}} = 0$. In this case, $1_{R,t} = 0$, but E_t^{id} is smaller. The optimal $\mathbf{a}_t^*$ is then the one that achieves the minimum objective value.

2) For $Z_t - H_t < 0 \leq Z_t - H_t + VP_t$: Because $Z_t - H_t + VP_t \geq 0$, to minimize the objective of $\mathbf{P4}_b$, one possible solution is to set E_t' as small as possible. This means E_t' should be only purchased to supply W_t, and not for storage, *i.e.,* $Q_t' = 0$.

When $S_{w,t} = W_t$, it is possible that $S_t - S_{w,t} \geq 0$. In this case, there is no need for discharging, *i.e.,* $D'_t = 0$, and the battery could be charged from renewable source $S'_{r,t} \geq 0$. On the other hand, when $S_{w,t} < W_t$, *i.e.,* S_t is fully used to supply W_t, we have $S'_{r,t} = 0$. To meet the demand in (4.9), we could either purchase E'_t and/or let battery discharge D'_t. Based on the above, we have the control solution $\mathbf{a}'_t$ as shown in (4.27). Charging or discharging will incur entry cost C_{rc} or C_{dc}, respectively. Similar to Case 1), there exists an alternatively way which is to keep the battery idle. Thus, the optimal $\mathbf{a}^*_t$ is chosen from the three possible solutions whichever achieves the minimum objective value.

3) For $0 \leq Z_t - H_t < Z_t - H_t + VP_t$: One possible solution is to set both E'_t and $S'_{r,t}$ as small as possible to minimize the objective value of $\mathbf{P4}_b$. Thus, the battery should not be charged, *i.e.,* $Q'_t + S'_{r,t} = 0$. To satisfy the rest of demand $W_t - S_{w,t}$, energy should be discharged from the battery. Following this, we can similarly derive the control solution $\mathbf{a}'_t$ in (4.28). Under this assumption, the entry cost C_{dc} for discharging is paid. Alternatively, we can keep the battery idle and only purchase energy E^{id}_t from the grid. This will result in more E^{id}_t purchased but avoid battery cost C_{dc}. The optimal $\mathbf{a}^*_t$ is the one that achieves the minimum objective value. ■

4.7.5 Proof of Proposition 4.2

Proof. To prove Proposition 4.2, we first introduce Lemma 4.4 and Lemma 4.5 below.

Lemma 4.4. *Under the proposed solution in Lemma 4.4 and Proposition 4.1, we have*

1) If $Z_t < -VP_{\max} + H_{\min}$*, then* $D^*_t = 0$*;*

2) If $Z_t > H_{\max}$*, then* $S^*_{r,t} + Q^*_t = 0$*,*

where $H_{\min} \triangleq \min\{H_t\}$ *and* $H_{\max} \triangleq \max\{H_t\}$*.*

Proof. 1) This case corresponds to Case 1) of Proposition 4.1. If $Z_t < -VP_{\max}+H_{\min}$, it is easy to see that $D^*_t = 0$ is the optimal control action.

2) This case corresponds to Case 3) of Proposition 4.1. It is easy to see that $S^*_{r,t} = Q^*_t = 0$ are the optimal control action. ■

Lemma 4.5. *For* γ^*_t *in* (4.25)*,* H_t *is bounded by*

$$-VC'(\Gamma) - \Gamma \leq H_t \leq \Gamma. \tag{4.67}$$

where $H_{\min} = -VC'(\Gamma) - \Gamma$ *and* $H_{\max} = \Gamma$*. Note* $\Gamma = \max\{R_{\max}, D_{\max}\}$ *as in* (4.25)*.*

Proof. 1) Upper bound of H_t: From (4.8), $x_{u,t} \geq 0$. If $H_t \geq 0$, from (4.25), we have $\gamma^*_t = 0$. Thus, based on the dynamics of H_t in (4.20), $H_{t+1} \leq H_t$, *i.e.,* non-increasing. When $H_t < 0$, from (4.25), the maximum increment of H_{t+1} in (4.20) is when $\gamma^*_t = \Gamma$ and $x_{u,t} = 0$, and thus $H_{t+1} \leq \Gamma$ as in (4.67).

2) Lower bound of H_t: From (4.25), if $H_t < -VC'(\Gamma)$, we have $\gamma^*_t = \Gamma$, and H_{t+1} is non-decreasing in (4.20). If $H_t \geq -VC'(\Gamma)$, the maximum decrement of H_{t+1} from H_t in (4.20) is when $\gamma^*_t = 0$ and $x_{u,t} = \Gamma$, and $H_{t+1} \geq -VC'(\Gamma) - \Gamma$. ■

Now, we are ready to prove Proposition 4.2. When first show that under A_o and V in (4.29) and (4.30), B_t is always upper bounded by $B_{\max}$; Then we prove that B_t is lower bounded by $B_{\min}$.

1) Upper Boundedness of B_t*, i.e.,* $B_t \leq B_{\max}$: Based on Lemma 4.4.1, we have $D^*_t = 0$, if $Z_t < -VP_{\max} + H_{\min}$. Equivalently, if $Z_t - \frac{\Delta_a}{T_o} < -VP_{\max} + H_{\min} - \frac{\Delta_a}{T_o}$,

there is no discharge from the battery. When $Z_t - \frac{\Delta_a}{T_o} \geq -VP_{\max} + H_{\min} - \frac{\Delta_a}{T_o}$, from (4.4), the maximum decreasing amount of Z_t to Z_{t+1} in (4.19) in the next time slot is

$$Z_{t+1} \geq -VP_{\max} + H_{\min} - \frac{\Delta_a}{T_o} - D_{\max}, \ \forall t. \tag{4.68}$$

In (4.21), we have $B_t = Z_t + A_o + \frac{\Delta_a}{T_o}t$. To satisfy the lower bound of B_t in (4.6), we must ensure $Z_t + A_o + \frac{\Delta_a}{T_o}t \geq B_{\min}$. Substituting Z_t in (4.68) to the above equation, we obtain

$$-VP_{\max} + H_{\min} - \frac{\Delta_a}{T_o} - D_{\max} + A_o + \frac{\Delta_a}{T_o}t \geq B_{\min}$$

which results to

$$A_o \geq B_{\min} + VP_{\max} - H_{\min} + D_{\max} + \frac{\Delta_a}{T_o} - \frac{\Delta_a}{T_o}t. \tag{4.69}$$

We need to determine the minimum possible value of A_o based on the sign of Δ_a.

1) If $\Delta_a \geq 0$: The minimum value of A_o in (4.69) is given by

$$A_{o,\min} = B_{\min} + VP_{\max} - H_{\min} + D_{\max} + \frac{\Delta_a}{T_o}. \tag{4.70}$$

As a result, A_t is given by

$$A_t = A_{o,\min} + \frac{\Delta_a}{T_o}t = B_{\min} + VP_{\max} - H_{\min} + D_{\max} + \frac{\Delta_a}{T_o} + \frac{\Delta_a}{T_o}t. \tag{4.71}$$

Based on Lemma 4.4.2, we have $S^*_{r,t} + Q^*_t = 0$ if $Z_t > H_{\max}$. Equivalently, if $Z_t - \frac{\Delta_a}{T_o} > H_{\max} - \frac{\Delta_a}{T_o}$, there will be no charging into the battery. When $Z_t - \frac{\Delta_a}{T_o} \leq H_{\max} - \frac{\Delta_a}{T_o}$, the maximum increasing amount of Z_t to Z_{t+1} in (4.19) in the next time slot is

$$Z_{t+1} \leq H_{\max} + R_{\max} - \frac{\Delta_a}{T_o}, \ \forall t. \tag{4.72}$$

Substituting A_t in (4.71) into (4.21), we have

$$\begin{aligned} Z_t &= B_t - \left(B_{\min} + VP_{\max} - H_{\min} + D_{\max} + \frac{\Delta_a}{T_o} + \frac{\Delta_a}{T_o} t \right) \\ &\leq H_{\max} + R_{\max} - \frac{\Delta_a}{T_o} \end{aligned} \tag{4.73}$$

where inequality (4.73) follows (4.72).

From inequality (4.73), we have

$$B_t \leq H_{\max} + R_{\max} - \frac{\Delta_a}{T_o} + B_{\min} + VP_{\max} - H_{\min} + D_{\max} + \frac{\Delta_a}{T_o} + \frac{\Delta_a}{T_o} t. \tag{4.74}$$

For the solution to be feasible, we need $B_t \leq B_{\max}$. This would be satisfied if RHS of (4.74) $\leq B_{\max}$. This can be satisfied if $V \in (0, V_{\max}]$ where $V_{\max}$ is given by

$$V_{\max} = \frac{B_{\max} - B_{\min} - R_{\max} - D_{\max} - 2\Gamma - \Delta_a}{P_{\max} + C'(\Gamma)}. \tag{4.75}$$

2) If $\Delta_a < 0$: The minimum value of A_o in (4.69) is given by

$$A_{o,\min} = B_{\min} + VP_{\max} - H_{\min} + D_{\max} + \frac{\Delta_a}{T_o} - \Delta_a. \tag{4.76}$$

As a result, A_t is given by

$$A_t = A_{o,\min} + \frac{\Delta_a}{T_o} t = B_{\min} + VP_{\max} - H_{\min} + D_{\max} + \Delta_a \frac{1 - T_o + t}{T_o}. \tag{4.77}$$

Substituting A_t in (4.77) into (4.21), we have

$$\begin{aligned} Z_t &= B_t - \left(B_{\min} + VP_{\max} - H_{\min} + D_{\max} + \Delta_a \frac{1 - T_o + t}{T_o} \right) \\ &\leq H_{\max} + R_{\max} - \frac{\Delta_a}{T_o}. \end{aligned} \tag{4.78}$$

where inequality (4.78) follows (4.72).

From inequality (4.78), we have

$$B_t \leq H_{\max} + R_{\max} - \frac{\Delta_a}{T_o} + B_{\min} + VP_{\max} - H_{\min} + D_{\max} + \Delta_a \frac{1 - T_o + t}{T_o}. \tag{4.79}$$

For the solution to be feasible, we need $B_t \leq B_{\max}$. This would be satisfied if RHS of (4.79) $\leq B_{\max}$. This can be satisfied if $V \in (0, V_{\max}]$ where $V_{\max}$ is given by

$$V_{\max} = \frac{B_{\max} - B_{\min} - R_{\max} - D_{\max} - 2\Gamma + \Delta_a}{P_{\max} + C'(\Gamma)}. \tag{4.80}$$

2) Lower Boundedness of B_t, i.e., $B_t \geq B_{\min}$: We now show that using $A_{o,\min}$ in (4.70) or (4.76) for $\Delta_a \geq 0$ or $\Delta_a < 0$, respectively, and $V \in (0, V_{\max}]$ with $V_{\max}$ in (4.75) or (4.80), respectively, we have $B_t \geq B_{\min}$ for all t.

1) If $\Delta_a \geq 0$: Substitute A_t in (4.71) and Z_t in (4.21) into (4.68), we have

$$\begin{aligned} & -VP_{\max} + H_{\min} - \frac{\Delta_a}{T_o} - D_{\max} \\ & \leq B_t - \left(B_{\min} + VP_{\max} - H_{\min} + D_{\max} + \frac{\Delta_a}{T_o} + \frac{\Delta_a}{T_o} t \right) \end{aligned}$$

which gives $B_{\min} + \frac{\Delta_a}{T_o} t \leq B_t$. Since $\frac{\Delta_a}{T_o} t > 0,\ \forall t,\ B_t \geq B_{\min}$ is satisfied for $\Delta_a \geq 0$.

2) If $\Delta_a < 0$: Substitute A_t in (4.77) and Z_t in (4.21) into (4.68), we have

$$\begin{aligned} & -VP_{\max} + H_{\min} - \frac{\Delta_a}{T_o} - D_{\max} \\ & \leq B_t - B_{\min} - VP_{\max} + H_{\min} - D_{\max} - \frac{\Delta_a}{T_o} + \Delta_a - \frac{\Delta_a}{T_o} t \end{aligned}$$

which gives $B_{\min} + \Delta_a \left(\frac{t}{T_o} - 1 \right) \leq B_t$. Since $\Delta_a \left(\frac{t}{T_o} - 1 \right) > 0,\ \forall t,\ B_t \geq B_{\min}$ is satisfied for $\Delta_a < 0$. ■

4.7.6 Proof of Theorem 1

Proof. A T-slot sample path Lyapunov drift is defined by $\Delta_T(\Theta_t) \triangleq L(\mathbf{\Theta}_{t+T}) - L(\mathbf{\Theta}_t)$. We upper bound it as follows

$$\Delta_T(\Theta_t) = \frac{1}{2} \left(Z_{t+T}^2 - Z_t^2 + H_{t+T}^2 - H_t^2 \right)$$

$$= Z_t \sum_{\tau=t}^{t+T-1} \left(Q_\tau + S_{r,\tau} - D_\tau - \frac{\Delta_a}{T_o} \right) + H_t \sum_{\tau=t}^{t+T-1} (\gamma_\tau - x_{u,\tau})$$
$$+ \frac{\left[\sum_{\tau=t}^{t+T-1} (\gamma_\tau - x_{u,\tau})\right]^2}{2} + \frac{\left[\sum_{\tau=t}^{t+T-1} \left(Q_\tau + S_{r,\tau} - D_\tau - \frac{\Delta_a}{T_o} \right)\right]^2}{2}$$
$$\leq Z_t \sum_{\tau=t}^{t+T-1} \left(Q_\tau + S_{r,\tau} - D_\tau - \frac{\Delta_a}{T_o} \right) + H_t \sum_{\tau=t}^{t+T-1} (\gamma_\tau - x_{u,\tau}) + GT^2 \quad (4.81)$$

where G is defined in Lemma 4.2.

Assume $T_o = MT$. We consider a per-frame optimization problem below, with the objective of minimizing the time-averaged system cost within the mth frame of length T time slots.

$$\mathbf{P_f}: \min_{\{\mathbf{a}_t, \gamma_t\}} \frac{1}{T} \sum_{t=mT}^{(m+1)T-1} [E_t P_t + x_{e,t} + C(\gamma_t)]$$
$$\text{s.t } (4.1),\ (4.2),\ (4.5),\ (4.9),\ (4.13),\ (4.14),\ (4.17) \text{ and } (4.18).$$

We show that $\mathbf{P_f}$ is equivalent to $\mathbf{P1}$ in which T_o is replaced by T. Let u_m^f denote the minimum objective value of $\mathbf{P_f}$. The optimal solution of $\mathbf{P1}$ satisfies all constraints of $\mathbf{P_f}$ and therefore is feasible to $\mathbf{P_f}$. Thus, we have $u_m^f \leq u_m^{\text{opt}}$. By Jensen's inequality and convexity of $C(\cdot)$, we have $\overline{C(\gamma)} \geq C(\overline{\gamma}) = C(\overline{x_u})$. Note that introducing the auxiliary variable γ_t with constraints (4.17) and (4.18) does not modify the problem. This means $u_m^f \geq u_m^{\text{opt}}$. Hence, we have $u_m^f = u_m^{\text{opt}}$ and $\mathbf{P_f}$ and $\mathbf{P1}$ are equivalent.

From (4.81) and the objective of $\mathbf{P_f}$, we have the T-slot drift-plus-cost metric for the mth frame upper bounded by

$$\Delta_T(\Theta_t) + V \left[\sum_{t=mT}^{(m+1)T-1} [E_t P_t + x_{e,t} + C(\gamma_t)] \right]$$
$$\leq Z_t \sum_{t=mT}^{(m+1)T-1} \left(Q_t + S_{r,t} - D_t - \frac{\Delta_a}{T_o} \right) + H_t \sum_{t=mT}^{(m+1)T-1} (\gamma_t - x_{u,t}) + GT^2$$
$$+ V \left[\sum_{t=mT}^{(m+1)T-1} [E_t P_t + x_{e,t} + C(\gamma_t)] \right]. \quad (4.82)$$

Let $\{\tilde{\mathbf{a}}_t, \tilde{\gamma}_t\}$ denote a pair of feasible solution of $\mathbf{P_f}$, satisfying the following relations

$$\sum_{t=mT}^{(m+1)T-1} \left(\tilde{Q}_t + \tilde{S}_{r,t}\right) = \sum_{t=mT}^{(m+1)T-1} \left(\tilde{D}_t + \frac{\Delta_a}{T_o}\right) \tag{4.83}$$

$$\sum_{t=mT}^{(m+1)T-1} \tilde{\gamma}_t = \sum_{t=mT}^{(m+1)T-1} \tilde{x}_{u,t} \tag{4.84}$$

with the corresponding objective value denoted as $\tilde{u}_m^f$.

Note that comparing with **P1**, we impose per-frame constraints (4.83) and (4.84) as oppose to (4.16) and (4.18) for the T_o-slot period. Let $\delta \geq 0$ denote the gap of $\tilde{u}_m^f$ to the optimal objective value u_m^{opt}, *i.e.*, $\tilde{u}_m^f = u_m^{\text{opt}} + \delta$.

Among all feasible control solutions satisfying (4.83) and (4.84), there exists a solution which leads to $\delta \to 0$. The upper bound in (4.82) can be rewritten as

$$\begin{aligned} &\Delta_T(\Theta_t) + V\left[\sum_{t=mT}^{(m+1)T-1} [E_t P_t + x_{e,t} + C(\gamma_t)]\right] \\ &\leq GT^2 + VT \lim_{\delta \to 0} \left(u_m^{\text{opt}} + \delta\right) = GT^2 + VT u_m^{\text{opt}}. \end{aligned} \tag{4.85}$$

Summing both sides of (4.85) over m for $m = 0, \ldots, M-1$, and dividing them by VMT, we have

$$\frac{L(\mathbf{\Theta}_{T_o}) - L(\mathbf{\Theta}_0)}{VMT} + \frac{1}{MT} \sum_{m=0}^{M-1} \sum_{t=mT}^{(m+1)T-1} [E_t P_t + x_{e,t} + C(\gamma_t)] \leq \frac{1}{M} \sum_{m=0}^{M-1} u_m^{\text{opt}} + \frac{GT}{V}. \tag{4.86}$$

Since $\overline{C(\gamma)} \geq C(\overline{\gamma})$ for the convex function $C(\cdot)$ where $\overline{\gamma} \triangleq \frac{1}{T_o} \sum_{t=0}^{T_o-1} \gamma_t$, from (4.86), we have

$$\left(\frac{1}{T_o} \sum_{t=0}^{T_o-1} E_t P_t\right) + \overline{x_e} + C(\overline{\gamma}) \leq \frac{1}{T_o} \sum_{t=0}^{T_o-1} [E_t P_t + x_{e,t} + C(\gamma_t)] \tag{4.87}$$

For a continuously differentiable convex function $f(\cdot)$, the following inequality holds [61]

$$f(x) \geq f(y) + f'(y)(x - y). \tag{4.88}$$

Applying (4.88) to $C(\overline{x_u})$ and $C(\overline{\gamma})$, we have

$$C(\overline{x_u}) \leq C(\overline{\gamma}) + C'(\overline{x_u})(\overline{x_u} - \overline{\gamma}) \leq C(\overline{\gamma}) + C'(\Gamma)(\overline{x_u} - \overline{\gamma}) = C(\overline{\gamma}) - C'(\Gamma)\frac{H_{T_o} - H_0}{T_o} \tag{4.89}$$

where the last term in (4.89) is obtained by summing both sides of (4.20) over T_o.

Applying the inequality (4.89) to $C(\overline{\gamma})$ at the LHS of (4.87), and further applying the inequality (4.87) to the LHS of (4.86), we have the following bound of the objective value $u^*(V)$ of **P1** achieved by Algorithm 1

$$u^*(V) - \frac{1}{M}\sum_{m=0}^{M-1} u_m^{\text{opt}} \leq \frac{GT}{V} + \frac{C'(\Gamma)(H_0 - H_{T_o})}{T_o} + \frac{L(\mathbf{\Theta}_0) - L(\mathbf{\Theta}_{T_o})}{VT_o}. \tag{4.90}$$

Note that H_t is bounded as in (4.67), and Z_t is bounded by (4.68) and (4.72). It follows that $L(\mathbf{\Theta}_t)$ is bounded. As $T_o \to \infty$, we have $\frac{C'(\Gamma)(H_0 - H_{T_o})}{T_o} \to 0$ and $\frac{L(\mathbf{\Theta}_0) - L(\mathbf{\Theta}_{T_o})}{VT_o} \to 0$. From (4.90), it follows that

$$\lim_{T_o \to \infty} u^*(V) \leq \lim_{T_o \to \infty} \frac{1}{M}\sum_{m=0}^{M-1} u_m^{\text{opt}} + \frac{GT}{V}. \qquad \blacksquare$$

4.7.7 Proof of Proposition 4.3

Proof. For $t = T_o$, from the dynamic shifting in (4.21), we have $Z_{T_o} = B_{T_0} - A_o - \frac{\Delta_a}{T_o}T_o$; For $t = 0$, we have $Z_0 = B_0 - A_o$. Thus, we have the following relation

$$\frac{Z_{T_o} - Z_0}{T_o} = \frac{B_{T_0} - A_o - \Delta_a - B_0 + A_o}{T_o} = \frac{B_{T_o} - B_0}{T_o} - \frac{\Delta_a}{T_o}.$$

Substituting (4.15) into the above equation, we have

$$\frac{Z_{T_o} - Z_0}{T_o} = \frac{\sum_{\tau=0}^{T_o-1} Q_\tau + S_{r,\tau} - F_\tau}{T_o} - \frac{\Delta_a}{T_o}. \tag{4.91}$$

Note that the queue Z_t in (4.19) is derived from (4.91). Since this finite time horizon algorithm, (4.16) is satisfied with error $\epsilon = Z_{T_o} - Z_0$. Because Z_t is bounded by (4.68)

and (4.72) and H_t is bounded by (4.67), the error ϵ has the following upper bound

$$|\epsilon| = |Z_{T_o} - Z_0| \leq H_{\max} + R_{\max} - \frac{\Delta_a}{T_o} + VP_{\max} - H_{\min} + \frac{\Delta_a}{T_o} + D_{\max}$$
$$\leq 2\Gamma + R_{\max} + VP_{\max} + VC'(\Gamma) + D_{\max}.$$

Thus, we complete the proof. ■

4.7.8 Proof of Proposition 4.4

Proof. From the objective function of $\mathbf{P4_{b2}}$, we see that the optimal control action $F_{s,t}$ is determined by the value of $Z_t - |H_t| + VP_{s,t}$. Similarly, E_t is determined by $Z_t - H_t + VP_{b,t}$ and $S_{r,t}$ is by $Z_t - H_t$. It is easy to see that, for $H_t \geq 0$, we only have one possible relation, given as

$$Z_t - H_t < Z_t - H_t + VP_{s,t} < Z_t - H_t + VP_{b,t}; \tag{4.92}$$

For $H_t < 0$, we have the following two possible relations

$$Z_t - H_t < Z_t + H_t + VP_{s,t} < Z_t - H_t + VP_{b,t} \tag{4.93}$$

$$Z_t + H_t + VP_{s,t} < Z_t - H_t < Z_t - H_t + VP_{b,t}. \tag{4.94}$$

From the relations (4.92)-(4.94), we have the following conditions for the control action.

1 For any value of H_t, if $Z_t - H_t + VP_{b,t} \leq 0$, E_t has to be as large as possible to minimize the objectives of $\mathbf{P4_b}$. If $Z_t - H_t + VP_{b,t} > 0$, E_t has to be as small as possible and only ensure the demand balance (3.8) being satisfied.

2 For any value of H_t, if $Z_t - |H_t| + VP_{s,t} \geq 0$, $F_{s,t}$ has to be as large as possible; If $Z_t - |H_t| + VP_{s,t} < 0$, $F_{s,t} = 0$ can achieve the minimum objective value.

3 For any value of H_t, if $Z_t - H_t \leq 0$, $S_{r,t}$ has to be as large as possible; If $Z_t - H_t > 0$, $S_{r,t} = 0$ can achieve the minimum objective value.

4 Due to $VP_{s,t} > 0$, $S_{s,t}$ is not controlled by (4.92)-(4.94).

5 If $S'_{r,t}(Z_t - H_t) + VC_{\text{rc}} < -S'_{s,t}VP_{s,t}$, the remaining amount $S_t - S_{w,t}$ is used to first charge the battery Otherwise, the remaining amount is used to first sell back to the grid. This means the remaining amount $S_t - S_{w,t}$ is first used to whichever action achieves lower objective value.

We use the relations (4.92)-(4.94) to solve $\mathbf{P4_b}$. We show the solution in each case below.

1) For $Z_t - H_t + VP_{b,t} \leq 0$: From condition 1, we could choose to set E_t as large as possible to minimize the objective of $\mathbf{P4}_b$. This means that $1_{R,t} = 1$ and $1_{D,t} = 0$, and we achieve maximum charging rate, *i.e.,* $S_{r,t} + Q_t = R_{\max}$. We determine $S_{r,t}$ and $S_{s,t}$ by condition 5. In this case, due to charging, the entrance cost for charging C_{rc} needs to be paid. Alternatively, we could let the battery stay idle instead of charging, *i.e.,* $S_{r,t} + Q_t = 0$. In this case, $C_{\text{rc}}1_{R,t} = 0$, but E_t is smaller and $S_{r,t} = 0$. The optimal $\mathbf{a}_t^*$ is the one that achieves the minimum objective value.

2) For $\min\{Z_t - H_t, Z_t - |H_t| + VP_{s,t}\} > 0$: From conditions 1-3, we could choose to set E_t and $S_{r,t}$ as small as possible, thus $E_t = Q_t = 0$, and to set $F_{s,t}$ as large as possible to minimize the objective of $\mathbf{P4}_b$; This means that $1_{D,t} = 1$ and $1_{R,t} = 0$. To achieve maximum sell-back amount $U_{\max}$, if $-F_{s,t}(Z_t - |H_t| + VP_{s,t}) < -S_{s,t}VP_{s,t}$, we selling is first from the battery, then the renewable. Otherwise, we sell first from the renewable. Alternatively, we could let the battery stay idle instead of discharging,

i.e., $F_{s,t} + F_{d,t} = 0$. In this case, $C_{\text{dc}} 1_{D,t} = 0$. The optimal $\mathbf{a}_t^*$ is the one that achieves the minimum objective value.

3) For $\max\{Z_t - H_t, Z_t - |H_t| + VP_{s,t}\} < 0 \leq Z_t - H_t + VP_{b,t}$: We could choose to set E_t and $F_{s,t}$ as small as possible. This means the charging is only from $S_{r,t}$, but not from Q_t. Similar to case 1), we determine $S_{r,t}$ and $S_{s,t}$ by condition 5. When $S_{w,t} = W_t$, it is possible that $S_t - S_{w,t} > 0$. In this case, there is no need for discharging, *i.e.,* $F_{d,t} = 0$, and the battery could charge $S_{r,t} > 0$. On the other hand, when $S_{w,t} < W_t$, *i.e.,* S_t is fully used to supply demand W_t, $S_{r,t} = 0$. To meet demand, we could either purchase E_t and/or let battery discharge $F_{d,t}$. Charging or discharging will incur entrance cost C_{rc} or C_{dc}, respectively. There exists an alternatively way which is to keep the battery idle. Thus, the optimal $\mathbf{a}_t^*$ is chosen by whichever achieves the minimum objective value.

4) For $Z_t - H_t < 0 < Z_t - |H_t| + VP_{s,t}$: This is the condition when (4.92) and (4.93) hold. Under this case, we could choose to maximize $S_{r,t}$ and $F_{s,t}$ and minimize E_t to minimize the objective of $\mathbf{P4}_b$. But, due to constraint (3.5), we have to satisfy $S_{r,t} \cdot F_{s,t} = 0$. If set $F_{s,t} \geq 0$ and $S_{r,t} = 0$, it means the remaining amount $S_t - S_{w,t}$, if any, will be only used for sell. Due to $Z_t < H_t$ for $\forall H_t$, we have $0 < Z_t - |H_t| + VP_{s,t} < VP_{s,t}$. Thus, $S_{s,t}$ is prior to $F_{s,t}$; If set $S_{r,t} \geq 0$ and $F_{s,t} = 0$, we only charge battery from $S_{r,t}$. There is no selling from battery. The control action $\mathbf{a}_t'$ is chosen from whichever achieve the less value for the objective. The alternative way is to keep the battery idle. Thus, the optimal $\mathbf{a}_t^*$ is chosen by whichever achieves the minimum objective value.

5) For $H_t < 0$ *and* $Z_t + H_t + VP_{s,t} < 0 < Z_t - H_t$: This condition is specifically for

(4.94). Based on conditions 1-5, it is straightforward to obtain $\mathbf{a}'_t$. After comparing to the alternative idle battery option, the optimal $\mathbf{a}^*_t$ is chosen by whichever achieves the minimum objective value. ■

4.7.9 Proof of Proposition 4.7

Proof. To ensure (4.39) is satisfied, we must show that the optimal control solution (4.52)-(4.58) in Proposition 4.4 can ensure (4.39) to be satisfied.

For cases 1,3 and 5, from their optimal control solutions (4.52), (4.55) and (4.58), it is easy to see that (4.39) is satisfied;

For cases 2 and 4, from their optimal control solutions (4.53) or (4.54) and (4.56) or (4.57), if $F'_{d,t} = W_t - S_{w,t} < D_{\max}$, it means $E'_t = 0$ and $F_{s,t} \geq 0$; If $F'_{d,t} = D_{\max}$, we have $F'_{s,t} = 0$ and $E'_t \geq 0$. Thus, (4.39) is satisfied.

For idle state, *i.e.,* battery is in idle, we always have $F^{\text{id}}_{s,t} = 0$. Thus, (4.39) is a sufficient condition for our algorithm 1. ■

Chapter 5

Real-Time Joint Energy Storage Management and Load Scheduling with Renewable Integration

In the previous chapter, an energy storage management problem is considered without flexible user loads. Given the individual load modeling, delay constraints considered and the load interaction with energy usage over time, the extension to the joint design of load scheduling and energy storage management is highly non-trivial for both algorithm design and performance analysis. In this chapter, we develop a joint energy storage management and load scheduling problem to achieve more cost saving for consumer.

5.1 System Model

We consider an electricity consuming entity (residential home or business site) powered by the conventional grid and a local renewable generator (RG) (*e.g.,* wind or solar generators). An energy storage unit (battery) is co-located with RG and can store energy from both power sources and supply power for the user's loads. The energy storage management (ESM) system is shown in Fig. 5.1. As a part of the ESM

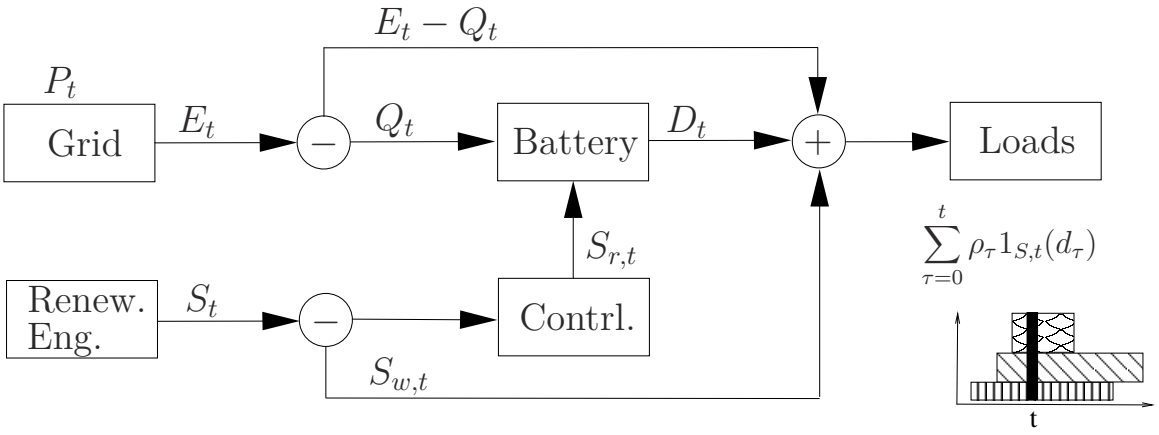

Figure 5.1: The residential energy storage management system.

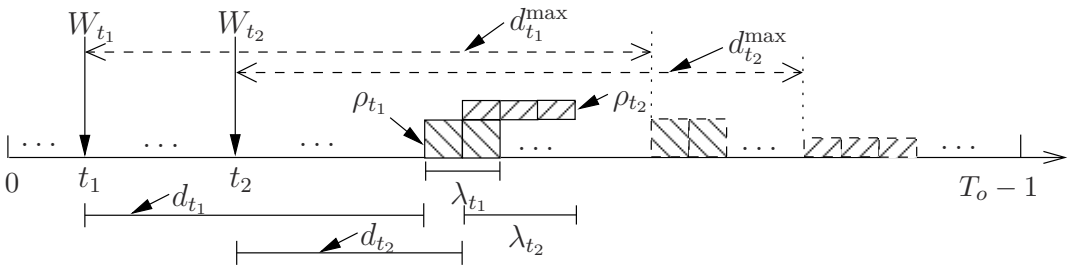

Figure 5.2: An example of load scheduling for two arrival loads W_{t_1} and W_{t_2}.

system, a load scheduling mechanism is implemented to schedule each load within its delay requirement. We assume the ESM system operates in discrete time slots with $t \in \{0, 1, \cdots\}$, and all operations are performed per time slot t. Each component of the EMS system is described below.

5.1.1 Load Scheduling

We assume the user has load tasks in various types arriving over time slots. An example of the scheduling time line of two loads is shown in Fig. 5.2. Let W_t denote the load that arrives at the beginning of time slot t. It is given by $W_t = \rho_t \lambda_t$, where ρ_t and λ_t are the load intensity and duration for W_t, respectively. We assume the load duration is an integer in multiple of time slots, and the minimum duration for

any load is 1, *i.e.,* $\lambda_t \in \{1, 2, \ldots\}$. Let $d_t^{\max}$ denote the maximum allowed delay for the load W_t before it is served (in multiple of time slots), and let d_t denote the actual scheduling delay incurred for W_t. We have

$$d_t \in \{0, 1 \ldots, d_t^{\max}\}, \ \forall t. \tag{5.1}$$

Thus, the earliest serving time duration for W_t is $[t, t + \lambda_t]$, and the latest serving time duration is $[t + d_t^{\max}, t + d_t^{\max} + \lambda_t]$. We define an indicator function $1_{S,t}(d_\tau) \triangleq \{1 : \text{if } t \in [\tau + d_\tau, \tau + d_\tau + \lambda_\tau);\ 0 : \text{otherwise}\}$, for $\forall \tau \leq t$. It indicates whether or not the load W_τ is being served at time slot t. Consider a T_o-slot period. We define $\overline{d_w}$ as the average scheduling delay of all arrived loads within this T_o-slot period, given by[1]

$$\overline{d_w} \triangleq \frac{1}{T_o} \sum_{\tau=0}^{T_o-1} d_\tau. \tag{5.2}$$

Besides the per load maximum delay $d_t^{\max}$ constraint in (5.1), we impose a constraint on the average delay $\overline{d_w}$ as

$$\overline{d_w} \in [0, d^{\max}] \tag{5.3}$$

where $d^{\max}$ is the maximum average delay for the loads within the T_o-slot period. It is straightforward to see that for the constraint (5.3) to be effective, we have $d^{\max} \leq \max_{t \in [0, T_o - 1]} \{d_t^{\max}\}$, for $\forall t$. The average delay $\overline{d_w}$ reflects the average quality of service for the loads within the T_o-slot period. We define a cost function $C_d(\overline{d_w})$ associated with $\overline{d_w}$. A longer delay reduces the quality of service and incurs a higher cost. Thus, we assume $C_d(\cdot)$ to be a continuous, convex, non-decreasing function with maximum derivative $C_d'(\cdot) < \infty$.

[1]Without loss of generality, we start the T_o-period at time slot $t = 0$.

5.1.2 Energy Sources and Storage

Since the storage model for power sources and battery operation has been similarly defined in Section 3.1, we summarize the identical equations with brief explanation and highlight the difference.

Power Sources: The user can purchase energy from the conventional grid with a real-time price P_t. The purchased amount E_t is bounded by

$$E_t \in [0, E_{\max}]\,. \tag{5.4}$$

The average cost for the purchased energy from the grid over a T_o-slot period is defined by $\overline{J} \triangleq \frac{1}{T_o}\sum_{t=0}^{T_o-1} E_t P_t$.

Renewable generator: An RG is used as an alternative energy source in the ESM system. Let S_t denote the amount of renewable energy harvested at time slot t. We assume S_t is first used to supply the currently scheduled loads. Denote this portion by $S_{w,t}$, we have

$$S_{w,t} = \min\left\{\sum_{\tau=0}^{t} \rho_\tau 1_{S,t}(d_\tau), S_t\right\} \tag{5.5}$$

where the first term in (5.5) represents the total energy over those scheduled loads that need to be served at time slot t (See Fig. 5.1 at time slot $t_2 + d_{t_2}$ for example). The remaining portion of S_t, if any, can be stored into the battery. Since there is a cost associated to the battery charging activity, we use a controller to determine whether or not to store the remaining portion into the battery. Let $S_{r,t}$ denote the amount of renewable energy charged into the battery at time slot t. It is bounded by

$$S_{r,t} \in [0, S_t - S_{w,t}]\,. \tag{5.6}$$

Battery Operation: The total charging amount at time slot t is bounded by

$$Q_t + S_{r,t} \in [0, R_{\max}]\,. \tag{5.7}$$

Similarly, the discharging amount from the battery at time slot t is bounded by

$$D_t \in [0, D_{\max}]\,. \tag{5.8}$$

We assume there is no simultaneous charging and discharging activities at the battery, *i.e.,*

$$(Q_t + S_{r,t}) \cdot D_t = 0. \tag{5.9}$$

With a finite capacity, B_t is bounded by

$$B_t \in [B_{\min}, B_{\max}]\,. \tag{5.10}$$

The dynamics of B_t over time due to charging and discharging activities are given by

$$B_{t+1} = B_t + Q_t + S_{r,t} - D_t. \tag{5.11}$$

The entry cost at time slot t is given by $x_{e,t} \triangleq 1_{R,t}C_{\rm rc} + 1_{D,t}C_{\rm dc}$. Thus, the time-averaged entry cost over the T_o-slot period is $\overline{x_e} \triangleq \frac{1}{T_o}\sum_{t=0}^{T_o-1} x_{e,t}$.

The net amount of energy change in battery at time slot t due to charging or discharging is given by $x_{u,t} = |Q_t + S_{r,t} - D_t|$. From (5.7) and (5.8), it follows that $x_{u,t}$ is bounded by

$$x_{u,t} \in [0, \max\{R_{\max}, D_{\max}\}]\,. \tag{5.12}$$

We model the usage cost as a function of $\overline{x_u}$, which is $C_u(\overline{x_u})$. We assume $C_u(\overline{x_u})$ is a continuous, convex, non-decreasing function with maximum derivative $C_u'(\overline{x_u}) < \infty$.

Based on the above, the average battery degradation cost over the T_o-slot period due to charging/discharging activities is given by $\overline{x_e} + C_u(\overline{x_u})$.

5.1.3 Supply and Demand Balance

For each load W_{t_o} arrived at time slot t_o, if it is scheduled to be served at time slot t ($\geq t_o$), the energy supply needs to meet the amount ρ_{t_o} scheduled for W_{t_o}. The overall energy supply must be equal to the total demands from those loads which need to be served at time slot t. Thus, we have supply and demand balance relation given by

$$E_t - Q_t + S_{w,t} + D_t = \sum_{\tau=0}^{t} \rho_\tau 1_{S,t}(d_\tau), \quad \forall t. \tag{5.13}$$

5.2 Joint Energy Storage Management and Load Scheduling: Problem Formulation

Our goal is to jointly optimize the load scheduling and energy flows and storage control for the ESM system to minimize an overall system cost over the T_o-slot period. Note that the loads, renewable energy, and pricing $\{W_t, S_t, P_t\}$ are the random inputs to the ESM system. Their complicated statistical behaviors are often difficult to acquire or predict. For example, for S_t generated from a renewable source such as solar, it is not only correlated over time, but also typically non-stationary over time. Thus, assuming certain known statistics on the process $\{S_t\}$ would not be realistic in practice. The same applies for $\{W_t\}$ and $\{P_t\}$. In light of this, in this work, we assume arbitrary dynamics for $\{W_t, S_t, P_t\}$ and do not assume their statistical knowledge is known. We intend to design a real-time control algorithm that is able to handle such arbitrary and unknown system inputs.

We model the overall system cost as a weighted sum of the cost from energy purchase and battery degradation, and the cost of scheduling delay. Define $\mathbf{a}_t \triangleq [E_t, Q_t, D_t, S_{w,t}, S_{r,t}]$ as the control action vector for the energy flow in the ESM system

at time slot t. Our goal is to optimize $\{\mathbf{a}_t, d_t\}$ to minimize the time-averaged system cost. This optimization problem is formulated as follows

$$\mathbf{P1:} \min_{\{\mathbf{a}_t, d_t\}} \ \overline{J} + \overline{x_e} + C_u(\overline{x_u}) + \alpha C_d(\overline{d_w})$$

$$\text{s.t.} \ \ (5.1), (5.3), (5.4), (5.6), (5.9), (5.13), \text{and}$$

$$0 \leq S_{r,t} + Q_t \leq \min\left\{R_{\max}, B_{\max} - B_t\right\} \tag{5.14}$$

$$0 \leq D_t \leq \min\left\{D_{\max}, B_t - B_{\min}\right\}. \tag{5.15}$$

where α is the positive weight for the cost of scheduling delay. It sets the relative weight between energy related cost and delay incurred in load scheduling in the joint optimization.

P1 is a finite time horizon stochastic joint optimization problem which is difficult to solve. It possesses the following challenges: The finite battery capacity imposes a hard constraint on the control actions $\{\mathbf{a}_t\}$. The constraints (5.14) and (5.15) on charging and discharging amounts depend on the SOB B_t. Due to the time-coupling dynamics of B_t in (5.11), this causes $\{\mathbf{a}_t\}$ being correlated over time. Furthermore, joint energy storage control and load scheduling complicates the problem which make it much more challenging than each separate problem alone. Finally, for the problem considered, the finite time horizon problem is much more difficult to tackle than the infinite time horizon problem as considered in most existing energy storage works. The techniques developed in the infinite time horizon problem no longer holds when a finite period is considered and new techniques need to be developed for a real-time control solution.

Instead of solving **P1**, in this work, we focus on proposing a real-time algorithm

to provide a suboptimal solution to **P1** which has a bounded guarantee of its sub-optimality. To do this, we first apply a sequence of modification and transformation of **P1**, which allows us to design a real-time algorithm for joint energy storage control and load scheduling at every time slot. Then, we discuss how our real-time solution can meet the constraints of **P1**.

5.2.1 Problem Modification

As mentioned above, due to finite battery capacity constraint, the control actions $\{\mathbf{a}_t\}$ is coupled over time. To remove this time coupling, similar to the technique used in Chapter 4 for energy storage only problem, we remove the finite battery capacity constraint, and instead, we impose a constraint on the change of battery energy level over the T_o-slot period. Specifically, by (5.11), the change of battery energy level over the T_o-slot period is $B_{T_o} - B_0 = \sum_{t=0}^{T_o-1} (Q_t + S_{r,t} - D_t)$. We now set this change to be a desired value Δ_u, *i.e.,*

$$\sum_{t=0}^{T_o-1} (Q_t + S_{r,t} - D_t) = \Delta_u. \tag{5.16}$$

Note that, Δ_u is only a desired value we set, which may not be achieved by an control algorithm at the end of T_o-slot period. We will quantify the amount of mismatch with respect to Δ_u under our proposed control algorithm in Section 5.4. By the battery capacity and (dis)charging constraint, it is easy to see that $|\Delta_u| \leq \Delta_{\max} \triangleq \min\{B_{\max} - B_{\min}, T_o \max\{R_{\max}, D_{\max}\}\}$.

We now modify **P1** to the follow optimization problem by adding the new con-

straint (5.16), and removing the battery capacity constraint (5.10)

$$\textbf{P2:} \min_{\{\mathbf{a}_t, d_t\}} \ \overline{J} + \overline{x_e} + C_u(\overline{x_u}) + \alpha C_d(\overline{d_w})$$
$$\text{s.t. } (5.1), (5.3) - (5.9), (5.13), (5.16).$$

Note that by removing the battery capacity constraint (5.10), we remove the dependency of per-slot charging/discharging amount on B_t in constraints (5.14) and (5.15), and replace them by (5.7) and (5.8), respectively.

5.2.2 Problem Transformation

In **P2**, both battery average usage cost $C_u(\overline{x_u})$ and scheduling delay cost $C_d(\overline{d_w})$ are functions of time-averaged variables, which complicates the problem. Using the technique introduced in [57], we now transform the problem into one that only contains the time-average of the functions. Specifically, we introduce auxiliary variables $\gamma_{u,t}$ and $\gamma_{d,t}$ for $x_{u,t}$ and d_t, respectively, and impose the following constraints

$$0 \leq \gamma_{u,t} \leq \max\{R_{\max}, D_{\max}\}, \ \forall t \tag{5.17}$$

$$\overline{\gamma_u} = \overline{x_u} \tag{5.18}$$

$$0 \leq \gamma_{d,t} \leq \min\{d_t^{\max}, d^{\max}\}, \ \forall t \tag{5.19}$$

$$\overline{\gamma_d} = \overline{d_w} \tag{5.20}$$

where $\overline{\gamma_i} \triangleq \frac{1}{T_o}\sum_{\tau=0}^{T_o-1}\gamma_{i,t}$, for $i = u, d$. The above constraints ensure that each auxiliary variable lies in the same range as its original variable, and its time average is the same as that of its original variable. Define $\overline{C_i(\gamma_i)} \triangleq \frac{1}{T_o}\sum_{t=0}^{T_o-1} C_i(\gamma_{i,t})$ as the time average of $C_i(\gamma_{i,t})$ over T_o slots, for $i = u, d$. Applying (5.18) and (5.20) to the objective of **P2**,

and defining $\boldsymbol{\pi}_t \triangleq [\mathbf{a}_t, d_t, \gamma_{u,t}, \gamma_{d,t}]$, we transform **P2** into the following optimization problem

$$\textbf{P3:} \min_{\{\boldsymbol{\pi}_t\}} \quad \overline{J} + \overline{x_e} + \overline{C_u(\gamma_u)} + \alpha\overline{C_d(\gamma_d)}$$

$$\text{s.t.} \quad (5.1), (5.3) - (5.9), (5.13), (5.16) - (5.20)$$

where the terms in the objective are all T_o-slot time-averaged cost functions. The equivalence of **P2** and **P3** is given in the following lemma.

Lemma 5.1. P2 *and* **P3** *are equivalent, with the same optimal objective values and optimal control solution* $\{\mathbf{a}_t^*, d_t^*\}$.

Proof. See Appendix 5.6.1.

Although **P3** is still difficult to solve, it enables us to design a dynamic control and scheduling policy for joint energy storage control and load scheduling by adopting Lyapunov optimization technique [25]. In the following, we propose our real-time algorithm for **P3**, and then design parameters to ensure the proposed solution meets the battery capacity constraint imposed in the original **P1** which is removed in **P2**.

5.3 Joint Energy Storage Management and Load Scheduling: Real-Time Algorithm

By Lyapunov optimization technique, we first introduce virtual queues for each time-averaged inequality and equality constraints of **P3** to transform them into queue stability problems. Then, we design a real-time algorithm based on minimizing the drift of Lyapunov function defined on these virtual queues.

5.3.1 Virtual Queues

We introduce a virtual queue X_t to meet constraint (5.3), evolving as follows

$$X_{t+1} = \max\left(X_t + d_t - d^{\max}, 0\right). \tag{5.21}$$

From (5.2), the above results in $\overline{d_w} \leq d^{\max} + (X_{T_o} - X_0)/T_o$. Thus, formulating the virtual queue X_t in (5.21) will guarantee to meet the average delay constraint (5.3) with a margin $(X_{T_o} - X_0)/T_o$. In Section 5.4, we will further discuss this constraint under our proposed algorithm.

For constraint (5.16), dividing both sides by T_o gives the time-averaged net change of battery energy level per slot being $\frac{\Delta_u}{T_o}$. To meet this constraint, we introduce a virtual queue Z_t, evolving as follows

$$Z_{t+1} = Z_t + Q_t + S_{r,t} - D_t - \frac{\Delta_u}{T_o}. \tag{5.22}$$

From B_t in (5.11) and Z_t above, we can show that they are different by a time-dependent shift as follows

$$Z_t = B_t - A_t, \text{ where } A_t \triangleq A_o + \frac{\Delta_u}{T_o}t. \tag{5.23}$$

The linear time function $\frac{\Delta_u}{T_o}t$ in A_t is to ensure that constraint (5.16) is satisfied. Due to this shift A_t, the range of Z_t is expanded to the entire real line, *i.e.,* $Z_t \in \mathbb{R}$ for $B_t \in \mathbb{R}^+$. Note that A_o is a design parameter. Later, we design A_o to ensure that our control solution $\{\mathbf{a}_t\}$ for the energy flows in our proposed algorithm satisfies the battery capacity constraint (5.10) imposed in **P1**.

Finally, to meet constraints (5.18) and (5.19), we establish virtual queues $H_{u,t}$

and $H_{d,t}$, respectively, as follows

$$H_{u,t+1} = H_{u,t} + \gamma_{u,t} - x_{u,t} \tag{5.24}$$

$$H_{d,t+1} = H_{d,t} + \gamma_{d,t} - d_t. \tag{5.25}$$

From the Lyapunov optimization, it can be shown that satisfying constraints (5.3), (5.16), (5.18), and (5.19) is equivalent to maintaining the stability of queues X_t, Z_t, $H_{u,t}$, and $H_{d,t}$, respectively [25].

5.3.2 Real-Time Algorithm

Note that Z_t and $H_{u,t}$ are the virtual queues related to the battery operation, while X_t and $H_{d,t}$ are those related to the scheduling delay. Let $\mathbf{\Theta}_t \triangleq [Z_t, H_{u,t}, X_t, H_{d,t}]$ denote the virtual queue vector. We define the quadratic Lyapunov function $L(\mathbf{\Theta}_t)$ for $\mathbf{\Theta}_t$ as follows

$$L(\mathbf{\Theta}_t) \triangleq \frac{1}{2}\left[Z_t^2 + H_{u,t}^2 + \mu\left(X_t^2 + H_{d,t}^2\right)\right] \tag{5.26}$$

where μ is a positive weight which is used to adjust the relative importance of delay related queues in the Lyapunov function. We define a one-slot sample path Lyapunov drift as $\Delta(\mathbf{\Theta}_t) \triangleq L\left(\mathbf{\Theta}_{t+1}\right) - L(\mathbf{\Theta}_t)$, which only depends on the current system inputs $\{W_t, S_t, P_t\}$.

Instead of directly minimizing the system cost objective in **P3**, we consider the *drift-plus-cost* metric given by $\Delta(\mathbf{\Theta}_t) + V[E_t P_t + x_{e,t} + C_u(\gamma_{u,t}) + \alpha C_d(\gamma_{d,t})]$. It is a weighted sum of the drift $\Delta(\mathbf{\Theta}_t)$ and the system cost at time slot t with $V > 0$ being the relative weight between the two terms.

Rather directly using the drift-plus-cost function which is still challenging, in the following, we will use an upper bound of this drift-plus-cost function to design our real-time algorithm. The upper bound is derived in Appendix 5.6.2 as (5.39). Using this upper bound, we formulate a per-slot real-time optimization problem and solve it at every time slot t. By removing all the constant terms independent of control action $\boldsymbol{\pi}_t$, we arrive at the following optimization problem

$$\begin{aligned}\mathbf{P4}: \min_{\boldsymbol{\pi}_t} \; & Z_t\left[E_t + S_{r,t} + S_{w,t} - \rho_t 1_{S,t}(d_t)\right] - |H_{u,t}|\, S_{w,t} \\ & + H_{u,t}\left[\gamma_{u,t} - (E_t + S_{r,t})\right] + |H_{u,t}|\, \rho_t 1_{S,t}(d_t) + \mu X_t d_t + \mu H_{d,t}(\gamma_{d,t} - d_t) \\ & + V\left[E_t P_t + x_{e,t} + C_u(\gamma_{u,t}) + \alpha C_d(\gamma_{d,t})\right] \\ \text{s.t.} \;\; & (5.1), (5.4) - (5.9), (5.13), (5.17), (5.19).\end{aligned}$$

Note that the term $\sum_{\tau=0}^{t} \rho_\tau 1_{S,t}(d_\tau)$ in the upper bound (5.39) is the total energy demand from the scheduled loads at time slot t. Since delay d_τ for $\tau \in \{0, 1, \ldots, t-1\}$ are determined in previous time slot $\tau \leq t-1$ by solving $\mathbf{P4}$, only $\rho_t 1_{S,t}(d_t)$ is a function of $\boldsymbol{\pi}_t$ at time slot t, and is part of the objective of $\mathbf{P4}$.

Denote the optimal solution of $\mathbf{P4}$ by $\boldsymbol{\pi}_t^* \triangleq [\mathbf{a}_t^*, d_t^*, \gamma_{u,t}^*, \gamma_{d,t}^*]$. After regrouping the terms in the objective of $\mathbf{P4}$ with respect to different control variables, we show that $\mathbf{P4}$ can be separated into four sub-problems to be solved sequentially and variables in $\boldsymbol{\pi}_t^*$ can be determined separately. The steps are described below.

S1) Determine d_t^* and $\gamma_{d,t}^*$ by solving the following $\mathbf{P4_{a1}}$ and $\mathbf{P4_{a2}}$, respectively.

$$\mathbf{P4_{a1}}: \min_{d_t} \;\; \mu d_t(X_t - H_{d,t}) - \rho_t 1_{S,t}(d_t)\left(Z_t - |H_{u,t}|\right) \quad \text{s.t. } (5.1).$$

$$\mathbf{P4_{a2}}: \min_{\gamma_{d,t}} \;\; \mu H_{d,t}\gamma_{d,t} + V\alpha C_d(\gamma_{d,t}) \quad \text{s.t. } (5.19).$$

S2) Determine $S^*_{w,t}$ in (5.5) using d^*_t obtained in S1).

S3) Using $S^*_{w,t}$ obtained in S2) in (5.13), determine $\gamma^*_{u,t}$ and $\mathbf{a}^*_t$ by solving the following $\mathbf{P4_{b1}}$ and $\mathbf{P4_{b2}}$, respectively.

$$\mathbf{P4_{b1}}: \min_{\gamma_{u,t}} \; H_{u,t}\gamma_{u,t} + VC_u(\gamma_{u,t}) \quad \text{s.t. (5.17).}$$

$$\mathbf{P4_{b2}}: \min_{\mathbf{a}_t} \; E_t(Z_t - H_{u,t} + VP_t) + S_{r,t}(Z_t - H_{u,t}) + V\left(1_{R,t}C_{\rm rc} + 1_{D,t}C_{\rm dc}\right)$$
$$\text{s.t.} \quad (5.4) - (5.9), (5.13).$$

Remark: An important and interesting observation of the above is that the joint optimization of load scheduling and energy storage control can in fact be separated: The scheduling decision (*i.e.,* d^*_t) is determined first in $\mathbf{P4_{a1}}$; Based on the resulting energy demand in the current time slot t, energy storage control decision (*i.e.,* $\mathbf{a}^*_t$) is then determined in $\mathbf{P4_{b2}}$. The two sub-problems are connected through the current virtual queue backlogs Z_t and $H_{u,t}$ related to the battery operation.

In the following, we solve each subproblem to obtain a closed-form solution. Thus, the optimal solution of $\boldsymbol{\pi}_t$ is obtained in closed-form, and our proposed algorithm bears minimum complexity and very simple to implement.

1) The optimal d^*_t: The optimal scheduling delay d^*_t for $\mathbf{P4_{a1}}$ is given below.

Proposition 5.1. *Let* $\omega_o \triangleq -\rho_t\left(Z_t - |H_{u,t}|\right)$, $\omega_1 \triangleq \mu\left(X_t - H_{d,t}\right)$, *and* $\omega_{d_t^{\max}} \triangleq \mu d_t^{\max}(X_t - H_{d,t})$.

1. *If* $X_t - H_{d,t} \geq 0$, *then*

$$d^*_t = \begin{cases} 0 & \textit{if } \omega_o \leq \omega_1 \\ 1 & \textit{otherwise}; \end{cases} \tag{5.27}$$

2. If $X_t - H_{d,t} < 0$, then

$$d_t^* = \begin{cases} 0 & \text{if } \omega_o \leq \omega_{d_t^{\max}} \\ d_t^{\max} & \text{otherwise.} \end{cases} \tag{5.28}$$

Proof. See Appendix 5.6.3.

Remark: Note that ω_o, ω_1, and $\omega_{d_t^{\max}}$ are the objective values of $\mathbf{P4_{a1}}$ when $d_t = 0, 1$, and $d_t^{\max}$, respectively. Furthermore, w_o depends on the virtual queue backlogs (Z_t and $H_{u,t}$) related to battery energy level, while ω_1 and $\omega_{d_t^{\max}}$ depend on the virtual queue backlogs (X_t and $H_{d,t}$) related to delay. Proposition 5.1 shows that the scheduling decision for load W_t is to either immediately serve it ($d_t^* = 0$) or delay its serving time ($d_t^* = 1$ or $d_t^{\max}$). This decision depends on whether the battery energy is high enough (so W_t will be served immediately) or the scheduling delays for the loads so far are low enough (so W_t will be delayed). When the load is delayed to serve, the delay should be either minimum or maximum depending on the existing scheduling delays of the past loads.

2) The optimal $\gamma_{d,t}^*$ and $\gamma_{u,t}^*$: Since $C_d(\cdot)$ and $C_u(\cdot)$ are both convex, the objective of $\mathbf{P4_{a2}}$ and $\mathbf{P4_{b1}}$ are convex. Let $C_i'(\cdot)$ denote the first derivative of $C_i(\cdot)$, and $C_i'^{-1}(\cdot)$ denote the inverse function of $C_i'(\cdot)$, for $i = d, u$. We obtain the optimal solution $\gamma_{i,t}^*$ for $\mathbf{P4_{a2}}$ and $\mathbf{P4_{b1}}$ as follows.

Lemma 5.2. *The optimal solution $\gamma_{i,t}^*$ for $i = d, u$ is given by*

$$\gamma_{i,t}^* = \begin{cases} 0 & \text{if } H_{i,t} \geq 0 \\ \Gamma_i & \text{if } H_{i,t} < -V\beta_i C_i'(\Gamma_i) \\ C_i'^{-1}\left(-\frac{H_{i,t}}{V\beta_i}\right) & \text{otherwise.} \end{cases} \tag{5.29}$$

where $\beta_u = 1$, $\beta_d = \frac{\alpha}{\mu}$, $\Gamma_u \triangleq \max\{R_{\max}, D_{\max}\}$, and $\Gamma_d \triangleq \min\{d_t^{\max}, d^{\max}\}$.

Proof. See Appendix 5.6.4.

3) The optimal $\mathbf{a}_t^*$: Once the scheduling decision d_t^* for W_t is determined, the total energy demand from the scheduled loads, *i.e.,* $\sum_{\tau=0}^{t} \rho_\tau 1_{S,t}(d_\tau^*)$, is determined. Given this energy demand, $\mathbf{P4_{b2}}$ is solved to obtain the optimal control solution $[E_t^*, Q_t^*, D_t^*, S_{r,t}^*]$ in $\mathbf{a}_t^*$. This subproblem for energy storage and control is essentially the same as in Chapter 4, where the energy storage only problem is considered. Thus, the solution can be readily obtained from Appendix 4.7.4. Here we directly state the result.

Define $L_t^* \triangleq \sum_{\tau=0}^{t} \rho_\tau 1_{S,t}(d_\tau^*)$ as the current energy demand at time slot t. Define the idle state of the battery as the state where there is no charging or discharging activity. The control solution under this idle state is denoted by $[E_t^{\text{id}}, Q_t^{\text{id}}, D_t^{\text{id}}, S_{r,t}^{\text{id}}]$. By supply-demand balancing equation (5.13), it is given by $E_t^{\text{id}} = L_t^* - S_{w,t}^*$, $Q_t^{\text{id}} = D_t^{\text{id}} = S_{r,t}^{\text{id}} = 0$. Let ξ_t denote the objective value in $\mathbf{P4_{b2}}$ for the battery being in the idle state. We have $\xi_t = (L_t^* - S_{w,t}^*)(Z_t - H_{u,t} + VP_t)$. Denote $\mathbf{a}_t' = [E_t', Q_t', D_t', S_{w,t}^*, S_{r,t}']$. The optimal control solution $\mathbf{a}_t^*$ of $\mathbf{P4_{b2}}$ is given in three cases below.

i) For $Z_t - H_{u,t} + VP_t \leq 0$: The battery is in either charging or idle state. The solution $\mathbf{a}_t'$ in charging state is give by

$$\begin{cases} D_t' = 0, \\ S_{r,t}' = \min\left\{S_t - S_{w,t}^*, R_{\max}\right\} \\ Q_t' = \min\left\{R_{\max} - S_{r,t}', E_{\max} - L_t^* + S_{w,t}^*\right\} \\ E_t' = \min\left\{L_t^* + R_{\max} - S_{w,t}^* - S_{r,t}', E_{\max}\right\}. \end{cases} \tag{5.30}$$

If $E_t'(Z_t - H_{u,t} + VP_t) + (Z_t - H_{u,t})S_{r,t}' + VC_{\text{rc}} 1_{R,t} < \xi_t$, then $\mathbf{a}_t^* = \mathbf{a}_t'$; Otherwise, $\mathbf{a}_t^* = \mathbf{a}_t^{\text{id}}$.

ii) For $Z_t - \mu_u H_{u,t} < 0 \leq Z_t - H_{u,t} + VP_t$: The battery is either in charging,

discharging, or idle state. The solution $\mathbf{a}'_t$ in charging or discharging state is give by

$$\begin{cases} D'_t = \min\left\{L^*_t - S^*_{w,t}, D_{\max}\right\} \\ S'_{r,t} = \min\left\{S_t - S^*_{w,t}, R_{\max}\right\} \\ Q'_t = 0, \\ E'_t = \left[L^*_t - S^*_{w,t} - D_{\max}\right]^+. \end{cases} \tag{5.31}$$

If $E'_t(Z_t - H_{u,t} + VP_t) + (Z_t - H_{u,t})S'_{r,t} + V(C_{\rm rc}1_{R,t} + C_{\rm dc}1_{D,t}) < \xi_t$, then $\mathbf{a}^*_t = \mathbf{a}'_t$; Otherwise, $\mathbf{a}^*_t = \mathbf{a}^{\rm id}_t$.

iii) *For* $0 \le Z_t - H_{u,t} < Z_t - H_{u,t} + VP_t$: The battery is in either discharging or idle state. The solution $\mathbf{a}'_t$ in discharging state is give by

$$\begin{cases} D'_t = \min\left\{L^*_t - S^*_{w,t}, D_{\max}\right\} \\ S'_{r,t} = Q'_t = 0, \\ E'_t = \left[L^*_t - S^*_{w,t} - D_{\max}\right]^+. \end{cases} \tag{5.32}$$

If $E'_t(Z_t - H_{u,t} + VP_t) + VC_{\rm dc}1_{D,t} < \xi_t$, then $\mathbf{a}^*_t = \mathbf{a}'_t$; Otherwise, $\mathbf{a}^*_t = \mathbf{a}^{\rm id}_t$.

In each case above, the cost of charging or discharging is compared with the cost ξ_t of being in an idle state, and the control solution of $\mathbf{P4_{b2}}$ is the one with the minimum cost. The condition for each case depends on Z_t, $H_{u,t}$ and P_t, where Z_t and $H_{u,t}$ are rated to battery energy level B_t and usage cost $x_{u,t}$, respectively. Thus, Cases i)-iii) represent the control actions at different battery energy levels (*i.e.,* low, moderate, or high) and electricity prices. For example, the ESM tends to store energy into the battery (or idle if the battery cost is high) , when the battery energy level and electricity price are both low, as shown in Case i); And the ESM tends to use the battery storage for energy supply (or idle if the battery cost is high), when battery energy level is high, as shown in Case iii).

4) Feasibility of $\mathbf{a}_t^*$ *to* **P1**: Recall that we have removed the battery capacity constraint (5.10) when modifying **P1** to **P2**. Thus, this constraint is no longer imposed in $\mathbf{P4_{b2}}$, and our real-time algorithm may not provide a feasible control solution $\{\mathbf{a}_t^*\}$ to **P1**. To ensure the solution is still feasible to the original problem **P1**, we design our control parameters A_o and V. The result readily follows Proposition 4.2 in Chapter 4. We omit the details and only state the final result below.

Proposition 5.2. *For the optimal solution* $\mathbf{a}_t^*$ *of* $\mathbf{P4_{b2}}$*, the resulting* B_t *satisfies the battery capacity constraint* (5.10)*, and* $\{\mathbf{a}_t^*\}$ *is feasible to* **P1***, if* A_o *in* (5.23) *is given by*

$$A_o = \begin{cases} A_o' & \text{if } \Delta_u \geq 0 \\ A_o' - \Delta_u & \text{if } \Delta_u < 0 \end{cases} \tag{5.33}$$

where $A_o' = B_{\min} + VP_{\max} + VC_u'(\Gamma_u) + \Gamma_u + D_{\max} + \frac{\Delta_u}{T_o}$*, and* $V \in [0, V_{\max}]$ *with*

$$V_{\max} = \frac{B_{\max} - B_{\min} - R_{\max} - D_{\max} - 2\Gamma_u - |\Delta_u|}{P_{\max} + C_u'(\Gamma_u)}. \tag{5.34}$$

5.3.3 Discussions

We summarize the proposed real-time joint load scheduling and energy storage management in Algorithm 2. Due to the separation of joint optimization, the algorithm provides a clear sequence of determination of control decisions at each time slot t.

Recall that we modify the original joint optimization problem **P1** to **P3**, and apply Lyapunov optimization to propose a real-time algorithm for **P3** which is to solve the per-slot optimization problem **P4**. We have the following discussions.

- In modifying **P1**, we remove the battery capacity constraint (5.10) and instead impose a new constraint (5.16) on the overall change of battery energy level

Algorithm 2 Real-Time Joint Load Scheduling and Energy Storage Management

Set the desired value of Δ_u. Set A_o and V as in (5.33) and (5.34), respectively.
At time slot 0: Set $Z_0 = X_0 = H_{u,0} = H_{d,0} = 0$.
At time slot t: Obtain the current values of $\{W_t, S_t, P_t\}$

1. *Load scheduling:* Determine d_t^* according to (5.27) and (5.28) and $\gamma_{d,t}^*$ according to (5.29), respectively.
2. *Energy Storage Control:*
   (a) Renewable contribution: Determine $S_{w,t}^*$ in (5.5) using d_t^* obtained above.
   (b) Energy purchase and storage: Determine $\gamma_{u,t}^*$ according to (5.29) and $\mathbf{a}_t^*$ according to Cases i)-iii) in Section 5.3.2.
3. *Updating virtual queues:* Use $\boldsymbol{\pi}_t^*$ to update B_t based on (5.11), and $X_t, Z_t, H_{u,t}, H_{d,t}$ based on (5.21)−(5.25).

over T_o slots to be Δ_u. Note that this constraint is set as a desired outcome, *i.e.,* Δ_u is a desired value. The actual solution $\mathbf{a}_t^*$ in the proposed algorithm may not satisfy this constraint at the end of the T_o-slot period, and thus may not be feasible to **P3**. Nonetheless, setting A_o and V as in (5.33) and (5.34) guarantees that $\{\mathbf{a}_t^*\}$ satisfy the battery capacity constraint (5.10) and therefore are feasible to **P1**.

- In designing the real-time algorithm by Lyapunov optimization, virtual queue X_t in (5.21) we introduce for the average delay constraint (5.3) can only ensure the constraint is satisfied with a margin as indicated below (5.21). As a result, constraint (5.3) can only be approximately satisfied. However, this relaxation is mild in practice for the average delay performance. Note that the per-load maximum delay constraint (5.1) is strictly satisfied for d_t^* by Algorithm 2. We will show in simulation that the achieved average delay $\overline{d_w}$ by Algorithm 2 in fact meets constraint (5.3).

- Finally, we point out that the load scheduling and energy storage control decisions are provided in closed-form by Algorithm 2. Thus, the algorithm can be easily implemented in real-time. Furthermore, no statistical assumptions on the loads, renewable source, and pricing $\{W_t, S_t, P_t\}$ are required in the algorithm, allowing it to be applied to general scenarios, especially when such statistics are difficult to predict. Despite being suboptimal for **P1**, we will show in Section 5.4 that Algorithm 2 provides a provable performance guarantee.

5.4 Performance Analysis

In this section, we analyze the performance of Algorithm 2 and discuss the mismatch involved in some constraints as a result of the real-time algorithm design.

5.4.1 Algorithm Performance

To evaluate the proposed algorithm, we consider a T-slot look-ahead problem. Specifically, we partition T_o slots into T frames with $T_o = MT$, for $M, T \in \mathbb{N}^+$. For each frame, we consider the same problem as **P1** but the objective is the T-slot averaged cost within the frame and the constraints are all related to time slots within the frame. In addition, we assume $\{W_t, S_t, P_t\}$ for the entire frame are known beforehand. Thus, the problem becomes a non-causal static optimization problem and we call it a T-slot lookahead problem. Let u_m^{opt} be the corresponding minimum objective value achieved by a T-slot look-ahead optimal solution over the mth frame.

We denote the objective value of **P1** achieved by Algorithm 2 over T_o-slot period by $u^*(V)$, where V is the weight value used in Algorithm 2. The following theorem

provides a bound of the cost performance under our proposed real-time algorithm to u_m^{opt} under the T-slot lookahead optimal solution.

Theorem 2. *Consider $\{W_t, S_t, P_t\}$ being any arbitrary processes over time. For any $M, T \in \mathbb{N}^+$ satisfying $T_o = MT$, the T_o-slot average system cost under Algorithm 2 is bounded by*

$$\begin{aligned} & u^*(V) - \frac{1}{M}\sum_{m=0}^{M-1} u_m^{opt} \\ & \leq \frac{GT}{V} + \frac{C_u'(\Gamma_u)(H_{u,0} - H_{u,T_o}) + \alpha C_d'(\Gamma_d)(H_{d,0} - H_{d,T_o})}{T_o} + \frac{L(\boldsymbol{\Theta}_0) - L(\boldsymbol{\Theta}_{T_o})}{VT_o} \end{aligned} \quad (5.35)$$

where the upper bound is finite.

In particular, as $T_o \to \infty$, we have

$$\lim_{T_o\to\infty} u^*(V) - \lim_{T_o\to\infty} \frac{1}{M}\sum_{m=0}^{M-1} u_m^{opt} \leq \frac{GT}{V}. \quad (5.36)$$

Proof. See Appendix 5.6.5.

Remark: Theorem 2 shows that our proposed algorithm is able to track the T-slot lookahead optimal solution with a bounded gap, for all possible M and T. Also, for the best performance, we should always choose $V = V_{\max}$. The bound in (5.36) gives the asymptotic performance as T_o increase. Since $V_{\max}$ in (5.34) increases with $B_{\max}$, it follows that Algorithm 2 is asymptotically equivalent to the optimal T-slot look-ahead solution as the battery capacity and T_o go to infinity. Note that, as $T_o \to \infty$, **P1** becomes an infinite time horizon problem with average sample path cost objective. The bound in (5.36) provides the performance gap of long-term time-averaged sample-path system cost of our proposed algorithm to the T-slot look-ahead policy.

5.4.2 Design Approximation

1) Average scheduling delay $d^{\max}$: Recall that, by Algorithm 2, using the virtual queue X_t in (5.21), the average delay constraint (5.3) is approximately satisfied with a margin, *i.e.,* $\overline{d_w} \leq d^{\max} + \epsilon_d$, where $\epsilon_d \triangleq (X_{T_o} - X_o)/T_o$ is the margin. We now bound ϵ_d below.

Proposition 5.3. *Under Algorithm 2, the margin* ϵ_d *for constraint* (5.3) *is bounded as follows*

$$|\epsilon_d| \leq \sqrt{\frac{2G}{\mu T_o} + \frac{L(\mathbf{\Theta}_o)}{\mu T_o}} + \frac{|X_o|}{T_o}. \tag{5.37}$$

Proof. See Appendix 5.6.6.

Proposition 5.3 indicates that the margin $\epsilon_d \to 0$ as $T_o \to 0$. Thus, the average delay is asymptotically satisfied. Note that, for $X_o = 0$, $\epsilon_d \geq 0$. If $X_o > 0$, it is possible that $\epsilon_d < 0$ and constraint (5.3) is satisfied with a negative margin. However, this will drive d_t^* to be smaller which may cause higher system cost. Thus, we set $X_o = 0$ in Algorithm 2.

2) Mismatch of Δ_u: In our design, we set Δ_u to be a desired value for the change of battery energy level over T_o-slot period as in new constraint (5.16). This value may not be achieved by Algorithm 2. Define the mismatch by $\epsilon_u \triangleq \sum_{\tau=0}^{T_o-1}(Q_\tau + S_{r,\tau} - D_\tau) - \Delta_u$. The bound for ϵ_u follows the result in Proposition 4.3 in Chapter 4 and is shown below.

$$|\epsilon_u| \leq 2\Gamma_u + R_{\max} + VP_{\max} + VC_u'(\Gamma_u) + D_{\max}. \tag{5.38}$$

Note that $V_{\max}$ in (5.34) increases as $|\Delta_u|$ decreases, and a larger $V_{\max}$ is preferred for better performance by Theorem 2. Thus, a smaller $|\Delta_u|$ is preferred. Note also

that our simulation study shows that the actual mismatch ϵ_u is much smaller than this upper bound.

5.5 Simulation Results

5.5.1 Simulation Configuration

We set each slot to be 5 minutes and consider a 24-hour duration. Thus, we have $T_o = 288$ slots for each day. We assume P_t, S_t and W_t do not change within each slot. We collect data from Ontario Energy Board [53] to set the price P_t. As shown Fig. 5.3 top, it follows a three-stage price pattern as $\{P_h, P_m, P_l\} = \{\$0.118, \$0.099, \$0.063\}$ and is periodic every 24 hours. We assume $\{S_t\}$ to be solar energy. It is a non-stationary process, with the mean amount $\overline{S}_t = \mathbb{E}[S_t]$ changing periodically over 24 hours, and having three-stage values as $\{\overline{S}_h, \overline{S}_m, \overline{S}_l\} = \{1.98, 0.96, 0.005\}/12$ kWh and standard deviation as $\sigma_{S_i} = 0.4\overline{S}_i$, for $i = h, m, l$, as shown in Fig. 5.3 middle. We assume the load $\{W_t\}$ is a non-stationary process, having three-stage mean values $\overline{W}_t = \mathbb{E}[W_t]$ as $\{\overline{W}_h, \overline{W}_m, \overline{W}_l\} = \{2.4, 1.38, 0.6\}/12$ kWh with standard deviation as $\sigma_{W_i} = 0.2\overline{W}_i$, for $i = h, m, l$, as shown in Fig. 5.3 bottom. For each load W_t, we generate λ_t from a uniformly distribution with interval $[1, 12]$, and $\rho_t = W_t/\lambda_t$. We set $d_t^{\max}$ in (5.1) to be identical for all t.

We set the battery related parameters as follows: $R_{\max} = 0.165$ kWh, $D_{\max} = 0.165$ kWh, $C_{\rm rc} = C_{\rm dc} = 0.001$, $B_{\min} = 0$ and the battery initial energy level $B_0 = 0$. Unless specified, we set $B_{\max} = 3$ kWh. We set $E_{\max} = 0.3$ kWh. Also, we set the weights $\alpha = 1$ and $\mu = 1$ as the default values. Since $V_{\max}$ increases as $|\Delta_u|$ decreases,

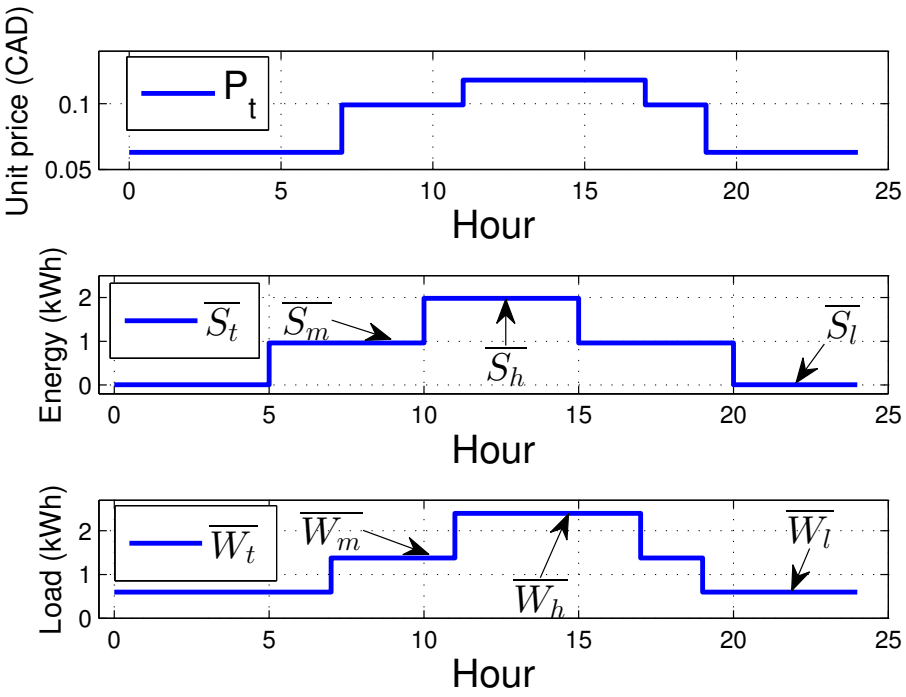

Figure 5.3: System inputs $\overline{W}_t, \overline{S}_t$, and P_t over 24 hours.

to achieve best performance[2], we set $\Delta_u = 0$ and $V = V_{\max}$.

For the battery cost, we consider an exemplary case where the battery usage cost and the delay cost are both quadratic functions, given by $C_u(\overline{x_u}) = k_u \overline{x_u}^2$ and $C_d(\overline{d_w}) = k_d \overline{d_w}^2$. The constant $k_u > 0$ is a battery cost coefficient depending on the battery characteristics, given by $k_u = 0.2$. The constant $k_d > 0$ is a normalization factor for the desired maximum average delay in (5.3), given by $k_d = \frac{1}{(d^{\max})^2}$. The optimal $\gamma^*_{i,t}$ in (5.29) can be determined with $C_i'(\Gamma_i) = 2k_i\Gamma_i$, and $C_i'^{-1}\left(-\frac{H_{i,t}}{V\beta_i}\right) = -\frac{H_{i,t}}{2\beta_i k_i V}$ for $i = u, d$.

[2]A detailed study of Δ_u can be found in Section 4.5

5.5.2 An Example of Load Scheduling

In Fig. 5.4, we show a fraction of the load scheduling results by Algorithm 2, where we set $d_t^{\max} = d^{\max} = 18$ and $\alpha = 0.005$. Each horizontal bar represents a scheduled load W_t with the width representing the intensity ρ_t and the length representing the total duration from arrival to service being completed. For a delayed load, the delay is indicated in different color before the load is scheduled. In this example, we see some loads are immediately scheduled, while others are scheduled at $d_t^{\max}$. The total energy demand at each time slot is the vertical summation over all loads that are scheduled in this slot.

5.5.3 Effect of Scheduling Delay Constraints

1) Effect of $d_t^{\max}$ and $d^{\max}$: We study how the average system cost objective of **P1** under our proposed algorithm varies with different delay requirements. We set $d_t^{\max} = d^{\max}$, $\forall t$, and plot the average system cost vs. $d_t^{\max}$ in Fig. 5.5, for different values of weight α in the cost objective. As can be seen, the system cost decreases as $d^{\max}(d_t^{\max})$ increases. This is shows that relaxing the average delay constraint gives more flexibility to load scheduling, where each load can be scheduled at lower electricity price, resulting in lower system cost. This demonstrates that flexible load scheduling is more beneficial to the overall system cost. In addition, we see that a larger value α gives more weight on minimizing the delay in the objective, resulting in a higher system cost.

Next, we study the effect of delay constraints on the monetary cost, *i.e.,* the cost of energy purchasing and battery degradation. This part of cost is given by

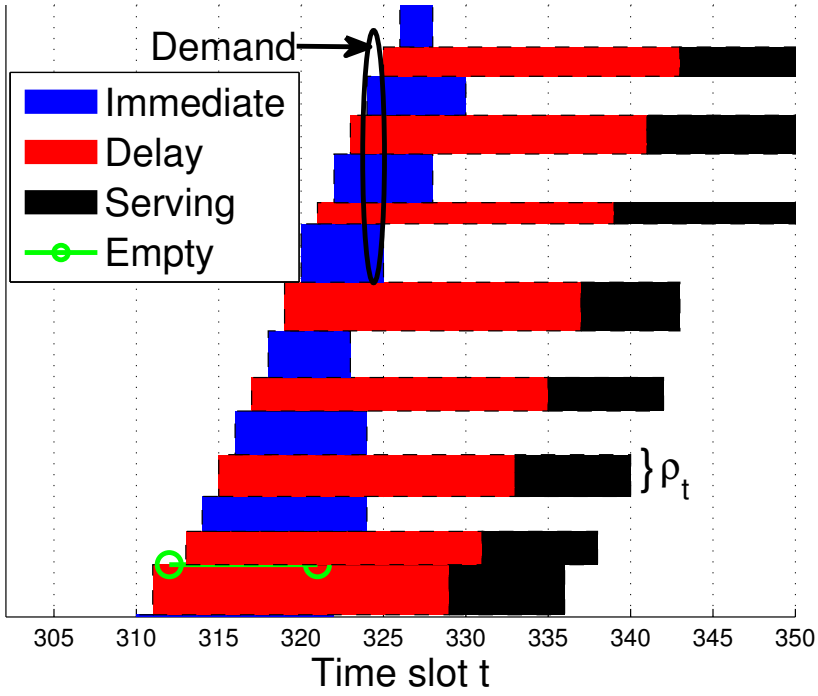

Figure 5.4: A trace of load scheduling results over time ($d_t^{\max} = d^{\max} = 18$, $\alpha = 0.005$).

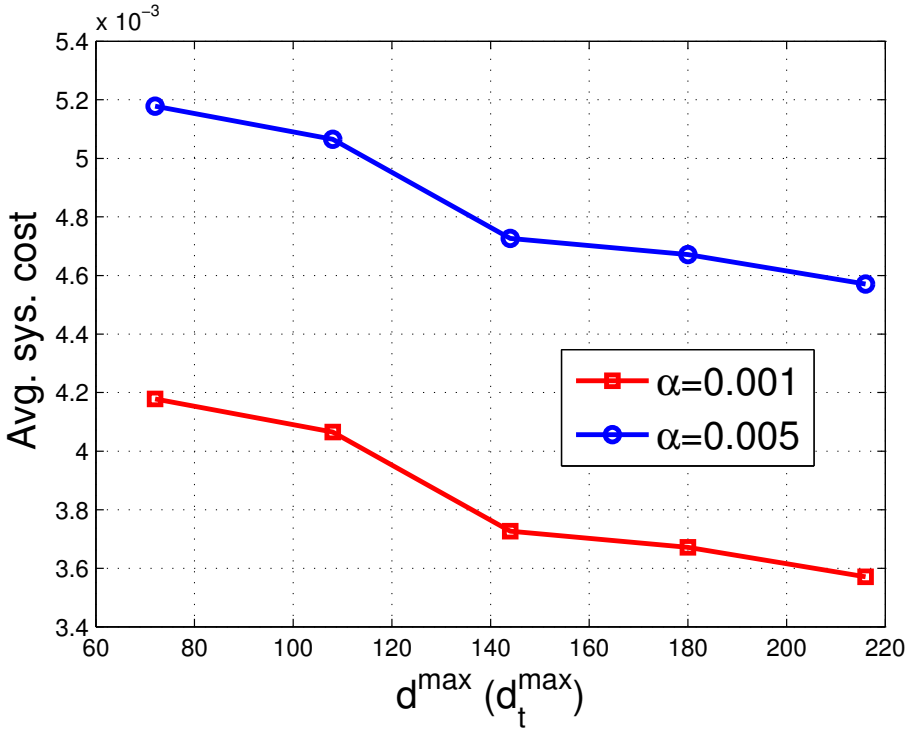

Figure 5.5: Average system cost vs. $d_t^{\max}$ ($d^{\max} = d_t^{\max}$).

$\overline{J} + \overline{x_e} + C_u(\overline{x_u})$ in the objective of **P1**. The monetary cost shows by allowing longer service delay, how much saving a consumer could actually have. In Fig. 5.6, we plot the monetary cost vs. $d^{\max}$ for $d_t^{\max} = 216$. We see a clear trade-off between the monetary cost and delay. Such trade-off curve can be used to determine the operating point. For comparison, we also consider the case in which all loads are served immediately after arrival, *i.e.,* $d_t^{\max} = 0$. This is essentially the case with only energy storage but no scheduling. Thus, the monetary cost is independent of $d^{\max}$. We see a substantial gap between the two curves and the gap increases with $d^{\max}$. This clearly shows the benefit of joint load scheduling and energy storage management.

2) Average delay $\overline{d_w}$: We now study the average delay $\overline{d_w}$ achieved by our proposed algorithm vs. $d^{\max}$ for various $d_t^{\max}$ in Fig. 5.7. As can be seen, the actual averaged delay $\overline{d_w}$ increases with the average delay $d^{\max}$ requirement. This is because, with a more relaxed constraint on the delay, loads can be shifted to a later time in order to reduce the system cost, resulting in larger average delay. However, the increase is sublinear with respect to $d^{\max}$. Similarly, we observe that increasing the per load maximum delay $d_t^{\max}$ increases $\overline{d_w}$. Finally, recall that we study the margin for average delay constraint (5.3) under our proposed algorithm in Proposition 5.3. To see how the resulting $\overline{d_w}$ meets constraint (5.3), we plot the line $d^{\max}$ in Fig. 5.7. As we see, $\overline{d_w}$ is below $d^{\max}$ for all values of $d^{\max}$ and $d_t^{\max}$.

3) Effect of μ: Weight μ is used to control the relative importance of virtual queues related to the battery and those to delay in Lyapunov function $L(\mathbf{\Theta}_t)$ in (5.26) and Lyapunov drift $\Delta(\mathbf{\Theta}_t)$. For Lyapunov drift $\Delta(\mathbf{\Theta}_t)$, if μ is large, the two queues X_t and $H_{d,t}$ related to the delay will dominate the drift. This will affect the drift-plus-cost

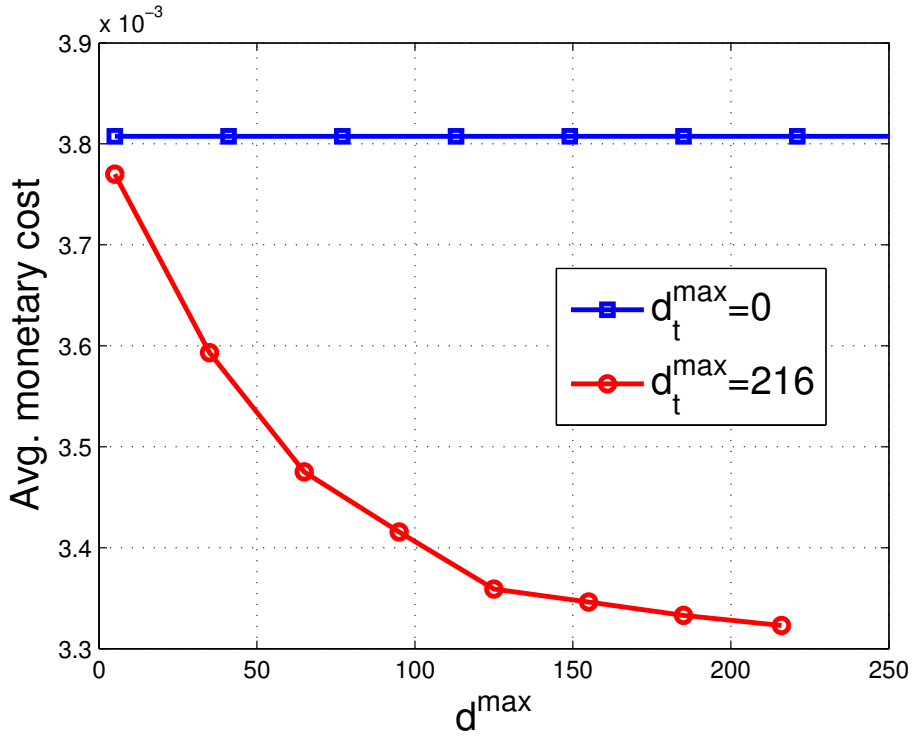

Figure 5.6: Monetary cost vs. $d^{\max}$ ($\alpha = 0.005$)

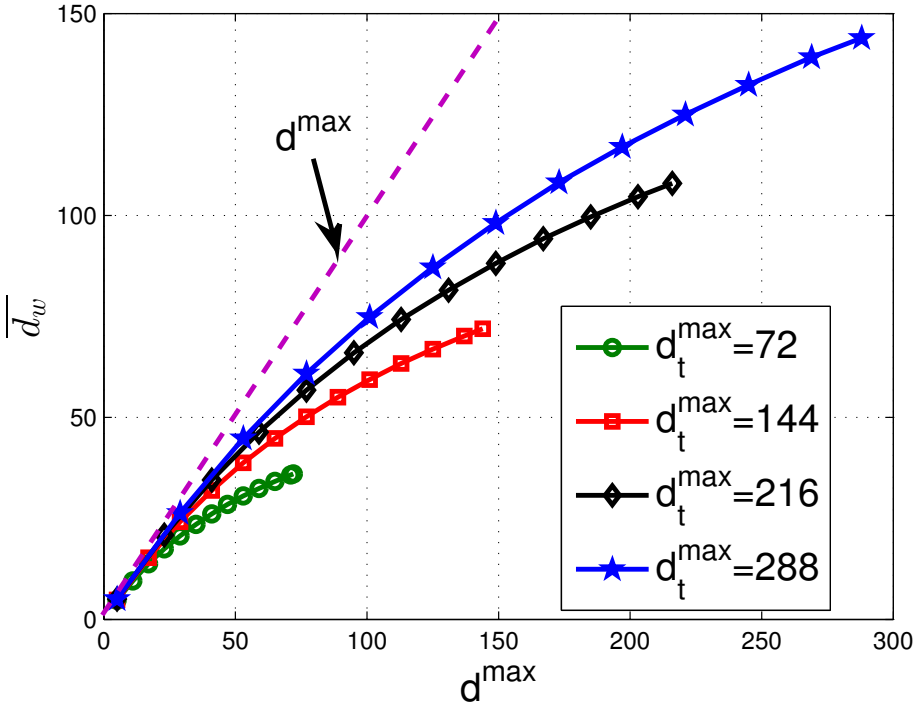

Figure 5.7: $\overline{d_w}$ vs. $d^{\max}$ ($\alpha = 0.005$).

objective considered in our proposed algorithm and thus the performance. To study the effect of μ on the performance, in Fig. 5.8, we evaluate the average system cost for different values of μ. We see that a lower system cost is achieved by smaller value of μ. This is because, with smaller μ, the drifts of X_t related to delay is less significant in the overall drift. This allows wider difference between $\overline{d_w}$ and $d^{\max}$, *i.e.,* smaller $\overline{d_w}$ and lower delay cost.

5.5.4 Performance vs. Battery Capacity

We consider two other algorithms for comparison: A) *No storage or scheduling*: In this case, neither energy storage nor load scheduling is considered. Each load is served immediately using energy purchased from the conventional grid and/or renewable generator. B) *Storage only*: In this method, only battery storage is considered but every load is served immediately without a delay. This is essentially the Algorithm 1 in Chapter 4.

In Fig. 5.9, we compare our proposed algorithm to the above two alternative algorithms under various battery capacity $B_{\max}$. Since algorithm A does not consider a battery, the system cost is unchanged over $B_{\max}$ and is 0.01. We do not plot the curve since the cost is much bigger than the rest of two algorithms we considered. For algorithm B and our proposed Algorithm 2, as can be seen, the system costs reduces as $B_{\max}$ increases. This is because a larger battery capacity allows charging/discharging to be more flexible based on the current demand and electricity price, resulting in the lower system costs. Comparing the two, we see that joint load scheduling and energy storage provides further reduction in system cost.

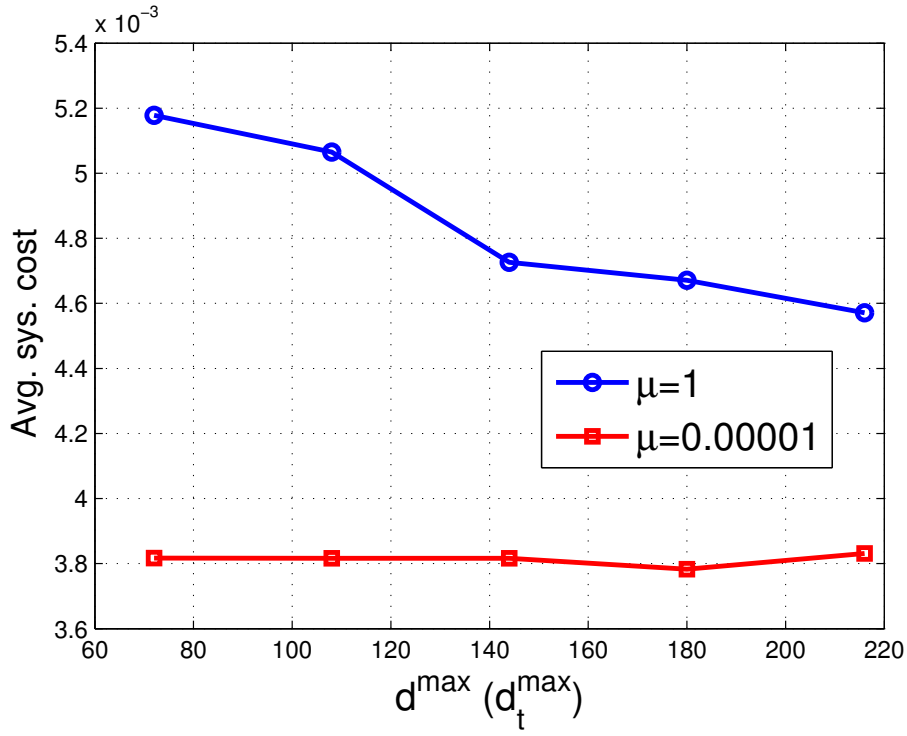

Figure 5.8: Average system cost vs. $d^{\max}$ ($d_t^{\max} = d^{\max}$).

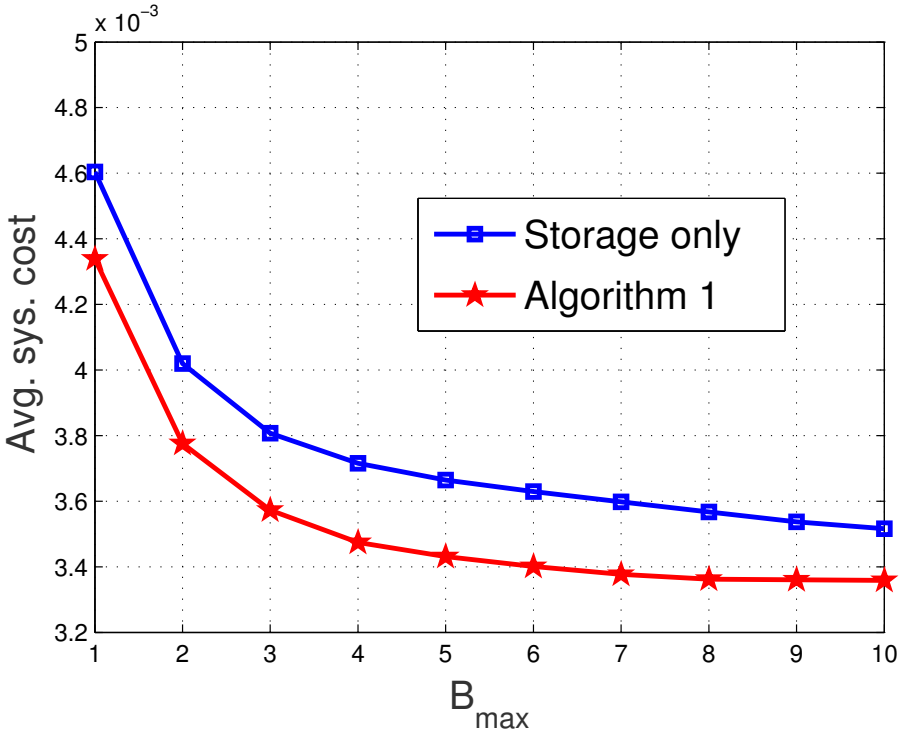

Figure 5.9: Average system cost vs. $B_{\max}$ ($\alpha = 0.001$). The average system cost for the method of no storage or scheduling is 0.01.

5.6 Appendices

5.6.1 Proof of Lemma 5.1

Proof. The proof follows the same approach as in Appendix 4.7.1. Let u_2^o and u_3^o denote the minimum objective values of **P2** and **P3**, respectively. Since the optimal solution of **P2** satisfies all constraints of **P3**, it is a feasible solution of **P3**. Thus, we have $u_3^o \leq u_2^o$. By Jensen's inequality and convexity of $C_i(\cdot)$ for $i = d, u$, we have $\overline{C_d(\gamma_d)} \geq C_d(\overline{\gamma_d}) = C_d(\overline{d_w})$ and $\overline{C_u(\gamma_u)} \geq C_u(\overline{\gamma_u}) = C_u(\overline{x_u})$. This means $u_3^o \geq u_2^o$. Hence, we have $u_2^o = u_3^o$ and **P3** and **P2** are equivalent. ■

5.6.2 Upper Bound on Drift-Plus-Cost Function

The following lemma shows the upper bound on the drift $\Delta(\mathbf{\Theta}_t)$.

Lemma 5.3. *The one-slot Lyapunov drift $\Delta(\mathbf{\Theta}_t)$ is upper bounded by*

$$\begin{aligned}\Delta(\mathbf{\Theta}_t) \leq & Z_t \left(E_t + S_{r,t} + S_{w,t} - \sum_{\tau=0}^{t} \rho_\tau 1_{S,t}(d_\tau) - \frac{\Delta_u}{T_o} \right) \\ & + H_{u,t}\gamma_{u,t} - H_{u,t}\left(E_t + S_{r,t}\right) - |H_{u,t}| \left(S_{w,t} - \sum_{\tau=0}^{t} \rho_\tau 1_{S,t}(d_\tau) \right) + G \\ & + \mu X_t \left(d_t - d^{\max}\right) + \mu H_{d,t}(\gamma_{d,t} - d_t) \end{aligned} \tag{5.39}$$

where $G = \frac{1}{2}\max\left\{\left(R_{\max} - \frac{\Delta_u}{T_o}\right)^2, \left(D_{\max} + \frac{\Delta_u}{T_o}\right)^2\right\} + \frac{1}{2}\max\left\{R_{\max}^2, D_{\max}^2\right\}$
$+ \frac{\mu}{2}\max\left\{\left(d^{\max}\right)^2, \left(d_t^{\max} - d^{\max}\right)^2\right\} + \frac{\mu}{2}(d_t^{\max})^2$.

Proof. From the definition of $\Delta(\mathbf{\Theta}_t)$, we have

$$\begin{aligned}\Delta(\mathbf{\Theta}_t) &\triangleq L(\mathbf{\Theta}_{t+1}) - L(\mathbf{\Theta}_t) \\ &= \frac{1}{2}[Z_{t+1}^2 - Z_t^2 + \left(H_{u,t+1}^2 - H_{u,t}^2\right) + \mu(X_{t+1}^2 - X_t^2 + H_{d,t+1}^2 - H_{d,t}^2)] \end{aligned} \tag{5.40}$$

where from queue (5.22), $Z_{t+1}^2 - Z_t^2$ can be presented by

$$\frac{Z_{t+1}^2 - Z_t^2}{2} = Z_t \left(Q_t + S_{r,t} - D_t - \frac{\Delta_u}{T_o} \right) + \frac{(Q_t + S_{r,t} - D_t - \frac{\Delta_u}{T_o})^2}{2}. \tag{5.41}$$

Note that from (5.16), we have $\frac{\Delta_u}{T_o} \leq \max\{R_{\max}, D_{\max}\}$. For a given value of Δ_u, by (5.7) and (5.8), $(Q_t + S_{r,t} - D_t - \frac{\Delta_u}{T_o})^2$ is upper bound by $\max\left\{(R_{\max} - \frac{\Delta_u}{T_o})^2, (D_{\max} + \frac{\Delta_u}{T_o})^2\right\}$. By the supply-demand balance (5.13), the first term on RHS of (5.41) can be replaced by

$$Z_t \left(Q_t + S_{r,t} - D_t - \frac{\Delta_u}{T_o} \right) = Z_t \left(E_t + S_{r,t} + S_{w,t} - \sum_{\tau=0}^{t} \rho_\tau 1_{S,t}(d_\tau) - \frac{\Delta_u}{T_o} \right). \tag{5.42}$$

From (5.24), $H_{u,t+1}^2 - H_{u,t}^2$ in (5.40) can be presented by

$$\frac{H_{u,t+1}^2 - H_{u,t}^2}{2} = H_{u,t}(\gamma_{u,t} - x_{u,t}) + \frac{(\gamma_{u,t} - x_{u,t})^2}{2}. \tag{5.43}$$

Note that from (5.12) and (5.17), the second term of RHS in (5.43) is upper bounded by $(\gamma_{u,t} - x_{u,t})^2 \leq \max\{R_{\max}^2, D_{\max}^2\}$.

We now find the upper bound for $-H_t x_{u,t}$ in the first term on RHS of (5.43). By the supply-demand balance (5.13), $-H_t x_{u,t}$ can be replaced by

$$\begin{aligned} -H_t x_{u,t} &= -H_{u,t}(|Q_t + S_{r,t} - D_t|) \\ &= -H_{u,t} \left(\left| E_t + S_{r,t} + S_{w,t} - \sum_{\tau=0}^{t} \rho_\tau 1_{S,t}(d_\tau) \right| \right). \end{aligned} \tag{5.44}$$

The upper bound of $-H_t x_{u,t}$ in (5.44) is obtained as follows.

1) For $H_{u,t} \geq 0$: It is easy to see that the following inequality holds

$$\begin{aligned} &- H_{u,t} \left(\left| E_t + S_{r,t} + S_{w,t} - \sum_{\tau=0}^{t} \rho_\tau 1_{S,t}(d_\tau) \right| \right) \\ &\leq -H_{u,t} \left(E_t + S_{r,t} + S_{w,t} - \sum_{\tau=0}^{t} \rho_\tau 1_{S,t}(d_\tau) \right) \\ &= -H_{u,t} \left(E_t + S_{r,t} \right) - H_{u,t} \left(S_{w,t} - \sum_{\tau=0}^{t} \rho_\tau 1_{S,t}(d_\tau) \right). \end{aligned}$$

2) For $H_{u,t} < 0$: We have

$$\begin{aligned}
&- H_{u,t}\left(\left|E_t + S_{r,t} + S_{w,t} - \sum_{\tau=0}^{t} \rho_\tau 1_{S,t}(d_\tau)\right|\right) \\
&\leq -H_{u,t}\left(|E_t + S_{r,t}| + \left|S_{w,t} - \sum_{\tau=0}^{t} \rho_\tau 1_{S,t}(d_\tau)\right|\right) \\
&\leq -H_{u,t}\left(E_t + S_{r,t} + \sum_{\tau=0}^{t} \rho_\tau 1_{S,t}(d_\tau) - S_{w,t}\right) \\
&= -H_{u,t}\left(E_t + S_{r,t}\right) + H_{u,t}\left(S_{w,t} - \sum_{\tau=0}^{t} \rho_\tau 1_{S,t}(d_\tau)\right).
\end{aligned}$$

Combine the above cases for $H_{u,t}$, we have $-H_t x_{u,t}$ in (5.44) upper bounded by

$$\begin{aligned}
&- H_{u,t}\left(\left|E_t + S_{r,t} + S_{w,t} - \sum_{\tau=0}^{t} \rho_\tau 1_{S,t}(d_\tau)\right|\right) \\
&\leq -H_{u,t}\left(E_t + S_{r,t}\right) - |H_{u,t}|\left(S_{w,t} - \sum_{\tau=0}^{t} \rho_\tau 1_{S,t}(d_\tau)\right).
\end{aligned}$$

From (5.21), $X_{t+1}^2 - X_t^2$ in (5.40) can be presented by

$$\begin{aligned}
X_{t+1}^2 &\leq \left(X_t + d_t - d^{\max}\right)^2 \\
&\leq X_t^2 + 2X_t\left(d_t - d^{\max}\right) + \left(d_t - d^{\max}\right)^2 \\
\frac{X_{t+1}^2 - X_t^2}{2} &\leq X_t\left(d_t - d^{\max}\right) + \frac{1}{2}\left(d_t - d^{\max}\right)^2 \qquad (5.45)
\end{aligned}$$

where by (5.1), the last term in RHS of (5.45) can be upper bounded by $(d_t - d^{\max})^2 \leq \max\left\{\left(d^{\max}\right)^2, \left(d_t^{\max} - d^{\max}\right)^2\right\}$.

From (5.25), $H_{d,t+1}^2 - H_{d,t}^2$ in (5.40) can be presented by

$$\frac{H_{d,t+1}^2 - H_{d,t}^2}{2} = H_{d,t}(\gamma_{d,t} - d_t) + \frac{(\gamma_{d,t} - d_t)^2}{2} \leq H_{d,t}(\gamma_{d,t} - d_t) + \frac{1}{2}(d_t^{\max})^2 \qquad (5.46)$$

where the last inequality is derived from the bounds of γ_d in (5.19) and d_t in (5.1).

Now, we give the upper bond of (5.40) as follows

$$\begin{aligned}\Delta(\mathbf{\Theta}_t) &\triangleq L(\mathbf{\Theta}_{t+1}) - L(\mathbf{\Theta}_t) \\ &\leq Z_t\left(E_t + S_{r,t} + S_{w,t} - \sum_{\tau=0}^{t}\rho_\tau 1_{S,t}(d_\tau) - \frac{\Delta_u}{T_o}\right) \\ &\quad + H_{u,t}\gamma_{u,t} - H_{u,t}(E_t + S_{r,t}) - |H_{u,t}|\left(S_{w,t} - \sum_{\tau=0}^{t}\rho_\tau 1_{S,t}(d_\tau)\right) \\ &\quad + \mu X_t\left(d_t - d^{\max}\right) + \mu H_{d,t}(\gamma_{d,t} - d_t) + G \end{aligned} \tag{5.47}$$

where G includes all constant terms from the upper bounds of (5.41), (5.43), (5.45) and (5.46), and is defined as

$$\begin{aligned}G \triangleq &\frac{1}{2}\max\left\{\left(R_{\max} - \frac{\Delta_u}{T_o}\right)^2, \left(D_{\max} + \frac{\Delta_u}{T_o}\right)^2\right\} + \frac{1}{2}\max\left\{R_{\max}^2, D_{\max}^2\right\} + \frac{\mu}{2}(d_t^{\max})^2 \\ &+ \frac{\mu}{2}\max\left\{(d^{\max})^2, (d_t^{\max} - d^{\max})^2\right\}. \quad \blacksquare \end{aligned} \tag{5.48}$$

5.6.3 Proof of Proposition 5.1

Proof. To determine the optimal scheduling delay d_t^*, we need to compare the objective values of $\mathbf{P4_{a1}}$ under all serving options. The optimal delay d_t^* is the one that achieves the minimum objective value.

Due to the fact $d_t \cdot 1_{S,t}(d_t) = 0$, we have the following cases.

1) If the load is immediately served, we have $1_{S,t}(d_t) = 1$ and $d_t = 0$. The objective value becomes ω_o;

2) If the load is delayed, we have $d_t > 0$ and $1_{S,t}(d_t) = 0$. The objective function is reduced to $\mu d_t(X_t - H_{d,t})$. For $X_t - H_{d,t} \geq 0$, the objective value is ω_1; Otherwise, the value is $\omega_{d_t^{\max}}$.

Comparing ω_o to ω_1 or $\omega_{d_t^{\max}}$, we obtain d_t^*. $\blacksquare$

5.6.4 Proof of Lemma 5.2

Proof. Since μ, α and V are all positive weights, and $C_i(\gamma_t)$ are both assumed to be continuous, convex and non-decreasing function with respect to $\gamma_{i,t}$ with maximum derivatives $C_i'(\Gamma_i) < \infty$ for $i = d, u$, the optimal $\gamma_{i,t}^*$ values are determined by examining the derivatives of the objective functions of $\mathbf{P4_{a2}}$ and $\mathbf{P4_{b1}}$. Note that, given $\gamma_{u,t}$ in (5.17) and $\gamma_{d,t}$ in (5.19), $C_i'(\gamma_{i,t}) \geq 0$ and is increasing with $\gamma_{i,t}$ for $i = d, u$. For β_i defined in Lemma 5.2, we have

1) For $H_{i,t} \geq 0$: We have $\mu_d H_{d,t} + V\alpha C_d'(\gamma_{d,t}) > 0$ and $H_{u,t} + VC_u'(\gamma_{u,t}) > 0$. Thus, the objectives of $\mathbf{P4_{a2}}$ and $\mathbf{P4_{b1}}$ are both monotonically increasing functions, and the minimum values are obtained with $\gamma_{i,t}^* = 0$ for $i = d, u$.

2) For $H_{i,t} < -V\beta C_i'(\Gamma_i)$: Since $VC_i'(\Gamma_i) \geq VC_i'(\gamma_{i,t})$ for $i = d, u$, we have $\mu_d H_{d,t} + V\alpha C_d'(\gamma_{d,t}) < 0$ and $H_{u,t} + VC_u'(\gamma_{u,t}) < 0$. The objectives of $\mathbf{P4_{a2}}$ and $\mathbf{P4_{b1}}$ are both monotonically decreasing functions. From (5.19), the minimum objective value of $\mathbf{P4_{a2}}$ is reached with $\gamma_{d,t}^* = \Gamma_d$ where $\Gamma_d \triangleq \min\{d_t^{\max}, d^{\max}\}$; The minimum objective value of $\mathbf{P4_{b1}}$ is reached with $\gamma_{u,t}^* = \Gamma_u$ where by (5.17), we have $\Gamma_u \triangleq \min\{R_{\max}, D_{\max}\}$;

3) For $-V\beta_i C_i'(\Gamma_i) \leq H_{i,t} \leq 0$: In this case, $\gamma_{d,t}^*$ and $\gamma_{u,t}^*$ are the roots of $\mu_d H_{d,t} + V\alpha C_d'(\gamma_{d,t}) = 0$ and $H_{u,t} + VC_u'(\gamma_{u,t}) = 0$, respectively. We have $\gamma_{i,t}^* = C_i'^{-1}\left(-\frac{H_{i,t}}{V\beta_i}\right)$ for $i = d, u$.

Thus, we have $\gamma_{i,t}^*$ for $i = d, u$ as in (5.29). ■

5.6.5 Proof of Theorem 2

Proof. A T-slot sample path Lyapunov drift is defined by $\Delta_T(\mathbf{\Theta}_t) \triangleq L(\mathbf{\Theta}_{t+T}) - L(\mathbf{\Theta}_t)$. We upper bound it as follows

$$\begin{aligned}
\Delta_T(\mathbf{\Theta}_t) &= \frac{Z_{t+T}^2 - Z_t^2 + \left(H_{u,t+T}^2 - H_{u,t}^2\right)}{2} + \frac{\mu\left(X_{t+T}^2 - X_t^2 + H_{d,t+T}^2 - H_{d,t}^2\right)}{2} \\
&\leq Z_t \sum_{\tau=t}^{t+T-1}\left(Q_\tau + S_{r,\tau} - D_\tau - \frac{\Delta_u}{T_o}\right) + \frac{1}{2}\left[\sum_{\tau=t}^{t+T-1}\left(Q_\tau + S_{r,\tau} - D_\tau - \frac{\Delta_u}{T_o}\right)\right]^2 \\
&\quad + H_{u,t}\sum_{\tau=t}^{t+T-1}(\gamma_{u,\tau} - x_{u,\tau}) + \frac{1}{2}\left[\sum_{\tau=t}^{t+T-1}(\gamma_{u,\tau} - x_{u,\tau})\right]^2 \\
&\quad + X_t\sum_{\tau=t}^{t+T-1}(d_\tau - d^{\max}) + \frac{\mu}{2}\left[\sum_{\tau=t}^{t+T-1}(d_t - d^{\max})\right]^2 \\
&\quad + H_{d,t}\sum_{\tau=t}^{t+T-1}(\gamma_{d,\tau} - x_{d,\tau}) + \frac{\mu}{2}\left[\sum_{\tau=t}^{t+T-1}(\gamma_{d,\tau} - x_{d,\tau})\right]^2 \\
&\leq Z_t \sum_{\tau=t}^{t+T-1}\left(Q_\tau + S_{r,\tau} - D_\tau - \frac{\Delta_u}{T_o}\right) + H_{d,t}\sum_{\tau=t}^{t+T-1}(\gamma_{d,\tau} - x_{d,\tau}) + GT^2 \\
&\quad + H_{u,t}\sum_{\tau=t}^{t+T-1}(\gamma_\tau - x_{u,\tau}) + X_t\sum_{\tau=t}^{t+T-1}(d_\tau - d^{\max}) \qquad (5.49)
\end{aligned}$$

where G is defined in Lemma 5.3.

Assume $T_o = MT$. We consider a per-frame optimization problem below, with the objective of minimizing the time-averaged system cost within the mth frame of length T time slots.

$$\begin{aligned}
\mathbf{P_f}: \min_{\{\mathbf{a}_t, \gamma_t\}} \quad & \frac{1}{T}\sum_{t=mT}^{(m+1)T-1}\left[E_t P_t + x_{e,t} + C_u(\gamma_{u,t}) + \alpha C_d(\gamma_{d,t})\right] \\
\text{s.t} \quad & (5.1), (5.4), (5.6), (5.9), (5.13) - (5.15), (5.17) - (5.20).
\end{aligned}$$

We show that $\mathbf{P_f}$ is equivalent to $\mathbf{P1}$ in which T_o is replaced by T. Let u_m^f denote the minimum objective value of $\mathbf{P_f}$. The optimal solution of $\mathbf{P1}$ satisfies all constraints of $\mathbf{P_f}$ and therefore is feasible to $\mathbf{P_f}$. Thus, we have $u_m^f \leq u_m^{\text{opt}}$. By Jensen's inequality and convexity of $C_i(\cdot)$ for $i = d, u$, we have $\overline{C_d(\gamma_d)} \geq C_d(\overline{\gamma_d}) = C_d(\overline{d_w})$ and $\overline{C_u(\gamma_u)} \geq$

$C_u(\overline{\gamma_u}) = C_u(\overline{x_u})$. Note that introducing the auxiliary variables $\gamma_{u,t}$ with constraints (5.17) and (5.18), and $\gamma_{d,t}$ with constraints (5.19) and (5.20) does not modify the problem. This means $u_m^f \geq u_m^{\text{opt}}$. Hence, we have $u_m^f = u_m^{\text{opt}}$ and $\mathbf{P_f}$ and **P1** are equivalent.

From (5.49) and the objective of $\mathbf{P_f}$, we have the T-slot drift-plus-cost metric for the mth frame upper bounded by

$$\begin{aligned}
&\Delta_T(\mathbf{\Theta}_t) + V\left[\sum_{t=mT}^{(m+1)T-1}\left[E_tP_t + x_{e,t} + C_u(\gamma_{u,t}) + \alpha C_d(\gamma_{d,t})\right]\right] \\
&\leq Z_t\sum_{t=mT}^{(m+1)T-1}\left(Q_t + S_{r,t} - D_t - \frac{\Delta_u}{T_o}\right) + H_{u,t}\sum_{\tau=t}^{t+T-1}(\gamma_{u,\tau} - x_{u,\tau}) + GT^2 \\
&\quad + X_t\sum_{\tau=t}^{t+T-1}(d_\tau - d^{\max}) + H_{d,t}\sum_{\tau=t}^{t+T-1}(\gamma_{d,\tau} - x_{d,\tau}) \\
&\quad + V\left[\sum_{t=mT}^{(m+1)T-1}\left[E_tP_t + x_{e,t} + C_u(\gamma_{u,t}) + \alpha C_d(\gamma_{d,t})\right]\right].
\end{aligned} \tag{5.50}$$

Let $\{\tilde{\boldsymbol{\pi}}_t\}$ denote a set of feasible solutions of $\mathbf{P_f}$, satisfying the following relations

$$\sum_{t=mT}^{(m+1)T-1}\left(\tilde{Q}_t + \tilde{S}_{r,t}\right) = \sum_{t=mT}^{(m+1)T-1}\left(\tilde{D}_t + \frac{\Delta_u}{T_o}\right) \tag{5.51}$$

$$\sum_{t=mT}^{(m+1)T-1}\tilde{\gamma}_{i,t} = \sum_{t=mT}^{(m+1)T-1}\tilde{x}_{i,t}, \text{ for } i = u, d \tag{5.52}$$

$$\sum_{t=mT}^{(m+1)T-1}\tilde{d}_t \leq \sum_{t=mT}^{(m+1)T-1}d^{\max} \tag{5.53}$$

with the corresponding objective value denoted as $\tilde{u}_m^f$.

Note that comparing with **P1**, we impose per-frame constraints (5.51)-(5.53) as oppose to (5.16), (5.18), (5.20) and (5.3) for the T_o-slot period, respectively. Let $\delta \geq 0$ denote the gap of $\tilde{u}_m^f$ to the optimal objective value u_m^{opt}, *i.e.,* $\tilde{u}_m^f = u_m^{\text{opt}} + \delta$.

Among all feasible control solutions satisfying (5.51)-(5.53), there exists a solution

which leads to $\delta \to 0$. The upper bound in (5.50) can be rewritten as

$$\Delta_T(\mathbf{\Theta}_t) + V\left[\sum_{t=mT}^{(m+1)T-1}[E_tP_t + x_{e,t} + C_u(\gamma_{u,t}) + \alpha C_d(\gamma_{d,t})]\right]$$
$$\leq GT^2 + VT\lim_{\delta\to 0}\left(u_m^{\text{opt}} + \delta\right) = GT^2 + VTu_m^{\text{opt}}.$$

Summing both sides of above over m for $m = 0, \ldots, M-1$, and dividing them by VMT, we have

$$\frac{L(\mathbf{\Theta}_{T_o}) - L(\mathbf{\Theta}_0)}{VMT} + \frac{1}{MT}\sum_{m=0}^{M-1}\sum_{t=mT}^{(m+1)T-1}[E_tP_t + x_{e,t} + C_u(\gamma_{u,t}) + \alpha C_d(\gamma_{d,t})]$$
$$\leq \frac{GT}{V} + \frac{1}{M}\sum_{m=0}^{M-1}u_m^{\text{opt}}. \tag{5.54}$$

Since $C_i(\overline{\gamma_i}) \leq \overline{C_i(\gamma_i)}$ for the convex function $C_i(\cdot)$ where $\overline{\gamma_i} \triangleq \frac{1}{T_o}\sum_{t=0}^{T_o-1}\gamma_{i,t}$ for $i = u, d$, from (5.54), we have

$$\left(\frac{1}{T_o}\sum_{t=0}^{T_o-1}E_tP_t\right) + \overline{x_e} + C_u(\overline{\gamma_u}) + \alpha C_d(\overline{\gamma_d}) \leq \frac{1}{T_o}\sum_{t=0}^{T_o-1}[E_tP_t + x_{e,t} + C_u(\gamma_{u,t}) + \alpha C_d(\gamma_{d,t})] \tag{5.55}$$

For a continuously differentiable convex function $f(\cdot)$, the following inequality holds [61]

$$f(x) \geq f(y) + f'(y)(x - y). \tag{5.56}$$

Applying (5.56) to $C_u(\overline{x_u})$ and $C_u(\overline{\gamma_u})$, we have

$$C_u(\overline{x_u}) \leq C_u(\overline{\gamma_u}) + C_u'(\overline{x_u})(\overline{x_u} - \overline{\gamma_u}) \leq C_u(\overline{\gamma_u}) + C_u'(\Gamma_u)(\overline{x_u} - \overline{\gamma_u})$$
$$= C_u(\overline{\gamma_u}) - C_u'(\Gamma_u)\frac{H_{u,T_o} - H_{u,0}}{T_o} \tag{5.57}$$

where the last term in (5.57) is obtained by summing both sides of (5.24) over T_o. Similarly, we obtain

$$C_d(\overline{d_w}) \leq C_d(\overline{\gamma_d}) - C_d'(\Gamma_d)\frac{H_{d,T_o} - H_{d,0}}{T_o}. \tag{5.58}$$

Apply the inequalities (5.57) and (5.58) to $C_u(\overline{\gamma_u})$ and $C_d(\overline{\gamma_d})$ respectively to the LHS of (5.55). From (5.54) and (5.55), we have the following bound of the objective value $u^*(V)$ of **P1** achieved by our proposed algorithm

$$\begin{aligned} & u^*(V) - \frac{1}{M}\sum_{m=0}^{M-1} u_m^{\text{opt}} \\ & \leq \frac{GT}{V} + \frac{C_u'(\Gamma_u)(H_{u,0} - H_{u,T_o}) + \alpha C_d'(\Gamma_d)(H_{d,0} - H_{d,T_o})}{T_o} + \frac{L(\boldsymbol{\Theta}_0) - L(\boldsymbol{\Theta}_{T_o})}{VT_o}. \end{aligned} \tag{5.59}$$

Now, we prove the bound of (5.59), *i.e.,* as $T_o \to \infty$, we have the bound (5.36). To show this, it is suffice to show that both $H_{u,t}$ and $H_{d,t}$ in (5.59) are bounded. To show these bounds, we need to show that the one-slot Lyapunov drift in (5.40) is upper bounded as follows

$$L(\boldsymbol{\Theta}_{t+1}) - L(\boldsymbol{\Theta}_t) \leq G. \tag{5.60}$$

To show the above bound for the drift, we choose an alternative feasible solution $\tilde{\boldsymbol{\pi}}_t$, satisfying the following per slot relations

$$\tilde{Q}_t + \tilde{S}_{r,t} = \tilde{D}_t + \frac{\Delta_u}{T_o} \tag{5.61}$$

$$\tilde{\gamma}_{i,t} = \tilde{x}_{i,t}, \text{ for } i = u, d \tag{5.62}$$

$$\tilde{d}_t \leq d^{\max}. \tag{5.63}$$

Under the above (5.61)-(5.63), the first terms on the RHS of (5.41), (5.43), (5.45) and (5.46) become zeros. It follows that $L(\boldsymbol{\Theta}_{t+1}) - L(\boldsymbol{\Theta}_t) \leq G$. Note that the upper bound for (5.45) in (5.60) is obtained by chosen $\tilde{d}_t = d^{\max}$ in (5.63). Averaging (5.60) over T_o-slot period, we have

$$\frac{1}{T_o}\left[L(\boldsymbol{\Theta}_{T_o}) - L(\boldsymbol{\Theta}_0)\right] \leq G. \tag{5.64}$$

For any initial value of Lyapunov function $L(\mathbf{\Theta}_0) < +\infty$, (5.64) can be presented by

$$\frac{1}{2T_o}\left[Z_{T_o}^2 + H_{u,T_o}^2 + \mu\left(X_{T_o}^2 + H_{d,T_o}^2\right)\right] \leq G + \frac{L(\mathbf{\Theta}_0)}{T_o}. \tag{5.65}$$

It follows that

$$H_{i,T_o} \leq \sqrt{2T_oG + 2L(\mathbf{\Theta}_0)}, \text{ for } i = u, d. \tag{5.66}$$

Since $\frac{\sqrt{2T_oG+2L(\mathbf{\Theta}_0)}}{T_o} \to 0$ as $T_o \to \infty$, we have the second term on RHS of (5.59) goes to zero. Thus, we have (5.36). ■

5.6.6 Proof of Proposition 5.3

Proof. To prove ϵ_d is bounded, we see that

$$|\epsilon_d| = \frac{|X_{T_o} - X_0|}{T_0} \leq \frac{|X_{T_o}| + |X_0|}{T_0}. \tag{5.67}$$

From (5.65), it follows that

$$|X_{T_o}| \leq \sqrt{\frac{2T_oG}{\mu} + \frac{2L(\mathbf{\Theta}_0)}{\mu}}. \tag{5.68}$$

Substituting the above upper bound of $|X_{T_o}|$ in (5.67), we have (5.37). ■

Chapter 6

Conclusions

In this dissertation, we first proposed a real-time control policy to minimize the long-term time-averaged cost for energy storage management with renewable energy integration. We incorporated the system dynamics and the batter operation cost in the problem formulation, and applied Lyapunov optimization technique to design the real-time control policy with a bounded performance from the optimal scheme. Our control decision was derived in closed-form resulting in minimum implementation complexity. Simulations showed the effectiveness of integrating renewable energy for energy storage in reducing the long-term cost as well as improving the efficiency of energy storage relative to the battery operation cost.

Due to the unpredictable stochastic nature of the renewable source, load and pricing, whose statistics are difficult to obtain and likely to be non-stationary, we considered arbitrary system input dynamics in formulating the second problem. We included the battery operation costs in the formulation, and modeled the battery costs due to charging/discharging as part of the system cost. Our design aimed to minimize the system cost over a finite period of time. We provided a real-time control algorithm for such arbitrary system input dynamics. Our proposed algorithm is a

result of a sequence of problem modification and transformation, and employing the Lyapunov optimization framework. We further showed that our proposed algorithm resulted in a guaranteed bounded performance from the optimal T-slot lookahead scheme. Simulation results demonstrated the effectiveness of our proposed algorithm as compared with other alterative approaches.

In our last problem, we considered an ESM system which included a renewable generator and a battery for energy storage. We considered joint energy storage and load scheduling for the ESM system, where renewable source, loads, and pricing might be non-stationary and the statistics were unknown. For load scheduling, our model considered random load arrival with different energy intensities and durations, and both per load maximum delay and average delay constraints were considered. For energy storage, our model included the battery operation cost due to charging and discharging. Formulating the joint optimization problem to minimize the overall system cost over a finite period of time, we designed a real-time algorithm for joint scheduling and energy storage control. With a sequence of problem modification and transformation and the application of Lyapunov optimization, we were able to provide a close-form per slot scheduling and energy storage decision. Interestingly, we showed that the joint scheduling and energy storage could be separately and sequentially determined in our real-time algorithm. We showed that our proposed real-time algorithm had a bounded performance guarantee from an optimal T-slot look-ahead solution and is asymptotically equivalent to the optimal T-slot look-ahead solution as the battery capacity and time period go to infinity. Simulation results demonstrated the effectiveness of our proposed algorithm for joint load scheduling and energy stor-

age as compared with other real-time schemes which consider neither storage nor scheduling, or storage only.

Chapter 7

Future Work

Energy storage management is a relatively new research topic in recent years. Some potential directions as future works are given as follows:

1. Real-Time Algorithm with Predictable Information

With the increasing penetration of renewable and storage, the future grid demand and supply management are expected to be quite dynamic. Similarly, the prediction of intermittent renewable source is also a challenging task. Although the complete long-term information of demand, renewable and pricing is difficult to obtain, some information, such as pricing, is still predictable in a short period of time.

If certain type of full/partial statistical information is known, it potentially can be used in designing the algorithm to improve the performance gap to the optimal solution. For example, the per-slot control decision will be made based on the future pricing information, besides the current input. Specifically, whether the future price will (likely) be higher or lower will be factored the current decision on whether to store energy or use the stored energy. This will further reduce the system cost. Exactly how to incorporate such full/partial statistical information into the design is non-trivial; it may require new technique and in-depth investigation.

2. More Detailed Modeling for Battery Degradation

Battery technology has been evolving slowly in the past and has only recently picked up the pace. The battery degradation and the associated cost function are complicated and have yet to be better understood. The precise cost function is difficult to model and it may also depend on the type of degradation one is concerned about.

In our developed models, we have modeled the cost function due to the battery charging and discharging activities. For a more detailed modeling of battery degradation, we may study the battery aging effect to the battery capacity. As well known, batteries begin fading from the day they are manufactured. The aging process occurs naturally as part of usage, which cannot be reversed. To design our real-time algorithm, we may face some new challenges. For example, we need to consider a decreasing capacity of battery, but ensure the battery capacity constraint being satisfied over time due to the charging and discharging activities. New technique may be required to overcome this unique challenge. Also, since the performance of our proposed algorithm has a tight connection with the battery capacity, how good the new algorithm can perform still needs in-depth investigation.

3. From Residential-Level to System-Level

We have designed the energy storage management and load scheduling scheme for the residential consumers, in helping them reduce the electricity cost. Our proposed algorithm shows that the load scheduling can optimally respond to the real-time pricing information, provided by the utility. As the result, each consumer can significantly save the energy cost.

However, the demand responses by a large number of consumers may cause the

issue of rebound peak. To combat this issue, we may consider studying a problem that aims at saving the energy cost for the consumers and ensuring the grid reliability for the system operator, simultaneously. To design such a problem, it is normally assumed that certain level of statistical information is known. However, it is non-trivial to design a real-time algorithm which does not rely on any statistical information. It requires new technique and in-depth investigation.

Bibliography

[1] D. Callaway and I. Hiskens, "Achieving controllability of electric loads," *Proc. IEEE*, vol. 99, pp. 184–199, Jan 2011.

[2] "The smart grid: An introduction," U.S Department of Energy, 2009. [Online]. Available: http://energy.gov

[3] F. Katiraei, R. Iravani, N. Hatziargyriou, and A. Dimeas, "Microgrids management: Controls and operation aspects of microgrids," *IEEE Power Energy Mag.*, vol. 6, pp. 54–65, May 2008.

[4] P. Denholm, E. Ela, B. Kirby, and M. Milligan, "The role of energy storage with renewable electricity generation," National Renewable Energy Laboratory, Tech. Rep., Jan 2010.

[5] "Lower u.s. electricity demand growth would reduce fossil fuelsâĂŹ frojected generation share," U.S Energy Information Administration, 2014. [Online]. Available: http://www.eia.gov

[6] J. Ma, Y. V. Makarov, C. Loutan, and Z. xie, "Impact of wind and solar generation on the california iso's intra-hour balancing needs," in *Proc. IEEE PES*, Jul 2011.

[7] R. Huang, T. Huang, and R. Gadh, "Solar generation prediction using the arma model in a laboratory-level micro-grid," in *Proc. IEEE SmartGridComm*, Nov 2012.

[8] A. Castillo and D. F. Gayme, "Grid-scale energy storage applications in renewable energy integration: A survey," *Energy Convers. Manage*, vol. 87, pp. 885–894, Nov. 2014.

[9] W. Su, H. Eichi, W. Zeng, and M.-Y. Chow, "A survey on the electrification of transportation in a smart grid environment," *IEEE Trans. Ind. Informat.*, vol. 8, pp. 1–10, Feb 2012.

[10] "Status and prospects of battery technology for hybrid electric vehicles, including plug-in hybrid electric vehicles," U.S Senate Committee on energy and Natural Resources, transportation Sector Fuel Efficiency, 2007. [Online]. Available: http://energy.senate.gov

[11] S. Borenstein, "The long-run efficiency of real-time electricity pricing," *The Energy Journal*, vol. Volume 26, pp. 93–116, 2005.

[12] A. Papavasiliou and S. Oren, "Supplying renewable energy to deferrable loads: Algorithms and economic analysis," in *Proc. IEEE Power and Energy Society General Meeting*, July 2010.

[13] J. H. Kim and W. B. Powell, "Optimal energy commitments with storage and intermittent supply," *Operations Research*, vol. 59, pp. 1347–1360, Dec 2011.

[14] Y. Kanoria, A. Montanari, D. Tse, and B. Zhang, "Distributed storage for intermittent energy sources: Control design and performance limits," in *Proc. Allerton Conf. on Commun., Control, and Comput.*, 2011.

[15] H.-I. Su and A. El Gamal, "Modeling and analysis of the role of energy storage for renewable integration: Power balancing," *IEEE Trans. Power Syst.*, vol. 28, pp. 4109–4117, Nov 2013.

[16] S. Sun, M. Dong, and B. Liang, "Real-time welfare-maximizing regulation allocation in dynamic aggregator-evs system," *IEEE Trans. Smart Grid*, vol. 5, pp. 1397–1409, May 2014.

[17] ——, "Real-time power balancing in electric grids with distributed storage," *IEEE J. Select. Areas Commun.*, Jun. 2014, iEEEXplore early access.

[18] Y. Wang, X. Lin, and M. Pedram, "Adaptive control for energy storage systems in households with photovoltaic modules," *IEEE Trans. Smart Grid*, vol. 5, pp. 992–1001, March 2014.

[19] M. Lin, A. Wierman, L. L. H. Andrew, and E. Thereska, "Dynamic right-sizing for power-proportional data centers," in *Proc. IEEE INFOCOM*, Apr. 2011.

[20] Y. Zhang and M. van der Schaar, "Structure-aware stochastic storage management in smart grids," *IEEE J. Sel. Topics Signal Process.*, vol. 8, pp. 1098–1110, Dec 2014.

[21] R. Urgaonkar, B. Urgaonkar, M. J. Neely, and A. Sivasubramaniam, "Optimal power cost management using stored energy in data centers," in *Proc. ACM SIGMETRICS*, Jun. 2011.

[22] L. Huang, J. Walrand, and K. Ramchandran, "Optimal demand response with energy storage management," in *Proc. IEEE SmartGridComm*, Nov. 2012.

[23] S. Salinas, M. Li, P. Li, and Y. Fu, "Dynamic energy management for the smart grid with distributed energy resources," *IEEE Trans. Smart Grid*, vol. 4, pp. 2139–2151, Sep. 2013.

[24] S. Chen, N. B. Shroff, and P. Sinha, "Heterogeneous delay tolerant task scheduling and energy management in the smart grid with renewable energy," *IEEE J. Sel. Areas Commum.*, vol. 31, pp. 1258–1267, Jul. 2013.

[25] M. J. Neely, *Stochastic Network Optimization with Application to Communication and Queueing Systems*. Morgan & Claypool, 2010.

[26] J. Yang and S. Ulukus, "Optimal packet scheduling in an energy harvesting communication system," *IEEE Trans. Commun.*, vol. 60, pp. 220–230, Jan. 2012.

[27] K. Tutuncuoglu and A. Yener, "Optimum transmission policies for battery limited energy harvesting nodes," *IEEE Trans. Wireless Commun.*, vol. 11, pp. 4808–4818, Mar. 2012.

[28] O. Orhan, D. Gunduz, and E. Erkip, "Delay-constrained distortion minimization for energy harvesting transmission over a fading channel," in *Proc. IEEE Int. Symp. on Infor. Theory (ISIT)*, July 2013.

[29] K. Tutuncuoglu, A. Yener, and S. Ulukus, "Optimum policies for an energy harvesting transmitter under energy storage losses," *IEEE J. Select. Areas Commun.*, vol. 33, pp. 467–481, Mar. 2015.

[30] C. Chen, J. Wang, and S. Kishore, "A distributed direct load control approach for large-scale residential demand response," *IEEE Trans. Power Syst.*, vol. 29, pp. 2219–2228, Sept 2014.

[31] M. He, S. Murugesan, and J. Zhang, "A multi-timescale scheduling approach for stochastic reliability in smart grids with wind generation and opportunistic demand," *IEEE Trans. Smart Grid*, vol. 4, pp. 521–529, Mar. 2013.

[32] I. Koutsopoulos and L. Tassiulas, "Optimal control policies for power demand scheduling in the smart grid," *IEEE J. Sel. Areas Commum.*, vol. 30, pp. 1049–1060, Jul. 2012.

[33] C. Joe-Wong, S. Sen, S. Ha, and M. Chiang, "Optimized day-ahead pricing for smart grids with device-specific scheduling flexibility," *IEEE J. Sel. Areas Commum.*, vol. 30, pp. 1075–1085, July 2012.

[34] P. Samadi, A.-H. Mohsenian-Rad, R. Schober, V. W. Wong, and J. Jatskevich, "Optimal real-time pricing algorithm based on utility maximization for smart grid," in *Proc. IEEE SmartGridComm*, Oct. 2010.

[35] A.-H. Mohsenian-Rad and A. Leon-Garcia, "Optimal residential load control with price prediction in real-time electricity pricing environments," *IEEE Trans. Smart Grid*, vol. 1, pp. 120–133, Sept 2010.

[36] P. Du and N. Lu, "Appliance commitment for household load scheduling," *IEEE Trans. Smart Grid*, vol. 2, pp. 411–419, June 2011.

[37] S. Kishore and L. Snyder, "Control mechanisms for residential electricity demand in smartgrids," in *Proc. IEEE SmartGridComm*, Oct 2010.

[38] T. Kim and H. Poor, "Scheduling power consumption with price uncertainty," *IEEE Trans. Smart Grid*, vol. 2, pp. 519–527, Sept 2011.

[39] G. Xiong, C. Chen, S. Kishore, and A. Yener, "Smart (in-home) power scheduling for demand response on the smart grid," in *Proc. IEEE ISGT*, Jan. 2011.

[40] P. Yi, X. Dong, A. Iwayemi, C. Zhou, and S. Li, "Real-time opportunistic scheduling for residential demand response," *IEEE Trans. Smart Grid*, vol. 4, pp. 227–234, March 2013.

[41] A.-H. Mohsenian-Rad, V. Wong, J. Jatskevich, R. Schober, and A. Leon-Garcia, "Autonomous demand-side management based on game-theoretic energy consumption scheduling for the future smart grid," *IEEE Trans. Smart Grid*, vol. 1, pp. 320–331, Dec 2010.

[42] S. Bu and F. Yu, "A game-theoretical scheme in the smart grid with demand-side management: Towards a smart cyber-physical power infrastructure," *IEEE Trans. Emerg. Topics Comput.*, vol. 1, pp. 22–32, June 2013.

[43] L. P. Qian, Y. J. Zhang, J. Huang, and Y. Wu, "Demand response management via real-time electricity price control in smart grids," *IEEE J. Sel. Areas Commum.*, vol. 31, pp. 1268–1280, Jul. 2013.

[44] W. Saad, Z. Han, H. Poor, and T. Basar, "Game-theoretic methods for the smart grid: An overview of microgrid systems, demand-side management, and smart grid communications," *IEEE Signal Process. Mag.*, vol. 29, pp. 86–105, Sept 2012.

[45] Y. Huang, S. Mao, and R. Nelms, "Adaptive electricity scheduling in microgrids," *IEEE Trans. Smart Grid*, vol. 5, pp. 270–281, Jan 2014.

[46] Y. Guo, M. Pan, Y. Fang, and P. Khargonekar, "Decentralized coordination of energy utilization for residential households in the smart grid," *IEEE Trans. Smart Grid*, vol. 4, pp. 1341–1350, Sept 2014.

[47] Y. Guo, Y. Gong, Y. Fang, P. Khargonekar, and X. Geng, "Energy and network aware workload management for sustainable data centers with thermal storage," *IEEE Trans. Parallel Distrib. Syst.*, vol. 25, pp. 2030–2042, Aug 2014.

[48] L. Huang and M. Neely, "Utility optimal scheduling in energy-harvesting networks," *IEEE/ACM Trans. Netw.*, vol. 21, pp. 1117–1130, Aug 2013.

[49] K. Zhou, J. Pan, and L. Cai, "Optimal combined heat and power system scheduling in smart grid," in *Proc. IEEE INFOCOM*, April 2014.

[50] S. Sun, M. Dong, and B. Liang, "Distributed real-time power balancing in renewable-integrated power grids with storage and flexible loads," *IEEE Trans. Smart Grid*, vol. PP, pp. 1–1, 2015.

[51] L. Tassiulas and A. Ephremides, "Stability properties of constrained queueing systems and scheduling policies for maximum throughput in multihop radio networks," *IEEE Trans. Automat. Contr.*, vol. 37, pp. 1936–1948, Dec. 1992.

[52] ——, "Dynamic server allocation to parallel queues with randomly varying connectivity," *IEEE Trans. Inform. Theory*, vol. 39, pp. 466–478, Mar. 1993.

[53] "Electricity prices," Ontario Energy Board, 2012. [Online]. Available: http://www.ontarioenergyboard.ca/OEB/Consumers/Electricity

[54] P. Ramadass, B. Haran, R. White, and B. N. Popov, "Performance study of commercial licoo2 and spinel-based li-ion cells," *J. Power Sources*, vol. 111, pp. 210–220, Sept 2002.

[55] Z. Ma, S. Zou, and X. Liu, "A distributed charging coordination for large-scale plug-in electric vehicles considering battery degradation cost," *IEEE Trans. Control Syst. Technol.*, Feb. 2015, available through IEEEXplore early access.

[56] Z. Mao, C. E. Koksal, and N. B. Shroff, "Near optimal power and rate control of multi-hop sensor networks with energy replenishment: Basic limitations with finite energy and data storage," *IEEE Trans. Automat. Contr.*, vol. 57, pp. 815–829, Apr. 2012.

[57] M. J. Neely, "Universal scheduling for networks with arbitrary traffic, channels, and mobility," 2010, preprint available at http://arxiv.org/abs/1001.0960.

[58] "Sony fortelion," SONY, 2011. [Online]. Available: http://www.solarshop-europe.net/product_info.php?products_id=2562

[59] "Lg resu 5.0," LG Chem, 2013. [Online]. Available: http://de.krannich-solar.com/en/products/storage-solutions/lg-chem.html

[60] "Tesla powerwall," TESLA, 2015. [Online]. Available: http://www.teslamotors.com/powerwall

[61] S. Boyd and L. Vandenberghe, *Convex Optimization*. Cambridge University Press, 2004.